ISSN: 1863-5598

ZKZ 64717
11-16

Bodo´s Power Systems®

Electronics in Motion and Conversion

November 2016

The Gallery

HIOKI

www.hioki.com/pw6001 ✉os-com@hioki.co.jp

HIOKI @electronica2016
Booth #179, Hall A1

POWER ANALYZER PW6001

Improve Power Conversion Efficiency and Minimize Loss
Enhance the Development of SiC, GaN and IGBT Inverters

- Diverse array of sensors from **10mA** to **1000A**
- **6CH** per unit, **12CH** when synchronizing 2 power analyzers
- **±0.02%** rdg. basic accuracy for power
- **5MS/s** sampling and **18-bit** A/D resolution
- **DC, 0.1Hz to 2MHz** bandwidth
- CMRR performance of **80dB/100kHz**
- FFT analysis up to **2MHz**
- Compensate current sensor phase error with **0.01°** resolution
- Harmonic analysis up to **1.5 MHz**
- **Dual** motor analysis
- Large capacity waveform storage up to **1MWord x 6CH**
- **MATLAB toolkit** support
  (MATLAB is a registered trademark of Mathworks Inc.)

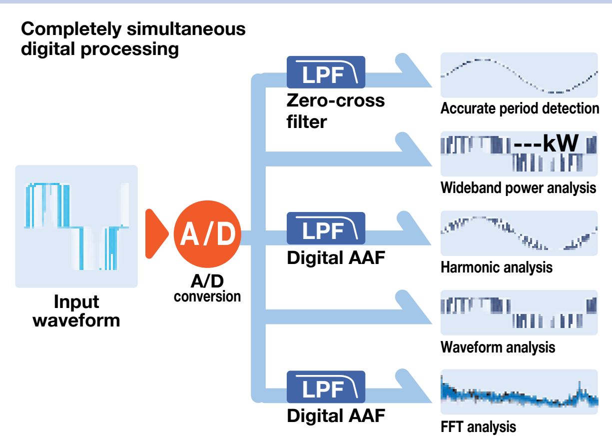

Fast, simultaneous calculations with Power Analysis Engine II

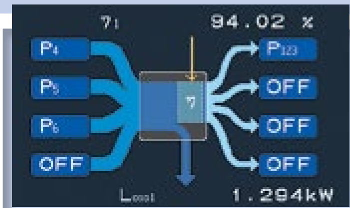

Assess efficiencyand loss at a glance

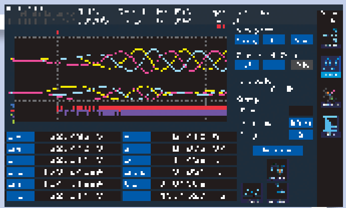

Analyze power waveforms without an oscilloscope

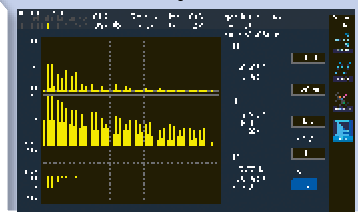

Harmonic analysis -critical for linking systems

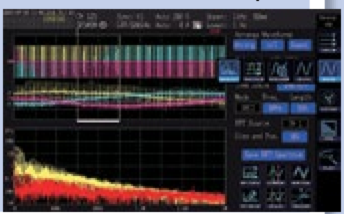

FFT analysis oftarget waveforms

Bodo´s Power Systems®

A Media
Katzbek 17a
D-24235 Laboe, Germany
Phone: +49 4343 42 17 90
Fax: +49 4343 42 17 89
editor@bodospower.com
www.bodospower.com

Publishing Editor
Bodo Arlt, Dipl.-Ing.
editor@bodospower.com

Junior Editor
Holger Moscheik
Phone + 49 4343 428 5017
holger@bodospower.com

Senior Editor
Donald E. Burke, BSEE, Dr. Sc(hc)
don@bodospower.com

UK Support
June Hulme
Phone: +44(0) 1270 872315
junehulme@geminimarketing.co.uk

Creative Direction & Production
Repro Studio Peschke
Repro.Peschke@t-online.de

Free Subscription to qualified readers

Bodo´s Power Systems
is available for the following
subscription charges:
Annual charge (12 issues)
is 150 € world wide
Single issue is 18 €
subscription@bodospower.com

circulation print run 24 000

Printing by:
Brühlsche Universitätsdruckerei GmbH
& Co KG; 35396 Gießen, Germany

Events

ESARS-ITEC 2016,
Toulouse, France November 2-4
http://www.esars-itec.org

Power Integrity Seminar 2016,
Munich Germany, November 3,
https://www.omicron-lab.com/trainings-events/1-day-workshop-with-steve-sandler-new-ways-to-vrm-modelling.html

electronica 2016,
Munich, Germany, November 8-11
http://electronica.de

sps ipc drives 2016,
Nuremberg, Germany, November 22-26
http://www.mesago.de/de/SPS/home.htm

Novemberfest in Munich,

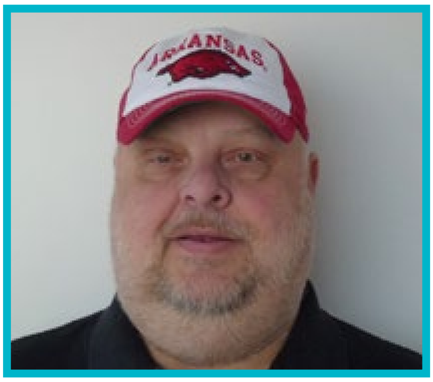

Those that missed Oktoberfest in Munich can now come to the electronica - the Novemberfest for electronics. The whole world of electronics comes to Munich bi-annually for the electronica, a big party ! For almost a full week, Munich is at the center of world of electronics. Two weeks later, in Nuremberg, the SPS IPC Drives will take place. November will be a busy time.

As I write this, I am surprising a lot of my industry friends with visits along the East Coast of the USA, and up into the New England area. Manhattan left a strong impression, as I had once been up in the World Trade Center, looking out over the city. This year I was in the Freedom Tower, overwhelmed by how fast buildings have replaced the wounds at Ground Zero. New York is always worth a visit, if for nothing else, just to take in its vibrant life and activity. But it is especially moving to look down at the Statue of Liberty. It was a gift to Americans from the French people. A good opportunity to take a rest, think about freedom, and the Thanksgiving holiday soon to come. Each of us can form our worlds and work for peace and freedom – you will have my full support.

Respect for people is so important and it seems surprising to have a candidate for President denigrating so many people including parents who have lost their son in war. It does not matter what religion the parents have. Their son gave his life for the USA and for freedom! My wish is that the voters will be mature enough to recognize trash-talking for what it is, and opt for a mature, experienced lady. In Germany we have Chancellor Angela Merkel and it would be very good for the USA to choose Hillary Clinton for the next President.

Everywhere I visit, innovation is moving fast. Wide band gap devices are taking over critical design activities for systems. Cost is no longer an issue, as reductions show up at the system level. SiC and GaN are more efficient in all applications, with transportation and computer systems leading the way. We are moving towards more electric automobiles. Power is being produced by green resources; water, wind or solar. Coal, gas and nuclear will be the past, as pollution and efficiency become paramount.

I now look forward to seeing you at the electronica or sps ipc drives. Bodo's Power Systems reaches readers across the globe. If you are using any kind of tablet or smart phone, you will now find all of our content on the new website www.eepower.com.
If you speak the language, or just want to have a look, don't miss our Chinese version: www.bodospowerchina.com

My Green Power Tip for November:
Turning off every street light during daylight should be possible. If you observe one not responding, have a talk to the town officials. That will save a lot of energy.

Best Regards

EPE ECCE Call for Papers

The Power Electronics community will gather in Warsaw, Poland, from 11 to 14 September 2017, to exchange views on research progresses and technological developments in the various topics described hereunder. On Monday 11 September a number of tutorials will be organised and several technical visits are planned on Friday 15 September. The 19th Conference on Power Electronics and Applications (and Exhibition), EPE'17 ECCE (Energy Conversion Congress and Expo) Europe is co-sponsored by the EPE Association and IEEE PELS. It will take place at the Gromada Airport Hotel and Conference Centre. EPE ECCE Europe is the place for specialists in power electronics, systems and components, to present papers and attend sessions on state-of-the-art technology in this challenging and evolutionary sector. The conference aims to be a meeting forum for researchers, developers and specialists from academia and industry. Papers are encouraged on all topics described hereunder for interdisciplinary discussions of new ideas, research, development, applications and the latest advances in the field of power electronics and adjustable speed drives.
Especially, wide bandgap materials (SiC & GaN) are a serious chance to big step forward in broad range of applications.
Several tutorials will be held prior to the conference. Authors willing to propose a tutorial at EPE'17 ECCE Europe are invited to send a proposal to Brigitte Sneyers at the scientific secretariat (EPE Association, c/o VUB-IrW-ETEC, Pleinlaan 2, B-1050 Brussels, Belgium, e-mail: bsneyers@vub.ac.be) before 15 January, 2017.

www.epe2017.com

The Future of Mobility at lectronica 2016: From Data Security to Autonomous Driving

In the future, mobility will be shaped by developments in automotive electronics: Smart lighting, autonomous driving and connected vehicles—to name just a few catchwords—are closely related to electronic components and software developed around the world now and in the future. electronica, the World's Leading Trade Fair for Electronic Components, Systems and Applications to be held in Munich from November 8–11, 2016, will shed light on the latest developments.

Experts will also discuss the industry's latest challenges and developments at the Automotive Conference and the Automotive Forum. Automotive electronics is on the rise around the world: According to the German Electrical and Electronic Manufacturers' Association (ZVEI), global demand for semiconductors for automotive electronics was worth nearly 35 billion dollars in 2014. Today, electrical and electronic components account for 30 percent of an automobile's production value—with an upward trend. The ZVEI expects the industry to grow at a rate of 4.5 percent over the next five years. No wonder, because according to the association, 80 percent of innovations in automobile manufacturing are driven by microelectronics and software.*
Expert knowledge at the electronica Automotive Conference
"Automotive" will be a focal point of electronica again in 2016. More than 800 exhibitors from this sector have already registered for the fair. All in all, more than 2,800 companies will present their products and services at the fair. On November 7, the day before the fair begins, leading managers and experts will meet at the electronica Automotive Conference to discuss the industry's key issues. The main topics of this year's lectures are safety, automated driving and interior electronics. Steve Nadig from Daimler Trucks North America has agreed to give a keynote address on "Autonomous Trucks: A Global Perspective." In another keynote address titled "Automotive meets CE," Dr. Ludger Laufenberg (Kostal) will explain how autonomous driving is effecting interior electronics. And Dr. Reinhard Ploss (Infineon Technologies) will examine the current role of electronics in the automotive industry in a keynote titled "Semiconductors as a key enabler for the transition of the automotive industry."

http://electronica.de

Redundant Power Supplies using GaN FETs

Telcodium, a leader in power supply design, in collaboration with Transphorm Inc. released the industry's first redundant power supplies using gallium nitride (GaN) field-effect transistors (FETs). Telcodium's AC Series replaces a typical three-module power supply architecture (two power supply bricks and one intermediate bus converter (IBC)) with a single power module with redundant AC feeds. Telcodium's power module operates at 94 percent True System Efficiency (TSE)* or higher—reducing average energy loss by 13 percent or more. To achieve the same TSE with the typical three-module power supply, the bricks and IBC would each need to yield a 97 percent efficiency—which exceeds the 80Plus Titanium specification and has yet to be demonstrated by any power supply manufacturer. Further, the new module is 30 percent smaller than the abovementioned two bricks and eliminates the standalone IBC—freeing considerable, critical space inside a host system.

www.transphormusa.com

www.telcodium.com

power integrations™

SCALE-iDriver™ Family

Single-Channel Gate Driver ICs with Reinforced Isolation

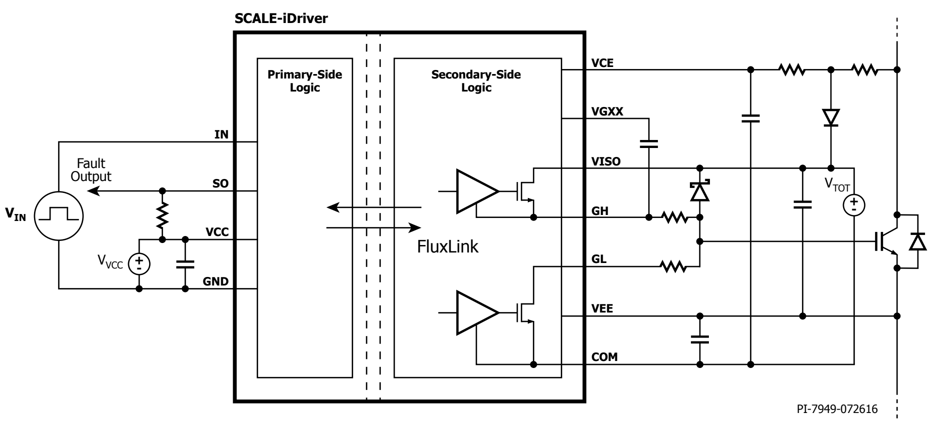

- 2.5 A, 5 A, 8 A output current devices
- Drives 1200 V IGBTs and MOSFETs up to 110 kW
- Revolutionary FluxLink™ communication technology
- Low profile with 9.5 mm creepage and reinforced isolation

www.power.com

ac-dc converters

led drivers

igbt drivers

20 Years of Effective Collaboration

Toshiba Electronics Europe and EBV Elektronik, a leading European distributor of semiconductors, are celebrating the 20th anniversary of their highly successful working relationship. In this time, collaboration between the two companies has grown from strength to strength and now sees EBV as one of Toshiba's most important world-wide distribution partners.

The association, which began on the 1st September 1996, originally covered selected countries in central Europe. However, after a successful, initial five months it was expanded to cover the whole of Europe. This partnership quickly saw yearly sales figures surpass $20 million, with a particular focus on couplers and MCU/Echelon interception systems.

Over the last 20 years EBV has been quick to introduce their customers to products and technologies pioneered by Toshiba, such as SRAMs and NAND Flash memories, backed up with joint customer visits and presentations. This has continued with the latest ranges of high-end photocouplers and MOSFETs, where opportunities for collaborative development and customer feedback have been taken by both parties to improve the experience of the end-user.

www.toshiba.semicon-storage.com

www.ebv.com

Picture: Klaus Michel, General Manager Distribution Sales, Toshiba & Slobodan Puljarevic, President EBV Elektronik

Promoting New Digital Age in India

STMicroelectronics, a global semiconductor leader serving customers across the spectrum of electronics applications, has showcased its latest technologies and products for Smart Driving, Smart Cities and Homes, and Smart Things at electronica India in the Bangalore International Exhibition Center.

ST's Smart Driving solutions focus on increasing safety and security with Assisted Driving, enhancing engine efficiency and accelerating vehicle electrification with Green Driving, and improving comfort and convenience with telematics and infotainment in Connected Driving.

Similarly, ST's offering for Smart Cities and Homes addresses energy efficiency along the entire power lifecycle through high-efficiency power supplies and energy-management technologies, smart (LED) lighting, and home automation. ST also provides all the building blocks for applications that make up the vast universe of Smart Things in our homes, offices, streets, and cars.

www.st.com

Non-Isolated Digital Point-of-Load Standard for 60 A Current

The Architects of Modern Power® (AMP Group) consortium announced an additional standard aimed at establishing common mechanical and electrical specifications for the development of advanced power conversion technology for distributed power systems. The 'gigaAMP™' standard, introduced to provide a higher current option in a land-grid array (LGA) footprint, builds on the previously-released 'picoAMP™' standard, published in September 2015, which defined standards for a lower range of non-isolated platforms ranging from 6 A to 18 A. The 60 A 'gigaAMP' standard defines a compact footprint of 25.1 x 14.1 mm in an LGA format.

The new 'gigaAMP' standard also adds to the previously released 'teraAMP™' standard for non-isolated digital point-of-load (POL) dc-dc converters, released in February 2015, and the 'microAMP™' and 'megaAMP™' standards released during electronica in November 2014. The first products to meet with this new 'gigaAMP' standard will be announced by AMP Group® members later in the year.

www.cui.com

www.murata.com

Completing Acquisition of Fairchild Semiconductor

ON Semiconductor Corporation and Fairchild Semiconductor International, Inc. jointly announced that ON Semiconductor has completed its announced acquisition of Fairchild.

On September 16, 2016, ON Semiconductor received confirmation that clearance related to the completion of its proposed acquisition of Fairchild from the Ministry of Commerce in the People's Republic of China had been obtained and that ON Semiconductor was entitled to close the transactions under PRC law. As such, the conditions to the acquisition of Fairchild relating to the termination or expiration of required waiting periods, and receipt of required approvals, under applicable antitrust laws were fully satisfied and ON Semiconductor's tender offer to purchase all of the outstanding shares of common stock of Fairchild for $20.00 per share in cash (the "Offer") expired as scheduled one minute following 11:59 p.m., New York City time, on September 16, 2016 and was not extended.

As a result of the Offer and the merger, Fairchild ceased to be a publicly traded company, its common stock will no longer be listed on NASDAQ, and Fairchild became a wholly owned subsidiary of ON Semiconductor.

http://www.onsemi.com

Allegro Stepper Motor Driver ICs

The Simplest Microstepping Control In The Industry

Allegro MicroSystems offers a full line of stepper motor driver and pre-driver ICs. These devices feature easy to use two wire step and direction translator interfaces as well as industry standard parallel or serial control.

- Microstepping
- Parallel, serial and step/direction interfaces
- PWM current control
- Robust protection features
- Diagnostic outputs
- Stall detect assistance
- Package options include exposed pad QFN, TSSOP, SOIC, and DIP. All packages are (Pb) free.

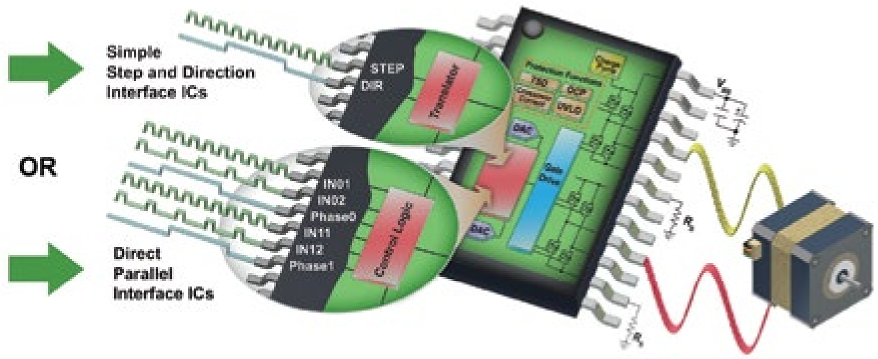

Applications include:

Office Automation
- Printers
- Scanners
- Copiers
- 3D Printing

Industrial
- Sewing machines
- Closed circuit television
- CNC milling machines
- Ticketing
- Vending
- Robotics

Automotive
- Throttle control
- Transmission
- Headlamp leveling
- Vent position control

Representatives

ALLREM
94616 Rungis Cedex, FRANCE
Tel: +33 (0) 1 56 70 03 80
E-mail: info@allrem.com

Allegro MicroSystems Germany GmbH
Adlerweg 1, D-79856 Hinterzarten, GERMANY
Phone: +49-(0)7652-9106-0
Fax: +49-(0)7652-767
E-mail: info.germany@allegromicro.com

Consystem S.r.l.
I-20144 Milano, ITALY
Tel: +39 02 4241471
Website: www.consystem.it
E-mail: support@consystem.it

Allegro™ MicroSystems Europe Ltd

www.allegromicro.com/MDP916BD

Maximize Productivity for Industry 4.0 Applications

Significantly increase manufacturing productivity with the Pocket IO programmable logic controller (PLC) development platform from Maxim Integrated Products, Inc.. The platform provides customers with the ability to achieve the smallest form factor and highest power efficiency for next-generation PLC designs.

Lost productivity is a common concern for Industry 4.0 designers challenged with keeping a manufacturing line running 24 hours a day, 7 days a week. Without intelligent data available at their fingertips, factory operators do not have the insight to make informed, real-time decisions which can significantly improve uptime, revenue, and gross margins. In addition to capturing real-time data, PLCs require fan-less operation due to harsh industrial environments. As a result, highly efficient power solutions are required to minimize heat dissipation.

Maxim's Pocket IO PLC development platform redefines how factories operate and enables Industry 4.0 applications. To maximize productivity, it provides real-time intelligence to quickly and effectively make decisions, adaptive manufacturing to avoid potential downtime, and distributed control to provide redundancy. The Pocket IO provides the following key advantages to increase productivity:

- Real-time intelligence: Fast data processing provides the necessary data to make intelligent decisions quickly and effectively to optimize yield.
- Adaptive manufacturing: Manufacturing flexibility allows for real-time changes and adjustments to avoid potential downtime.
- Distributed control: Ultra-small footprint of less than 10 cubic inches and smart energy consumption brings PLC down to the manufacturing line, re-distributing intelligent control and providing redundancy.

When compared to the Micro PLC Platform from two years ago, the Pocket IO decreases form factor by an additional 2.5x and reduces power consumption by another 30%.

Visit Maxim at electronica 2016 in Munich Hall A4, Stand 279.

http://bit.ly/Maxim_electronica_2016

http://www.maximintegrated.com

High-Performance Embedded Design with STM32F7 MCU Lines

STMicroelectronics has introduced STM32F7 microcontroller lines and added accessories and options to the development ecosystem, easing access to high-performance embedded design based on the ARM® Cortex®-M7 core.

The latest STM32F722 and STM32F723 microcontrollers in the very high-performance STM32F7 series reduce memory footprint by integrating value-added features including code-execution protection and high-speed USB physical-layer (PHY) circuitry that streamline development of connected applications. The STM32F732 and STM32F733 variants come with extra cryptographic features on-chip, such as an efficient AES256 HW engine. There are versatile package options from a 64-pin LQFP up to 176-pin LQFP or UFBGA for projects demanding high I/O count, and 256KB or 512KB of on-chip Flash memory with 256KB RAM.

Extensive pin, package, and software compatibility between the new devices and higher-end STM32F7 variants with 256KB to 2MB Flash memory and 256KB to 512KB RAM in packages up to 216-pin TFBGA simplifies design scaling for product differentiation and future-proofing. STM32F7 projects can also be readily ported throughout the large STM32 microcontroller family, which contains over 700 devices that cover all 32-bit Cortex-M cores and offer a wide range of peripheral, pin-count, and memory options.

www.st.com/stm32f7

World's Biggest Trade Fair for the Electronics Industry

electronica 2016 - Munich - 8 to 11 November, once again, electronica will bring the global electronics industry together in Munich for the World's largest trade fair dedicated to every aspect of electronics technology. electronica 2016 will offer visitors the chance to see all the major players from key industry sectors including semiconductors, power, interconnection, embedded and test and measurement. With the addition of an extra hall, electronica 2016 will have 13 halls full of innovations as well as an extensive programme of conferences and supporting events to provide visitors with the chance to learn more about developments that are considered key to the industry's future. Topics will include automotive, embedded solutions, LED technology, Internet of Things, cyber security, healthcare and wearables.

The program of conferences and forums will explore these exhibition topics in greater depth. By using the links in this newsletter, you can find out all there is to know about electronica 2016 and you can also save time and money by pre-registering.

Upcoming SMTA Space Coast Expo & Tech Forum

Alpha Assembly Solutions, the world leader in the production of electronic soldering and bonding materials, will be an exhibitor at the SMTA Space Coast Expo & Tech Forum to be held on November 17th in Melbourne, Florida.

Alpha will showcase their vast product portfolio of innovative materials and solutions for the electronics assembly industry with particular focus on ALPHA® Paste & Preforms for optimized process solutions and ALPHA® Wave Solder Alloy & Chemistries and Cored Solder Wire for optimal performance. ALPHA® Recycling Services will also be highlighted at the show to help customers realize their options for responsibly disposing of solder dross and waste.

"We are seeing more and more stringent specifications from our customers making it ever more critical for our product technology to yield consistent results while lowering overall costs," said Don Hosman, Southeast District Sales Manager for Alpha, a part of the MacDermid Performance Solutions group of businesses. "Our team works hard to exceed quality, efficiency and budget expectations to provide advanced products for a host of markets and applications."

In addition, Alpha will feature material set combinations to include paste, tacky flux, cored wire and wave soldering flux that are tested with one another to achieve greater reliability. These pairings, which were tested to IPC TM650 2.6.3.7/J-STD 004B requirements, will save customers a great deal of trial and error while increasing their throughput and time-to-market.

To receive information on successful material set combinations, be sure to visit Alpha during the SMTA Space Coast Expo or visit our site at AlphaAssembly.com.

www.AlphaAssembly.com

PhD Course in "the Smart Transformer"

The chair of power electronics of Kiel University offers a three-day industrial / Ph.D. course in "the Smart Transformer, its Impact on the Electric Grid and Technology Challenges". The Smart Transformer (ST), a power electronics-based transformer, can provide ancillary services to the distribution grids to support the grid management, in addition to the voltage adaptation. The Smart Transformer is a natural connection point for hybrid (AC and DC) grids both at MV and LV levels. The Smart Transformer is supposed to reach a market of US$204.3 million by 2020. This course investigates its possible services to the electric grid plus the power electronics technologies which could enable these services.

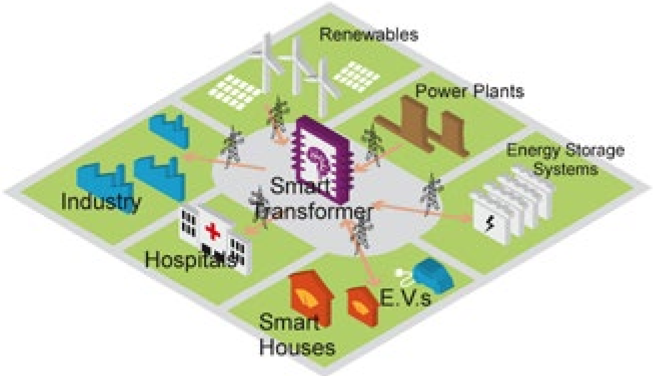

This course consists of lectures (2 ECTS) and laboratory experiments (2 ECTS). and takes place from February 22 till February 24, 2017 in faculty of engineering at Kiel university, Kiel, Germany. The registration is open till December 5, 2016 ("terasa@eek-sh.de").

The instructors are Prof. M. Liserre from University of Kiel; Prof. C. Vournas from University of Athens, and Dr. G. Buticchi form University of Kiel.

For more information about the course contents please visit:

www.pe.tf.uni.kiel.de/en

or contact: sha@tf.uni-kiel.de

Innovative Products and Concepts for Power & Energy Management

At the world's leading show for electronics, electronica in Munich (Nov. 8-11, 2016/Hall A5-Booth 542) ROHM Semiconductor will showcase cutting-edge power management solutions for numerous applications in the automotive, industrial and residential/home arenas. Utilising the latest SiC and Si technologies, proprietary processing and packaging technologies, these devices maximise efficiency and compactness, paving the way for cost and component reduction while delivering optimum performance. Combining ROHMs knowhow in analogue and digital power technology, they represent the most advanced developments of ROHM's global R&D centers and joint designs with industry partnerships. All these products are manufactured in the company's fully owned, vertically integrated production sites. Among others, key topics will include 3rd Gen SiC MOSFETs, Schottky barrier diodes (SBDs) and Modules, LED-Drivers for exterior Lighting, Design Kits for wireless power delivery and the technology partnership with Formula E-car developer Venturi.

The 3rd Gen of SiC Schottky Barrier Diodes (SBD) realise lowest forward voltage (VF) and lowest reverse leakage current (IR) over the entire temperature range among all of the SiC SBDs currently available on the market. In addition to this, they feature high surge

current capability which is ideal for power supply applications. Adding to the recently announced TO220AC devices at 650V/6, 8 and 10A, ROHM will introduce D2pak devices also adding lower current options, 2A and 4A to the family. ROHM's new full SiC modules including a chopper type module for converters integrating both, Trench SiC MOSFETs and SiC SBDs.

www.rohm.com/web/eu/electronica-2016

ECPE Workshops

Thermal and Reliability Modelling and Simulation of Power Electronics Components and Systems' and 'Model Predictive Control in Power Electronics - Expectations and Applications
30 November - 1 December 2016, Fuerth/Nuremberg, Germany
Chairmen: Prof. E. Wolfgang (ECPE),
Prof. B. Wunderle (TU Chemnitz), M. Thoben (Infineon)

Model Predictive Control in Power Electronics - Expectations and Applications
7 - 8 December 2016, Nuremberg, Germany
Chairmen: Prof. R. Kennel (TU Munich),
Dr. T. Geyer (ABB Corp. Research)

ECPE Tutorial
'Thermal Engineering of Power Electronic Systems - Part II
(Thermal Management and Reliability)
18 - 19 October 2016, Nuremberg, Germany
Chairmen: Prof. E. Wolfgang (ECPE),
Prof. U. Scheuermann (Semikron)

ECPE Tutorial 'Failure Mechanisms of Insulating Materials
27 October 2016, Kassel, Germany
Chairmen: Prof. A. Claudi (University of Kassel),
Dr. R. Bayerer (Infineon)

For the ECPE Calendar of Events 2016 and more Power Electronics Conferences & Events supported by ECPE please visit:

www.ecpe.org

Delivering Industry's First 1000V SiC MOSFET

Wolfspeed, a Cree Company and a leader in silicon carbide (SiC) power products, has introduced a 1000V MOSFET that enables a reduction in overall system cost, while improving system efficiency and decreasing system size. The new MOSFET, specially optimized for fast charging and industrial power supplies, enables a 30 percent reduction in component count while achieving more than 3x increase in power density and a 33 percent increase in output power.

"Supporting the widespread implementation of off-board charging stations, Wolfspeed's technology enables smaller, more efficient charging systems that provide higher power charging at lower overall cost. This market requires high efficiency and wide output voltage range to address the various electric vehicle battery voltages being introduced by automotive suppliers," explained John Palmour, CTO of Wolfspeed.

"Wolfspeed's new 1000V SiC MOSFET offers system designers ultra-fast switching speeds with a fraction of a silicon MOSFET's switching losses. The figure-of-merit delivered by this device is beyond the reach of any competing silicon-based MOSFET," Palmour added.

With the introduction of its 1000V SiC MOSFET, Wolfspeed leads the market with the industry's most complete device portfolio. Wolfspeed was the first company to release a commercially qualified SiC MOSFET in 2011 and remains a leader today, committed to delivering great technology and value.

Designers can reduce component count by moving from silicon-based, three-level topologies to simpler two-level topologies made possible by the 1000 Vds rating of the SiC MOSFET. The increase in output power in a reduced footprint is realized by the ultra-low output capacitance —as low as 60pF— which significantly lowers switching losses. This device enables operations at higher switching frequencies, which shrinks the size of the resonant tank elements and decreases overall losses, thus reducing heatsink requirements.

Wolfspeed has determined these proof-points by constructing a 20kW full-bridge resonant LLC converter and comparing it to a market-leading 15kW silicon system.

Wolfspeed offers a 20kW full-bridge resonant LLC converter reference design, listed as part number CRD-20DD09P-2. This fully assembled hardware set allows designers to quickly evaluate the new 1000V SiC MOSFET and demonstrate its faster switching capability, as well as the increased system power density the device enables.

The LLC converter's reference design files, which include full schematics, bill of materials, simulation files, and detailed a user guide, can be found online at go.wolfspeed.com/referencedesigns. The full hardware is available for purchase on demand from Wolfspeed.

www.wolfspeed.com

Sales Manager in Denmark

TDK-Lambda Germany has appointed a new sales manager in Denmark where it opened a subsidiary in April 2013. The global power supplies manufacturer established a local presence 3 years ago in response to an increase in demand in Scandinavia.

In order to be well prepared for current and future business and to promote cooperation between direct and distribution sales, Mr Allan Jakobsen has been appointed as the new "Sales Manager Nordic", serving Denmark, Sweden, Norway, Finland and the Baltic countries. "With his experience in direct customer service management, Mr Jakobsen will continue to serve our clients in the best possible way. He will also support the success of TDK-Lambda's distributor network," explained Ulrich Schwarz - Sales Director of TDK-Lambda Germany GmbH.

allan.jakobsen@de.tdk-lambda.com

electronica
8-11 November
Power & energy A2.547
Passives/modules B5.107
Murata IPDiA A4.518
Enabling your next power innovation
Mono-block converter
DC-DC converter with world's highest power density
Ultra small surface mount package 10.5 x 9.0 x 5.6mm
Quick response to load change
Outstanding thermal derating performance
High reliability / Telecom grade
New Product
UMAL energy device
Low-profile high capacity energy device.
Low profile,
Large capacity (12 mAh),
Low internal resistance (200 mΩ)
Long life
Continuous discharge
Constant voltage charge
Low power DC-DC
Murata's DC/DC converters can meet the needs for miniaturization,
Low profile,
High efficiency
Power-saving
Low noise
NXE1, NXE2, MGJ6 Low profile
info@murata.eu
go.murata.com/power
muRata
INNOVATOR IN ELECTRONICS

Dual Channel “Smart” Power Amplifier Uses Mixed-Signal Processing to Generate Multi-Pulse Waveforms Used in Industrial Ink Jet Printing

Apex Microtechnology is making the design of power analog drive circuitry for industrial ink jet printer nozzles less of a challenge by pairing a high performance power amplifier with a digital front end. The MP113 is a complete solution for implementing multi-pulse waveforms required to drive a changing number of print nozzles with quality and accuracy in large format printing applications.

The MP113 features onboard firmware that controls a dual channel amplifier that allows the user to define the desired waveform for their specific end system. The amplifier is rated at >10A PEAK per channel with a voltage supply operation of 180V and up to 135V of output voltage.

“The MP113’s graphical user interface provides a simplified solution that is easy to implement with an existing drive system or an entirely new design,” explains Apex Strategic Marketing Manager Jens Eltze. “The MP113 supports expanded printing capabilities including the use of grayscale and the ability to change droplet sizes for greater intensity which is needed to print higher resolution images.”

The modular design of the MP113 is in a broader sense its own evaluation kit. The embedded firmware allows users to test various parameters such as the size and speed of droplet formation and to optimize these specifications for specific types of ink. The MP113 also is designed with protection and diagnostic features to enhance the overall reliability of the system. In terms of electrical performance, the output for the MP113 is referenced to ground and not the negative supply rail, thus eliminating the need for a high current negative supply. A low current negative supply (≤50mA) allows input to zero volts without violating the common mode input range. The MP113 also provides thermal efficiency with a power dissipation rating of up to 100W per channel.

Key performance specifications include:

Parameter		MP113
Waveform Generator		
	Maxiumum ouput voltage	135V
	Maximum slew rate	50V/µs
	Maximum number of pulses per waveform	8
	Waveform generator resolution	≥125ns
	Voltage adjustment based on print head parameter	Yes (0.5V steps)
	Minimum pulse width	10µs
	Maximum print speed	50kHz
	Temperature protection	Yes
	Over-current protection	Option
Print Data Module		
	Maximum number of nozzles	1024
	Number of waveform generators	1 or 2
	Maximum Grayscale levels	4 (2-bit)
Module Size		110.5mm x 104.5mm

Pricing, Availability and Evaluation Tools

Sample units of the MP113 are available now for qualified applications, with production volumes targeted for Q4. Consult the factory for per unit pricing. Complete product information is online at www.apexanalog.com/apex-products/mp113. For technical support, contact Apex applications engineering at 800-546-2739, or apex.support@apexanalog.com.

Apex Microtechnology is an industry leader in high power analog components, designed to meet the performance and cost design targets of our customers’ precision control applications. Apex Microtechnology is headquartered in Tucson, AZ, USA. More information about Apex Microtechnology is available at www.apexanalog.com.

Apex Microtechnology,
Apex and the Apex logo are trademarks of Apex Microtechnology, Inc.

www.apexanalog.com

Magnetics: The Eternal Battle with Myths, Mysteries and Black Magic – or Maybe Really all Just a Matter of Basic Principles and Physics?

By Alexander Gerfer, CTO Würth Elektronik eiSos

Is magnetism an esoteric science of the 18th century or perhaps even black magic? Are magnetics really a closed book for the user? Or EMC ferrites an unknown entity?

We observe that the majority of engineers, including our own junior engineers, are not well trained in the basics. Much is omitted in training and higher education, but it already starting in high school. A classic example, Pythagoras' theorem, is no longer included in many curricula. It appears as though this is simply too trivial? Yet, without a foundation of well understood (!) basic knowledge, only superficial knowledge proliferates, or in the worst case, ignorance is not overcome.

This example demonstrates exactly where the problem lies with magnetics too. Regardless of which country's college and university curriculum you look at, EMC (Electromagnetic Compliance) and inductive components are often just side topics. In addition, the basic knowledge taught is not only diluted, but often outdated. Today's inductive components are based on the same physical principles – but the diversity of core materials has expanded rapidly; they work in quite different frequency ranges and in many other application areas than those described in the text books as "in practice". For instance, Dr. Ray Ridley impressively described at APEC2016 that students could not even recognize a transformer on a photo, but they could certainly identify the robotic comic figure, "Bumble Bee", as a "Transformer" on another photo!

Competitiveness in the market depends on companies being in a position to achieve a fast time-to-market. Whoever is faster to the market with their solution has a decisive influence on prices and market shares. Competitiveness also depends on whether this solution is achieved without interference emission and with interference immunity, whether it is efficient and of highly durable and reliable quality!

Speed to market is compromised if the basic principles on the origins of interference are not understood and then the devices have to be made EMC compliant in laborious EMC tests and redesigns. Inductive components are blamed for lack of efficiency in power supplies in over 60% of cases. However, going into more detail reveals that much would have been resolved by choosing the right topology, correct component selection and understanding, e.g. of current density and the associated limit of miniaturization. Service life depends largely in whether the design stays cool. High operating temperatures are a curse for all electronics!

So we can only hope that the young engineers actively keep abreast of their continuing education. Not only based on Wikipedia, but also in the numerous good seminars offered by the manufacturers.

We at Würth Elektronik eiSos have offered handbooks for many years and we provide enlightenment on this subject in seminars. But how was it in Kant's famous definition, "Enlightenment is man's emergence from his self-incurred immaturity." I can only appeal: Keep on learning! Don't be scared by black magic, demystify EMC and inductive components!

http://www.we-online.com/

Elektronics with Diamonds

Since quite some time, Silicon is still the workhorse of the electronics industry, but semiconductors with a broad bandgap (WBGS) are already winning ground in certain applications faster and faster. For instance Akhan Semiconductor concentrates on the diamond technology. Diamond is unmatched in its ability to diffuse heat, perform as a semiconductor, and create smaller and more powerful electronics. Our correspondent Henning Wriedt talked with its CEO Adam Khan about these WBGS.

By Henning Wriedt, Bodo's Power Systems, corresponding editor

Henning Wriedt: Mr. Khan, where do Wide Band Gap Semiconductors (WBGS) have their place in the semiconductor technology field and on the application side?

Adam Khan: Wide Band Gap Semiconductors have the potential to address nearly the entirety of the materials and device components of the global semiconductor market but perhaps nowhere more imminently than power electronics. Any user of technology understands heat is a major issue where cellphones, laptops, tablets, and the like, are warm to the touch even after limited usage. The performance demands of consumer technologies have forced the approach of the physical limitations of the existing silicon based technologies.

Henning Wriedt: Which are the current WBGS-Materials?

Adam Khan: The existing WBGS materials such as Silicon Carbide and Gallium Nitride have been in extensive development since the 1980s & 1990s, respectively, and have seen traction in power electronics applications, such as high voltage switching and power inverter systems, as well as wide usage in optoelectronics applications (such as LED in the case of Gallium Nitride).

Henning Wriedt: Which are the most important specifications of WBGS compared to other semiconductor materials?

Property	Si	GaAs	6H-SiC	4H-SiC	GaN	Diamond
Bandgap, E_g (eV)	1.12	1.43	3.03	3.26	3.45	5.45
Dielectric constant, ε_r[a]	11.9	13.1	9.66	10.1	9	5.5
Electric breakdown field, E_c (kV/cm)	300	400	2,500	2,200	2,000	10,000
Electron mobility, μ_n (cm^2/V·s)	1,500	8,500	500 80	1,000	1,250	2,200
Hole mobility, μ_p (cm^2/V·s)	600	400	101	115	850	850
Thermal conductivity, λ (W/cm·K)	1.5	0.46	4.9	4.9	1.3	22
Saturated electron drift velocity, v_{sat} ($\times 10^7$ cm/s)	1	1	2	2	2.2	2.7

[a] $\varepsilon = \varepsilon_r \cdot \varepsilon_o$, where ε_o=8.85×10^{-14} F/cm.

Figure 1: Physical characteristics of Si and the major WBG semiconductors (Credit: Oak Ridge National Laboratory)

Adam Khan: WBGS materials can operate at higher voltages, higher frequencies, and power densities as compared to silicon, allowing more power to be delivered using smaller and simpler components from fewer chips. Also unlike Silicon, they can both operate at higher temperatures and dissipate heat more efficiently, where diamond has the highest thermal conductivity. This enables cost efficiency, energy efficiency, and the next generation of design capability for semiconductor.

Henning Wriedt: What are the pros and cons of the current WBGS?

Adam Khan: Despite higher processing temperatures (700C) and dependence on costly substrates, the long maturation Silicon Carbide based technologies have made it the cheapest of the WBGS materials. Silicon Carbide is currently utilized in power devices, and is starting to play an important role in electric and hybrid electric vehicles (EV/HEV) markets due its higher operating temperature at higher voltages.

Less mature than Silicon Carbide, but more so than diamond, Gallium Nitride devices have had widespread deployment in primarily LED, but also Radio Frequency and high power electronics primarily due to the materials direct bandgap and high-frequency performance. Despite its advantages, Gallium Nitride materials remain more costly than both nanocrystalline diamond and Silicon Carbide with restrictions on large area wafer availability.

Diamond shows the best theoretical performance of all WBGS exceeding the performance capability of the competing materials by several orders of magnitude. Advances in synthesis and semiconductor doping have since opened the materials capability to address current and emerging market needs, but as it is the least mature of the WBGS materials, the availability of component devices is presently limited.

Henning Wriedt: Can WBGS somehow extend Moore's Law, since current technologies seem to reach a density plateau?

Adam Khan: Very much so. From the design perspective, WBGS materials are capable of faster switching speeds as compared to Silicon which allow for higher frequencies of operation translating to faster clockspeeds for logic circuits. More importantly perhaps, diamond is capable of direct integration with the existing silicon based chips, allowing direct cooling of chip junctions and increasing the performance capability of the existing silicon based circuitry.

Henning Wriedt: Do the R&D community and the Government support the WBGS technology adequately?

Adam Khan: More recently, there has been a marked increase in the grants supporting programs involving WBGS materials amongst the various U.S. based agencies. Further, with ambitious efforts on the part of the U.S. Department of Energy through programs like the Power America Initiative and the Materials Genome Initiative, the public sector R&D climate is very supportive.

Henning Wriedt: Your company focuses on one WBGS. Please explain your Miraj™ Diamond Platform

Adam Khan: At its core, the Miraj Diamond™ platform consists of two breakthrough innovations in diamond semiconductor research-- the CMOS compatible Nanocrystalline Diamond synthesis process, developed by Argonne National Laboratory, and the co-implantation n-type diamond process pioneered by AKHAN Semiconductor. Combined with related process intellectual property, the platform provides innovative solutions to the automotive, aerospace, telecommunications, consumer electronics, and military & defense markets rendering more reliability and efficiency in existing systems and allowing new design capabilities in next-generation systems.

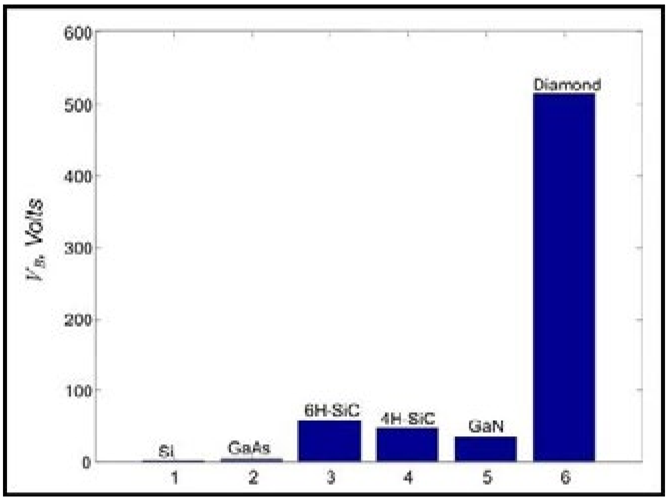

Figure 2: Maximum breakdown voltage of a power device at the same doping density normalized to Si.
(Credit: Oak Ridge National Laboratory)

Henning Wriedt: What are the manufacturing and integration aspects of this platform?

Adam Khan: AKHAN has recently entered the marketplace with its innovative thermal and optical Miraj Diamond™ products, with pilot commercial scale manufacturing capability of our initial product line with licensing product availability for vertically integrated/ high volume customers. The platform is currently compatible with 200mm process lines, normative to power electronics wafer sizes. Further the platform can be directly integrated with existing Silicon and a variety of Glass substrate processes.

Henning Wriedt: Your company is based in Illinois - no need to move to the Silicon Valley?

Adam Khan: The Illinois innovation ecosystem is rather unique as it possesses an existing skilled and largely untapped labor force--the byproduct of having two national laboratories, several world-class universities, and prolific technology companies such as Motorola. The state itself has also been supportive of AKHAN's efforts-- recognizing the importance of advanced materials manufacturing and the resultant creation of S.T.E.M. jobs-- crafting an incentive package totaling over $5 million (USD). The company does maintain a remote presence in Silicon Valley with both myself and the company's CTO, Bill Alberth being based out of our San Francisco office.

Contact:
AKHAN Semiconductor, Inc.
940 Lakeside Drive
Gurnee, IL 60031, USA
Tel: +847.855.8400

http://www.akhansemi.com

Picture : Adam Khan, Founder and CEO of AKHAN Semi

Adam Khan is the Founder and the Chief Executive Officer of AKHAN SEMI. Previous to AKHAN SEMI, Mr. Khan studied both physics and electrical engineering at the University of Illinois at Chicago before pursuing research at the graduate level at Stanford University's Stanford Nanofabrication Facility (SNF).

Mr. Khan has authored several patents, technical publications, is invited to technical talks regularly, and also co-chaired the 2014 New Diamond and Nano Carbons conference (Materials Research Society). Mr. Khan is co-inventor of the Miraj Diamond™ Platform, the world's first CMOS Compatible N-type Diamond Materials and Devices.

Peak Current Proof Input Filter with Multilayer Power Suppression Bead WE-MPSB

Power supplies are often designed for steady state operation, with transient conditions mainly considered as an afterthought. In practice, transient conditions such as startup, shutdown, and load transients are often far more stressful on the components of the power supply than operation in steady state. To suppress high frequency noise, chip bead ferrites are mainly placed at the input and output of power supplies.

By Ranjith Bramanpalli, Würth Elektronik eiSos

There are two good examples of transients that are often overlooked, but requires merit careful attention. The inrush current occurs when a power supply first starts up or when PWM used for variable loads such as dimming of LED drivers. Chip bead ferrites are often positioned at the inputs and outputs of power supplies where they must endure heavy transient currents, and this creates a need for compact, cost effective devices that are also highly reliable. Such ferrites are placed at the input and output because they are very effective at filtering the high frequency noise in switching regulators. The high frequency noise results from rapid switching currents ringing with parasitic inductance and capacitance. Such noise tends to occur at frequencies from 50 MHz to 500 MHz and is known as “ringing”, “spikes” or “periodic and random deviation noise” (PARD noise). Figure 1 shows PARD at the origin, the switching node, and also shows how PARD noise shows up at the input and output of the switcher.

Figure 1: PARD noise without Chip Bead Ferrites starts at the switching node of a buck converter (blue) and contaminates the input voltage (yellow) and the output voltage (green)

Zooming in and measuring the frequency of PARD noise in Figure 1 reveals a frequency of 170 MHz. Conducted noise like the waveforms in Figure 11 will generate radiated noise if it leaks onto input and output wiring harnesses.

In general, chip bead ferrites should be always placed as close as possible to the converter as source of noise. However, one effective method for preventing PARD noise from getting into the input and output leads of a switching power supply is to place chip bead ferrites in series with the inputs and outputs. These should be placed as close as possible to the edge of the PCB and/or to the connectors, and footprints for ferrites should be placed in series with both the positive and the negative of each connector.

Again, in general ferrites should be placed as close as possible to the source of the noise because the noise couples into the unfiltered traces and cables. But be aware that it is very likely that high frequency noise can couple around a ferrite via parasitic capacitance to GND and earth planes. Most EMC standards begin limiting radiated EMI at 30 MHz, so preventing this unwanted antenna effect of input and output leads is highly important. When a ground plane or a shielded enclosure is present, noise can couple around a ferrite placed towards the interior of a PCB, as shown in Figure 2.

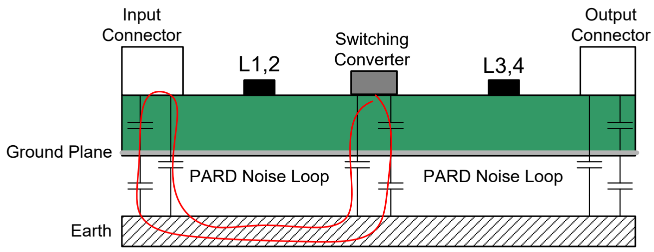

Figure 2: PARD noise gets around chip bead ferrite beads L1-L4 by coupling capacitive through the ground plane and earth to the input and output connectors

Würth Elektronik eiSos has recently developed a family of chip bead ferrites that feature high average / RMS current ratings, low DC resistance and are also tested and specified for high current pulses. This peak current proof series, the WE-MPSB Multilayer Power Suppression Bead family, is especially suitable for use in positions where short-duration currents far exceed the average currents.

Inrush Currents at Turn-On

At the moment when a power supply is turned on, any capacitors connected to the input bus will begin to charge. In some very rare cases, a soft-start of the input supply controls the ramp in a smooth,

monotonic behavior, but in most cases, the input voltage ramps up very quickly. For example, if the 12 VDC power bus in Figure 3 is already up and running when a mechanical switch connects it to the buck converter, the ramp slope is only limited by the source resistance and the resistance and parasitic inductance of the leads/PCB traces/switch. For this application note the resistance and inductance of a 30 cm banana-to-banana test cable was measured and came out to 8 mΩ and 0.3 µH, respectively. In practice all voltage sources are current limited, but if the 12 VDC bus had a large amount of output capacitance, a fact for the laboratory DC power supply used in this application note, then the charging current when the mechanical switch closed could easily exceed 30 A as shown in Figure 4.

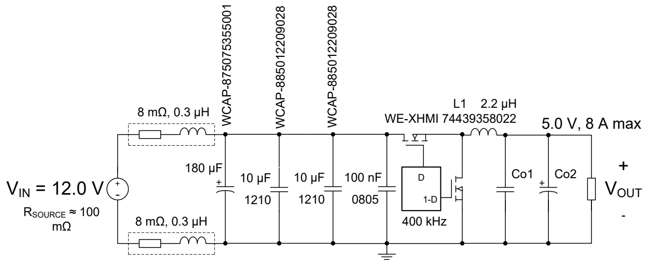

Figure 3: Schematic of the test buck converter showing source resistance, input lead resistance and inductance along with all input capacitors

Figure 4: Input inrush current of 33 A for a 12 VDC bus with a near-instantaneous connection charging 20 µF of ceramic and 180 µF of polymer aluminum input capacitance

Figure 4 shows a pulse that peaks at approximately 33 A and settles after around 100 µs to the 5 A current limit of the laboratory power supply used as the input source. It then takes another 200 µs to charge the input capacitors up to the target 12 V. Compare this waveform to the steady state input source current:

$$I_{source,\,max} = \frac{V_{out} \cdot I_{out,\,max}}{\eta \cdot V_{in,\,min}} = \frac{5\ V \cdot 8\ A}{0.95 \cdot 11.4\ V} = 3.7\ A$$

(η is the measured power efficiency of 95%)

The compromise facing the circuit designer becomes evident: any input filter components must be able to handle heavy current pulses each time the converter is switched on, but selecting ferrites rated to handle the full pulse current leads to overdesign for steady state.

Outrush Currents at Turn-On

The next ferrites will be placed at the output. The converter has two polymer aluminum 330 µF output capacitors with 20 mΩ of ESR each and two 100 µF multi-layer ceramic capacitors with approximately 3 mΩ of ESR each. This capacitor bank is capable of supplying large pulses of current in a short time. The same 30 cm cables were used to connect the 5.0 V output to a load that draws the maximum of 8 A of output current, and Figure 5 shows that when the 8 A load is connected with a fast rise time the current transient comes close to 25 A.

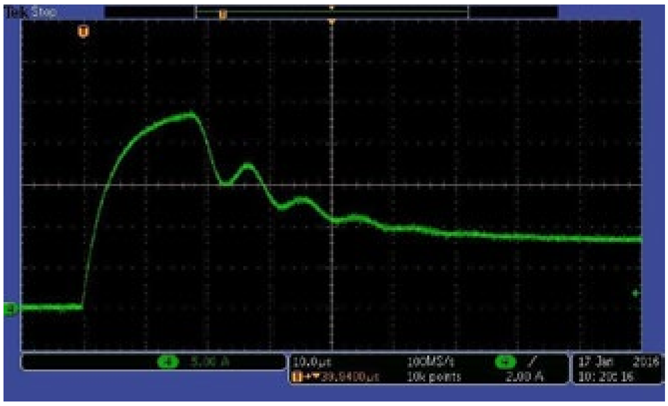

Figure 5: Outrush current for a 5 VDC bus with a near-instantaneous connection to an 8 A load with 200 µF of ceramic and 660 µF of polymer aluminum output capacitance

Using WE-MPSB Multilayer Power Suppression Bead Problems with Steady State Current Ratings

The WE-MPSB family was designed to provide a similar range of impedances as the standard, WE-CBF family of chip bead ferrites. The WE-CBF family provides RMS current ratings, but like nearly all other chip bead ferrites from any manufacturer, no peak or pulse current ratings. In this example, in order to handle a 33 A pulse with steady state specifications multiple WE-CBF family devices would be needed, since the highest RMS current rating in this family is 6 A, for the 1806 or 1812-sized devices. Just one WE-CBF family device, for example the 4 A-rated 742 792 150 with a 1206 case size and rated 80 Ω at 100 MHz would handle the steady state current, but repeated startup transients could lead to failures such as the ones depicted in Figure 6.

Six such devices would be needed for the positive input line and another six for the negative input line, and this is not practical for several reasons: First, chip bead ferrites can be paralleled for continuous currents and their positive temperature coefficient will ensure that they share current more or less evenly. However, such current sharing is neither tested nor guaranteed for short-duration pulse currents. Second, placing several components in parallel with impedance that is dominated by resistance and inductance causes the inductance, the

Figure 6: Melted and burned chip bead ferrites due to overcurrent and overheating

resistance and the impedance to drop, making them far less effective at filtering the desired noise. Third, six components cause high costs and need much PCB space.

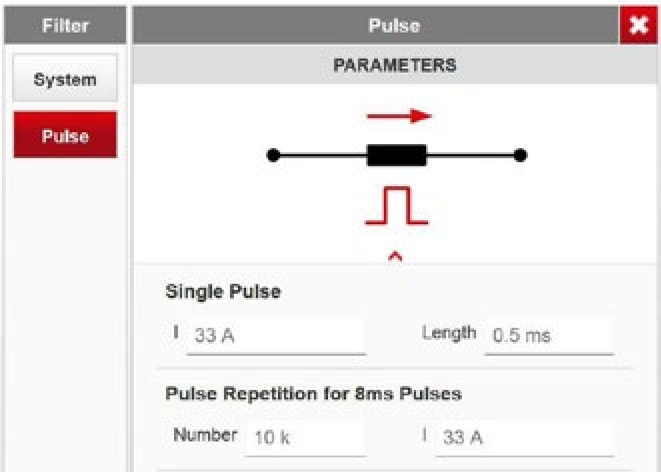

Figure 7: Enter the pulse length, peak current and number of pulses

Select the proper WE-MPSB
In situations where peak currents exceed average current by ratios from 3:1 to nearly 10:1 WE-MPSB are typical area of use. A first pass for selecting chip bead ferrites is to review all parts that can handle the RMS current of 3.7 A.

Peak Current Proof Ferrites for the Input
In our application we are expecting 10 000 switching cycles during lifetime, so 10 000 pulses with 33 A will stress the WE-MPSB of the input filter and needs to be survived. The first step and most comfortable way is to enter these data into the pulse designer of REDEXPERT. There are 9 parts left, which we took all in the product storage for easy comparison.

Validation of Effective Resistance
From the 9 left WE-MPSB we now select the one with the highest resistance (not total impedance) at the noise frequency. In general chip bead ferrites have their highest resistance at the frequency of their highest total impedance, but for other frequencies there is no general approximation possible. The fastest way to find the best part is using REDEXPERT from Würth Elektronik (www.weonline.com/redexpert). As a registered user you can place the chart slider at 170 MHz (see Figure 8), and read directly the resistance values of each part out of the grid, and even sort descending to get the part with highest resistance.

Considering all of above parameters the red highlighted part WE-MPSB 742 792 245 51 seems to be the best suitable component for our application. Its current rating is 4.0 A, and it can withstand about 18 700 pulses of 33 A and 8 ms length. Keeping in mind that this 8 ms is much longer than the initial pulse of 500 µs and the short peak of 100 µs, gives it a plenty safety margin. From all suitable components, it is the one with the highest resistance at 170 MHz.

Pulse-Stable Ferrites for the Output
The output RMS current is the same as the average output current of 8.0 A. Following the same guidelines, there are five candidates rated for greater than 8.0 A:

All five parts can handle more than 10 000 pulses and have more than 8 A rms current rating, so the final selection will require actual EMC testing to determine which part filters the most noise. The smaller parts are less expensive but provide less reduction of noise.

Testing of the selected components
For final lab testing we added the above mentioned WE-MPSB 742 792 245 51 to the input and WE-MPSB 742 792 251 01 to the output. You can easily see, that the green output voltage is now already silent.

Performing radiated EMI scans proves that the chip beads successfully suppress the PARD noise. Especially in the range of the 170 MHz PARD ringing, the EMI is significantly improved.

Further Considerations
Influence of RDC to overall efficiency
The used WE-MPSB 742 792 245 51 has a DC resistance of 35 mΩ, which adds additional conduction losses and therewith reduces the efficiency. The measurements in our lab shown just a slight decrease

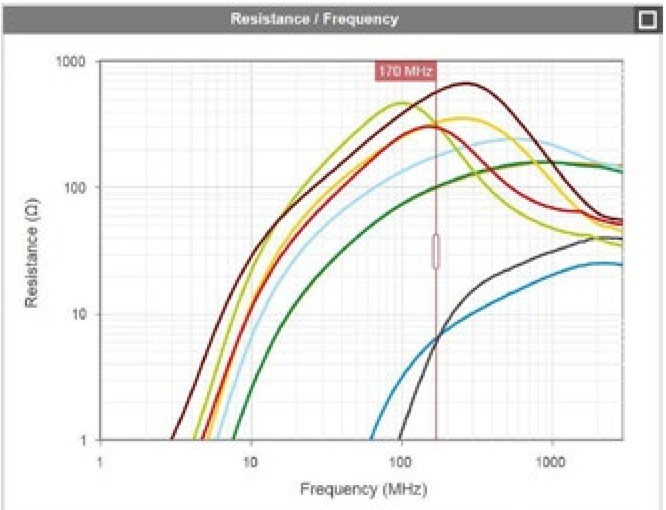

Filters: I_R ≥ 3.70 A | N @33.0 A ≥ 10.0 k | Series = WE-MPSB

	Order Code	Series	Size	Spec	Type	N @33.0 A	Z	R @170 MHz ▾	R_{DC}	I_R
✔	74279224251	WE-MPSB	2220		High Current	18.7 k	250 Ω @100 MHz	298 Ω	12.0 mΩ	4.00 A
✔	74279224181	WE-MPSB	2220		High Current	62.5 k	180 Ω @100 MHz	174 Ω	10.0 mΩ	5.00 A
✔	74279224101	WE-MPSB	2220		High Current	11.3 k	100 Ω @100 MHz	99.8 Ω	5.00 mΩ	7.00 A
✔	74279226101	WE-MPSB	1812		High Current	11.3 k	100 Ω @100 MHz	97.8 Ω	6.00 mΩ	8.00 A
✔	7427922808	WE-MPSB	0603		High Current	15.7 k	8.00 Ω @100 MHz	6.32 Ω	2.50 mΩ	9.50 A
✔	74279221100	WE-MPSB	1206		High Current	27.2 k	10.0 Ω @100 MHz	5.78 Ω	1.00 mΩ	10.5 A

Figure 8: Determine the best suitable WE-MPSB with REDEXPERT leads to 742 792 245 51

of the efficiency from 95% down to 94.5% for each used chip bead ferrite. To investigate it in detail, we calculate the efficiency as follow:

Influence of DC Bias to Impedance Characteristic

As all magnetic parts, also chip bead ferrites follow the physics principle of elementary magnets. With increasing DC current they will continuously saturate up to the level of complete saturation. This saturation effect shifts the impedance curve, as shown in figure 10. The peak inductance value remains almost constant with a drop of just 40% of its initial value, whereas the impedance at lower frequencies significantly drops by rates of up to 90%. In low frequencies the inductive part is dominating, which saturates with DC current. Above the SRF the capacitive part is dominating, which is not effected by the DC current.

Figure 9: Lab Results with Chip Bead Ferrites. The green output voltage is almost silent

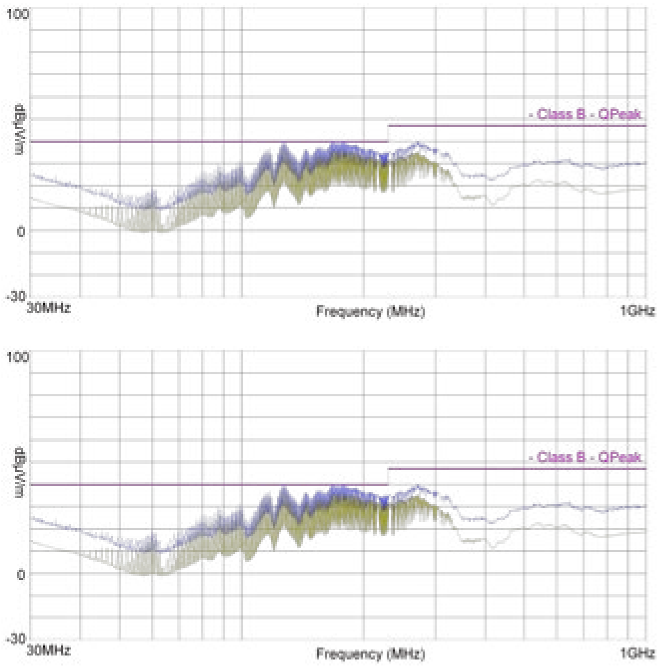

Figure 10: Lab Results of EMC-Testing. The user WE-MPSB chip beads significantly improve the radiated EMI in the range from 100 to 250 MHz

However, if you do your EMI measurements at full load current, this (worst case) impedance shift is already considered in your measurements, and you don't have to care about this effect. Important to know is, that the bigger the size of the chip bead ferrites, the lower is the shift of impedance caused by DC current.

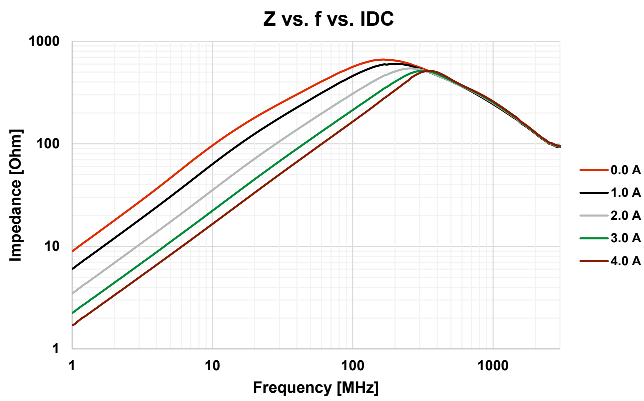

Figure11: Impedance of WE-MPSB 742 792 245 51 with DC bias current from 0A to 4A

Conclusion

Chip bead ferrites are the best components for reducing high frequency noise above 10 MHz. In power supply layouts they must be placed as close as possible to the source of noise which can be the input and output connectors, to properly filter conducted EMI from the input and output wiring harnesses. This prevents conducted EMI from becoming radiated EMI. Being the first components and the last components in the chain exposes chip bead ferrites to heavy transient currents, and circuit designers can now select parts that filter noise with minimal impact to power efficiency and will handle large current pulses with excellent reliability.

www.we-online.com

Control Method for a Reverse Conducting IGBT

When IGBT and diode functionality is combined into a single piece of silicon, a reverse conducting IGBT (RC-IGBT) is created. This allows a standard IGBT/diode-module to be built on a single silicon chip. This results in enhanced current carrying capability without increasing the foot print of the module and – depending on the device technology – allowing the diode´s electrical performance to be influenced by the control state of the IGBT gate. However, in order to manage the losses in the combined RC-IGBT, special control approaches need to be considered.

By Daniel Domes, Infineon Technologies AG

Device Introduction

Reverse conducting IGBTs can be built by partially interrupting the p-doped collector area with n-doped regions. This creates the diode functionality, yet there remains sufficient area for the IGBT to inject minority carriers into the drift region for low forward voltage ($V_{CE(sat)}$).

With this approach, the diode functionality is dependent on the state of the gate control. Devices of this type are designed for hard switching applications, and are known as Reverse Conducting IGBTs with Diode Control (RCDC-IGBT).

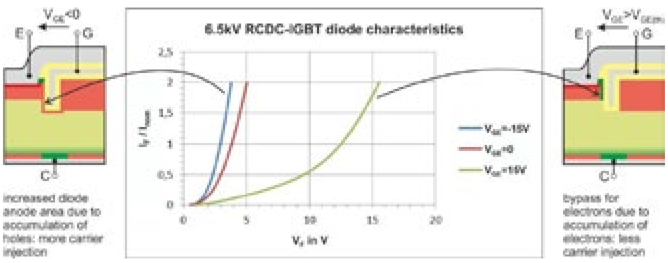

Figure 1: 6.5 kV RCDC-IGBT static diode performance as a function of gate voltage. In cross section: red color is p-type-doped, green color is n-type-doped. T_{vj}=125 °C

Loss Optimal RCDC-IGBT Performance

The RCDC-IGBT gate state has a significant impact on the forward characteristics of the diode. From the static loss perspective, in diode conduction mode the gate needs to be turned off. The lowest VF can be achieved when V_{GE}=-15 V, this is a little higher when V_{GE}=0 V. Since VF corresponds to the carrier density inside the chip, for the lowest dynamic losses and thus lowest Q_{rr}, V_F should be selected to be a high value.

Deciding how to drive the gate in diode conduction mode will depend on the pulse frequency of the application and the ability to desaturate the diode prior to it turning off.

Special Gate Drive Aspects

A gate driver for low loss RCDC-IGBT operation needs to be able to:

- detect the diode conduction mode and prevent turn on of the RCDC-IGBT gate
- desaturate the RCDC-IGBT diode by driving V_{GE} to 15 V prior to diode turn off

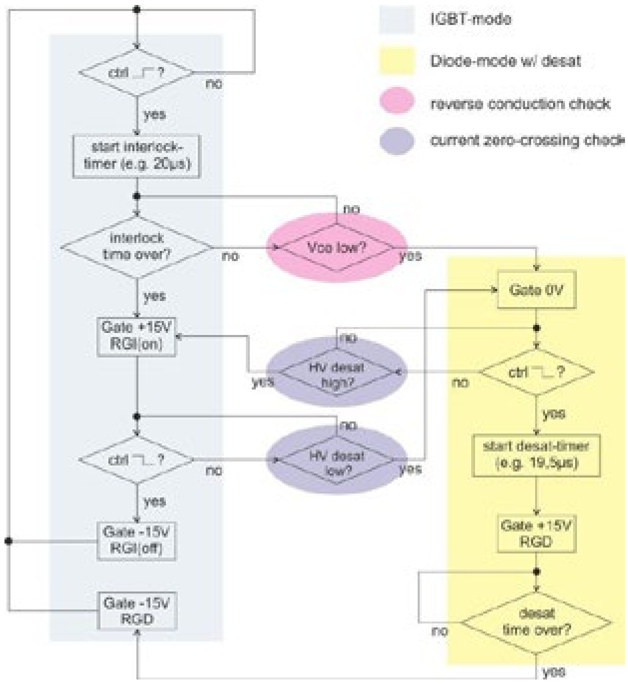

Figure 2: Flow chart of the RCDC gate driver control scheme

- drive V_{GE} to 0 V in diode conduction mode in the case of a typical 6.5 kV inverter pulse frequency and limited diode desaturation time
- detect a load current zero crossing in diode mode and turn on the RCDC-IGBT gate for smooth current transition from the diode to the IGBT of the same switch
- detect the load current zero crossing in IGBT mode and turn off the RCDC-IGBT gate for low loss diode operation

Detect the Diode Conduction Mode

In a classic inverter, a forward conducting IGBT is turned off at the start of the interlock time period. For the opposite diode, this means that first the blocking voltage decreases and then the current starts to rise. Once the interlock time period is over, the antiparallel IGBT gate of the diode is turned on. For an RCDC-IGBT, the turn on of the conducting diode´s antiparallel IGBT needs to be prevented by the gate driver logic.

It is recommended to monitor the V_{CE} of the switch before executing the turn on command from the control side. In this scenario, the voltage across the diode switch is low before the interlock time ends, clearly indicating that the diode is conducting.

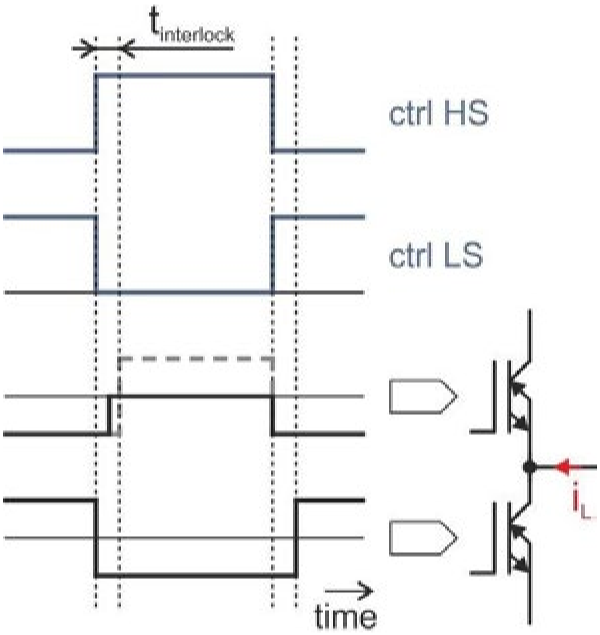

Figure 3: Diode detection without desaturation pulse

For diode desaturation purposes, the interlock time is calculated for each gate driver individually. Consequently, the high and low side gate driver input signals will change at the same time. Falling edges of the control signal are executed immediately, turning off the LS-IGBTs gate. The IGBT turns off normally and the voltage across the high side switch decreases. A voltage detector checks whether the V_{CE} of the high side switch drops below a defined threshold (displayed as “V_{CE} low”). In this case, the high side switch will go into diode conduction mode and the gate (V_{GE}) is switched from -15 V to 0 V as soon as the detector output “V_{CE} low” changes.

The high voltage detector is a simple frequency-compensated voltage divider. In high voltage applications, this circuit is often present in the gate driver stage for desaturation detection purposes and adds no additional parts to the Bill of Material (BOM).

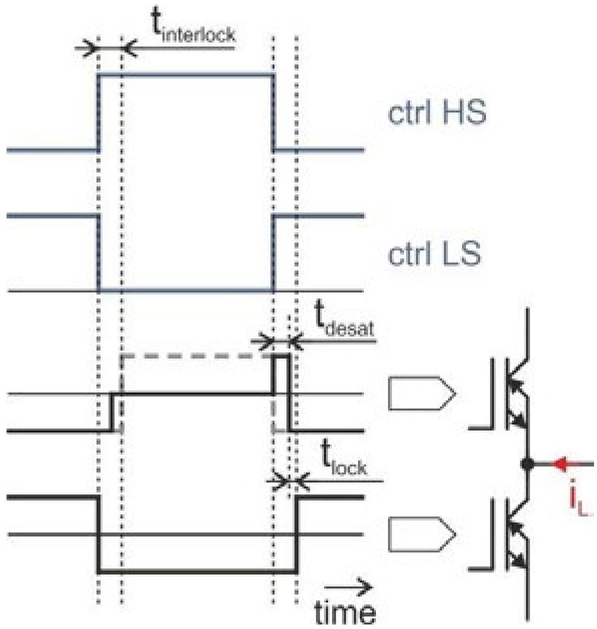

Figure 4: Diode detection with desaturation pulse

Diode Desaturation

Detecting the diode conduction state and keeping the corresponding switch gate in the off-state ensures a high carrier density inside the device thus maintaining low V_F-values. However, for dynamic loss reduction this condition is not desired as high carrier density causes high Q_{rr} and hence high IGBT turn on and diode turn off losses.

If the diode switch gate is turned on before the diode is turned off, the operation point is shifted from a low to a high V_F output curve and the diode carrier concentration is reduced with a strong effect on the dynamic losses. Typical desaturation time for a 6.5 kV RCDC-IGBT is 20 to 100 µs.

For practical implementation, the driver needs to accurately predict the point in time at which the diode turns off. This corresponds to the opposite IGBT turning on, which (based on the signal definitions) is executed after the IGBT switch control signal changes from low to high and the interlock time $t_{interlock}$ is over.

This approach is illustrated in Figure 4. The high side switch diode conduction state was detected and the gate switched to V_{GE}=0. Now, the high side and low side gate input signals change synchronously. The low side gate driver counts the interlock time and when it is over, turns on the low side IGBT.

The diodes switch gate driver creates the desaturation pulse by driving V_{GE} to 15 V. No active switching in the half bridge occurs until the interlock timer is over. The gate driver of the diode switch remains with V_{GE} at 15 V for the desaturation time (t_{desat}). The duration of t_{desat} is shorter than $t_{interlock}$ since the remaining locking time t_{lock} must be added. The locking time should be kept small to prevent the diode saturating again, reducing the effect of the desaturation. A typical value of t_{lock} for a 6.5 kV RCDC IGBT is 0.5 µs.

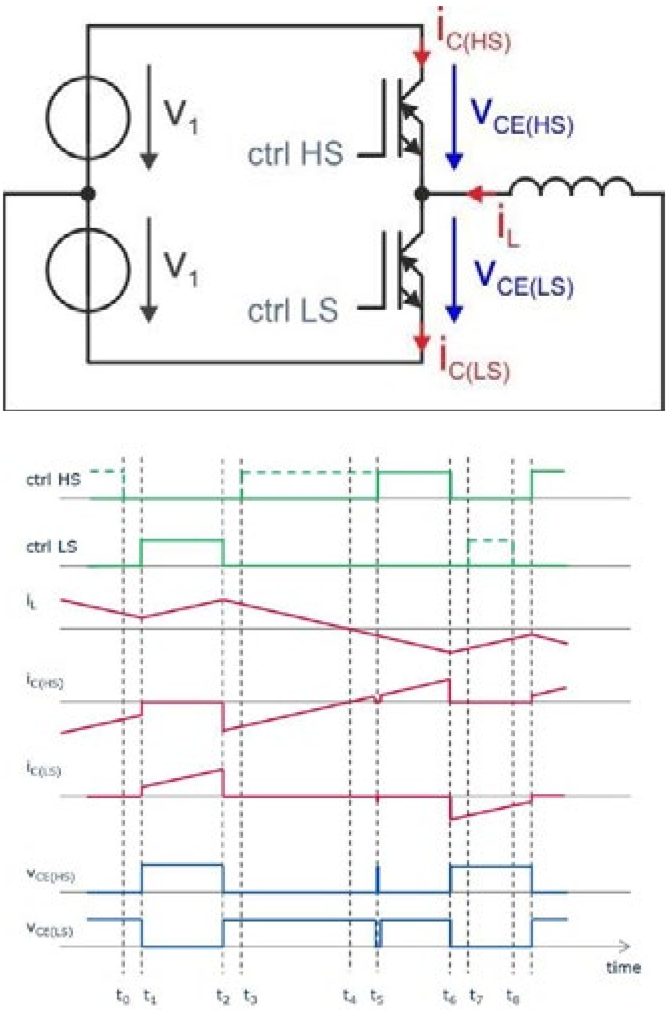

Figure 5: a) simplified RCDC-IGBT half bridge system, b) schematic waveforms for demonstration of load current zero crossing at t4, current IC(HS) goes through the diode for t2 ≤ t < t5 and changes into IGBT for t5 ≤ t < t6

With this approach, the diode desaturation duration corresponds to the maximum interlock time tolerated by the application. A long interlock time ensures best device performance but decreases the dynamic response of the system. Using a very small gate resistor applies the shortest time constants for the desaturation pulse and gives the best desaturation result. In Figure 2 references this resistor as R_{GD}, whereas the nominal gate resistors are named $R_{GI(on)}$ and $R_{GI(off)}$.

Considering a practical 6.5 kV traction inverter system with a frequency of several hundred Hertz and maximum interlock time of 20µs, the RCDC-IGBT performs best if the gate runs at 0 V in diode conduction mode. In this case, the static diode losses are slightly higher than with operation at V_{GE}=-15 V. Total losses are minimized as Q_{rr} is lower than with V_{GE}=-15 V diode operation. For other frequencies and longer desaturation times the optimal operation timing will be different.

Load Current Zero Crossing Approach: Diode to IGBT

If, in a classical inverter approach, a diode is conducting then the load current can change polarity as the antiparallel IGBT is normally turned on via the gate. For an RCDC-IGBT, this situation must be detected and the gate turned on immediately to avoid interrupting the load current.

If a PN-diode conducts and the current decreases to zero, the diode remains flooded with carriers allowing the load current to reverse direction even though the antiparallel IGBT gate is not turned on. In Figure 5a, the load current (I_L) changes direction at t4 but, as $I_{C(HS)}$, still flows through the diode. The high side IGBT gate remains in an off state, as its control signal is low. As soon as the carriers in the diode are depleted by the load current, the voltage across the diode reverses at time t_5. The load current di/dt is small compared to di/dt in a hard switching event.

The gate driver must check for positive V_{CE} while the diode is conducting. As soon as V_{CE} becomes positive, the gate is immediately turned on. The detection circuit must be able to react to low positive V_{CE} voltages, to avoid the output voltage change becoming unnecessarily high. In Figure 5a, at time t_5 this effect is exaggerated. It is advised to use a classical desaturation detection circuit with a high voltage diode chain, a current source and a comparator.

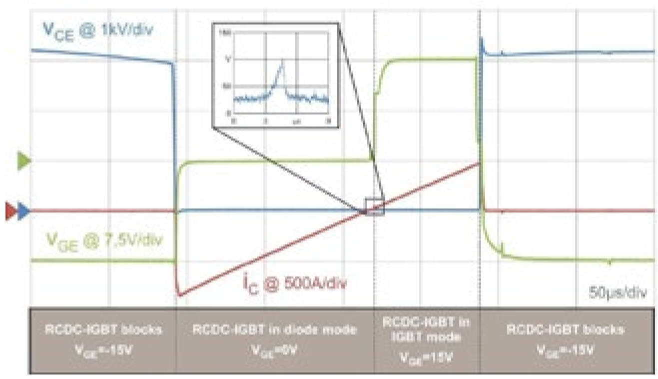

Figure 6: Load current zero crossing, commutating from diode (IC<0) at VGE=0 into the antiparallel IGBT (IC>0) with VGE=15 V; very small increase in VCE (see inset) at the time the detector recognizes the zero crossing event, load current without interruption

Figure 6 shows the load current commutation from the diode to the IGBT by means of RCDC IGBTs in an H-bridge configuration. The gate driver circuit detects the small increase in V_{CE} (inset) and turns on the RCDC-IGBTs gate. The load current changes polarity without interruption or excessive voltage distortion.

0Load Current Zero Crossing Approach: IGBT to Diode

As well as the transition of the load current from the diode to the IGBT, the current can also change its direction to flowing from the IGBT into the antiparallel diode. This does not risk interrupting the load current as the gate remains in an on state and the diode sinks the current. If VGE remained at 15 V, VF would be unnecessarily high and thus the static losses increase until the next control command is received. It is recommended to use the proposed desaturation circuit again, detecting a small VCE voltage across the RCDC-IGBT. Since VF is initially high, the voltage difference in VCE from IGBT to diode conduction also becomes high and can easily be detected.

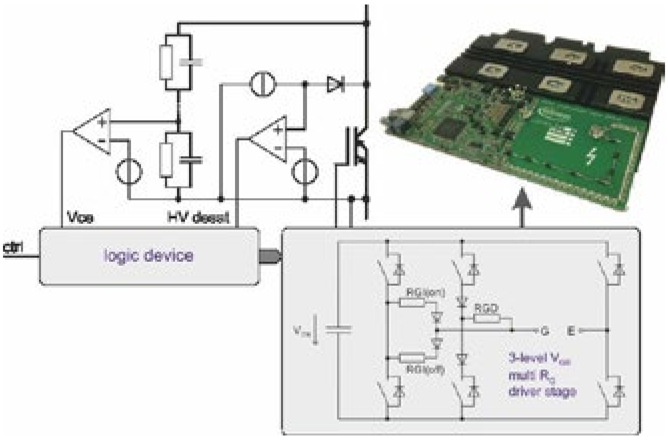

Figure 7: Schematic gate driver circuit for operating a RCDC-IGBT in a conventional inverter system, from the inverter control stage only the ctrl signal needs to be provided, all RCDC-IGBT specific information is generated and processed inside the gate driver circuit.

Drive Scheme

Figure 2 shows the complete RCDC-IGBT gate driver control scheme. The state machine is able to handle all basic RCDC-IGBT gate drive requirements including diode conduction mode detection, diode desaturation, load current zero crossing from diode to IGBT and vice versa.

Figure 7 shows the gate driver used. If IGBT switching is required, the gate resistors RGI(on) and RGI(off) are used. If minimum time constant switching is required to desaturate the diode, a comparatively small RGD is used. The advanced H-bridge concept allows VGE to be driven to 0 V when the diode is conducting.

In high voltage IGBT gate drivers a high voltage divider is commonly used for desaturation detection. The RCDC-IGBT gate driver has a desaturation circuit consisting of a high voltage diode chain, comparator and current source. Logically, three binary input signals “ctrl”, “VCE” and “HV desat” are processed by the state machine.

www.infineon.com/power

Innovative 7in1 IGBT Packages for Scalable and Easy Design of Industrial Drives and Inverters

Industrial drive applications require scalable IGBT modules to simplify the design and to provide the possibility of utilizing the same components like driver boards and bus bars for different inverter power ratings. The Mitsubishi NX-series 7in1 IGBT packages provide such scalable solutions combined with high power density and simplified inverter assembly.

By Thomas Radke and Narender Lakshmanan Mitsubishi Electric Europe B.V

Introduction

Different motor control inverters require different IGBT power module package sizes. Conventionally, for smaller inverter power ratings, the 6in1 IGBT power modules are used. For higher ratings, inverters are conventionally built by using three half bridge power modules. As a result the inverter construction is different for different power ratings, thus the driver boards, bus bars and heatsinks cannot be reused for achieving higher power ratings. This necessitates higher development expenditure alongside the requirement for complicated logistics for the sourcing of new and unique components. In several motor drive applications, reactive power required for the motor operation has to be considered and an additional brake unit has to be incorporated. To address the requirements of scalability and reducing the number of components, the NX-series 7in1 IGBT packages have been developed. The NX-series 7in1 packages include a three phase inverter bridge plus an additional brake chopper IGBT with a current rating between 75A and 300A in the 1200V class.

NX-series 7in1 IGBT Modules

The NX-series 7in1 IGBT modules contain a three phase inverter bridge and a brake chopper as shown in the internal circuit diagram in Figure 1. A thermistor is implemented to monitor the baseplate temperature.

	75A	100A	150A	200A	300A
650V/600V		CM100RX-12A small	CM150RX-13T small	CM200RX-13T small	
1200V	CM75RX-24S small	CM100RX-24T small	CM150RX-24T small	CM200RXL-24S large	CM300RXL-24S1 large
1700V	CM75RX-34SA small		CM150RXL-34SA large		
internal conection		small pkg. (RX)		large pkg. (RXL)	

Figure 1: Line-up and circuit diagram of NX-series 7in1 IGBT Modules

Two different packages were developed in order to cover the whole line-up from 75A to 300A. An inverter with the high power density can be achieved by implementing these current ratings into the 122x62mm² footprint (small pkg.) and the 122x122mm² footprint (large pkg). The 17mm module height is already compatible to other existing standard IGBT power module housings and therefore various compatible rectifier modules from different manufactures are available. To provide full scalability for small and large packages, the same arrangement of power and control terminals are designed. This offers the possibility of using the same components like driver boards and bus bars for different power ratings. This approach - multiple utilization of components is a key factor in minimizing the development effort, time and costs. The separation and the orthogonal arrangements of the dc-terminals (P/N) and the ac-output allows for a simplified inverter construction. In cases where the brake chopper is not required, the unused IGBT can be turned-off by short circuiting the gate and emitter pins. Therefore, depending on the requirement, the 7in1 module can also be easily utilized as a three phase inverter without the brake chopper.

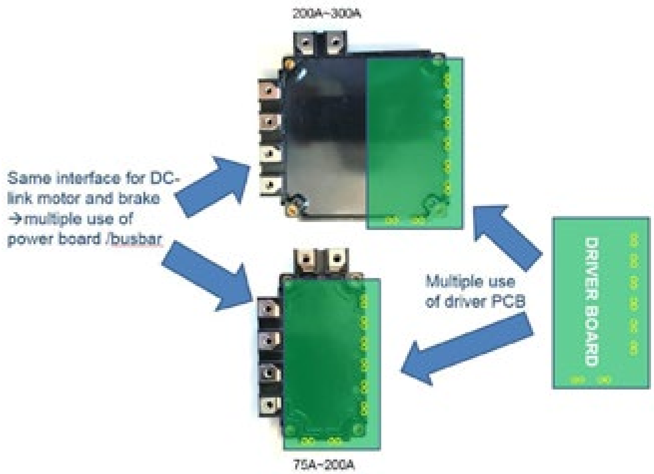

Figure 2 Multiple use of components enabling scalability

Inverter Benchmark

Conventionally, the 6in1 IGBT modules are available in a package with 122x62mm² footprint with a current rating up to 200A. Usually pin terminals are used which limit the current capability of the contacts. An additional limitation is the high heat concentration in air cooled heat sinks due to the small package footprint. Due to this reason, the inverter power rating based on 6in1 modules is limited to about 55kW. Inverters for power ratings above 55kW conventionally employ three half bridge modules with an additional optional brake

chopper module. This change from a compact 6in1 IGBT module to three half bridge modules translates into a heatsink size increase of about 210%, greater complexity in design and an expensive inverter construction. In place of just 1 power module four power modules have to be assembled. The compact NX-series 7in1 package offers a power range comparable to the conventional 6in1 module. The large package version of the NX-series 7in1 module allows for an extension of up to 90kW in the inverter power range. Therefore the large package version of the 7in1 modules offer an intermediate solution between the compact 6in1 / 7in1 modules and the high power half bridge modules. The high power density of the large 7in1 package is achieved by using low loss CSTBT™ IGBT chips combined with a thermally optimized package structure and additionally utilizing the maximum allowed junction temperature of 175°C. A thermal simulation by using Mitsubishi's Melcosim software ([3] publically accessible Ver. 5.3) has been performed and the result is shown in Figure 3. This simulation considers typical conditions for motor control applications with a switching frequency of 4 kHz. The heatsink temperature is considered as 100°C which is typical for air cooled applications. As demonstrated, one 200A / 1200V 7in1 module (CM200RXL-24S in the large package) has performance comparable to three 2in1 modules with 225A /1200V rating (CM225DX-24S1). This alternative 7in1 solution instead of three, (or with brake chopper - four) 2in1 modules reduces the size by about 50% as shown in Figure 4. The 300A / 1200V 7in1 (CM300RXL-24S1) module is able to deliver an even higher performance. The 6in1 module, with 200A rated current has thermal limitations and cannot provide the inverter output power equal to an inverter employing the 7in1 or the 2in1 modules as shown in Figure 3. Additionally an air cooled heat sink design which maintains the sink temperature (Ts) below 100°C will be quite difficult to achieve using the 6in1 module (considering the relatively small foot print of 122x62mm²). Considering an optimistic assessment where a heat sink temperature of 100°C can be maintained, the maximum output current of the 6in1 200A module is limited to 120Arms at an IGBT junction temperature of about 125°C. Considering the same condition (125°C junction temperature), the 7in1 200A/1200V module is able to deliver an output current of about 150Arms. The heat sink design for the baseplate of the 7in1 will be much simpler since the base plate area of the 7in1 module is two times greater than that of the 6in1 module. Therefore it is reasonable to consider operating the heat sink at 100°C while utilizing the large 7in1 module.

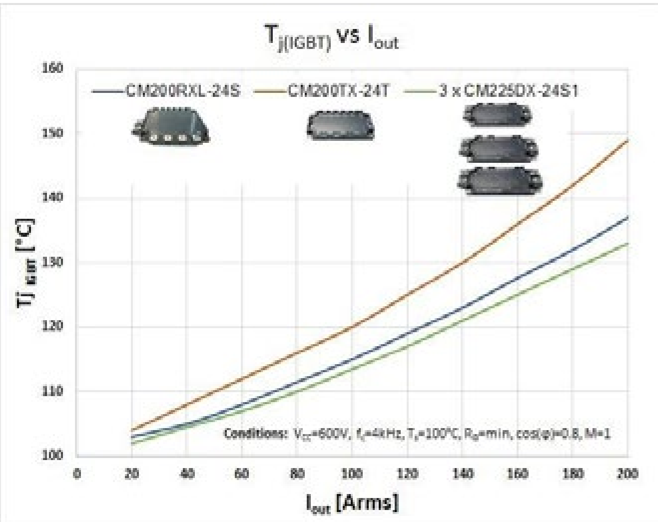

Figure 3: Thermal performance comparison

Conclusion

The NX-series 7in1 IGBT modules provide an optimized package for the requirements of motor control inverters. Taking advantage of this demonstrated scalability offered by the large and small packages, the same inverter construction concept can be utilized for developing an extended inverter series capable of delivering higher power levels. The efforts required for designing and implementing the extension of the inverter power range compared to the conventional approach (using 6in1 modules) is greatly reduced because components like bus bars and driver boards can be reused. The low loss CSTBT™ chips in combination with the superior thermal performance offered by the thermally optimized package structure in the large package delivers a high power density.

Therefore the 7in1 modules offer an optimized solution to design a scalable cost effective motor drive inverter.

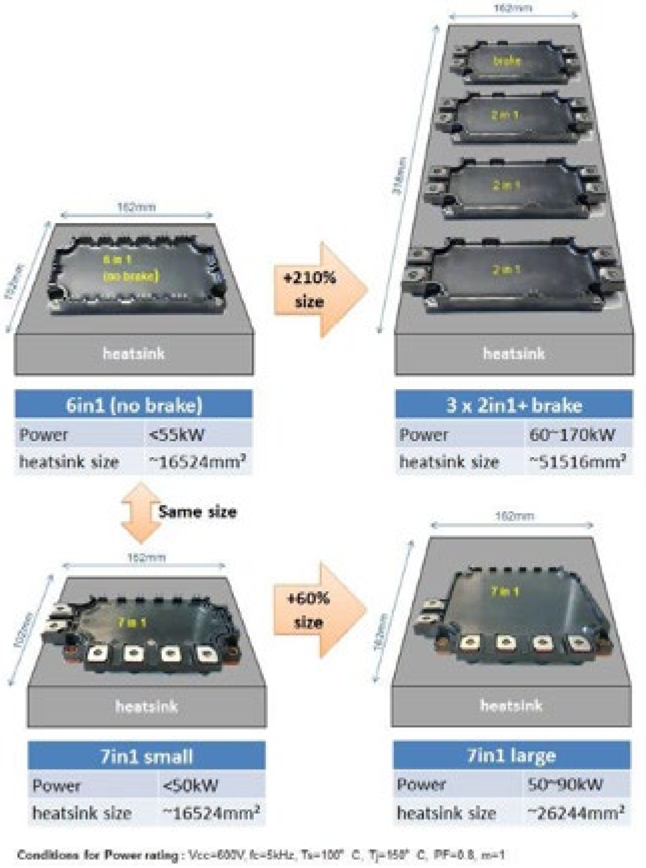

Figure 4: Heatsink size and inverter power comparison

References

[1] NX-series IGBT modules Application Note (http://www.mitsubishielectric.com/semiconductors/files/manuals/igbt_nx_note_e.pdf)
[2] Datasheet CM200RXL-24S (http://www.mitsubishielectric.com/semiconductors/php/oPartProfile.php?FILENAME=cm200rxl-24s_e.pdf&FOLDER=/product/powermodule/igbt/s_series)
[3] Melcosim Version 5.3 (https://www.mitsubishielectric.com/semiconductors/ssl/php/members/login/login_s.php)

www.mitsubishielectric.com/semiconductors

From IGBT to SiC MOSFET

A stone step for smooth replacement in Industrial Applications

Features and benefits of silicon carbide (SiC) have been extensively demonstrated. It has been proven to be the suitable material for high voltage, high frequency power switches. As shown in Figure 1, several SiC based devices have been launched in recent years.

By Dr. Vladimir Scarpa, Field Application Engineer-Power, ROHM Semicondcutor GmbH

In an initial phase, in early 2000s, Schottky barrier diodes (SBD) out of SiC have been implemented. SiC SBDs have been widely used in power factor correction (PFC) stage of single-phase switched mode power supplies (SMPS). They provided very low reverse recovery charge, saving significant amount of dynamic losses in the diode itself and in the counterpart switch. Lately, further applications, like photovoltaic inverters and uninterruptable power supplies (UPS) also adopted SiC SBDs.

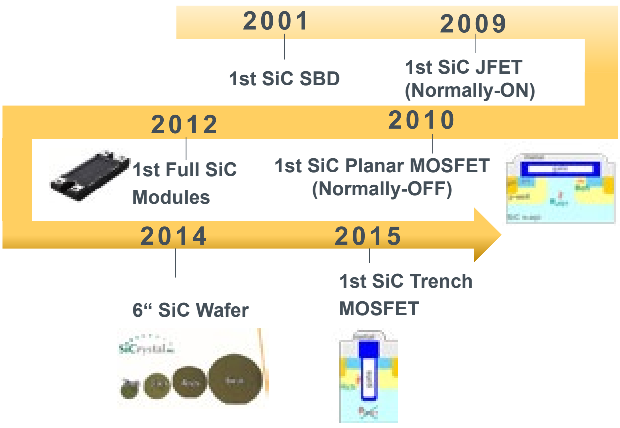

Figure 1: Timeline with main market events in the area of SiC devices

With respect to active switches, in 2010 the first normally-off silicon carbide switches were launched based on MOSFET structure. These devices simplified the gate driver circuitry, and enabled a smoother transition from standard silicon IGBTs and super junction MOSFETs. As consequence, many electronic companies from different application fields started to see SiC switches in their short-term horizon, and began development projects which include SiC MOSFETs. More recently, after extensive qualification procedure in system level, part of these projects turned out into products that were then introduced into the field.

There are however some particularities in the adoption of SiC MOSFETs. In order to get the maximum of their benefits, some changes in system design maybe required. This article will describe some of the issues faced before and during development phase. For each of these issues, some technical hints and, in some cases, practical examples will be shown in order to overcome these issues.

Quality and Reliability

One of the main concerns from development engineers is the reliability of SiC devices. This is understandable, since SiC does not have yet same time on the field than equivalent IGBTs and MOSFETs made out of silicon.

As it can be shown in Table 1, qualification processes of both silicon and SiC devices are following same standards and test conditions.

ROHM also does innumerous further tests to verify the quality and lifetime of its products. Results of these tests can be directly shared with customers. In addition, when customer requires special tests outside standard conditions, they can be performed by ROHM after agreement.

Gate oxide lifetime

As shown in Figure 1, ROHM recently launched the 3rd Gen of SiC MOSFETs, first devices with trench gate, different from planar gate from former generations. This new structure practically eliminates the resistance from the parasitic JFET inside the structure. As a consequence, the amount of on resistance per area unity has been reduced by half [2].

The trench structure adopted by ROHM, also known as U-structure, is shown in Figure 2 (a). As it can be seen, the electrical field around the interface SiC- SiO2 during blocking time is much lower than in the conventional trench structure. This guarantees long lifetime of gate oxide, also for operation voltage levels close to nominal.

Test	IEC Standard	Conditions[1]	Silicon[1]	SiC[2]	Remarks SiC[2]
High Temperature Reverse Bias	60747	1000 h @ 95% $V_{ds,max}$, T_{amb} = 125..145°C	✓	✓	@ 100% $V_{ds,max}$, T_{amb}= $T_{j,max}$ =175°C
High Temperature Gate Bias	60747	1000 h @ ±$V_{GS,max}$, T_{amb}= $T_{j,max}$	✓	✓	--
High Humidity High Temperature Reverse Bias	60068-67	1000 h @ $V_{ds,max}$= 80V 85% RH, T_{amb}= 85°C	✓	✓	$V_{ds,max}$=100V
High Temperature Storage	60068-2-2	1000 h @ $T_{STG,max}$	✓	✓	--
Low Temperature Storage	60068-2-1	1000 h @ $T_{STG,min}$	✓	✓	--
Thermal Cycle	60068-2-14	100 cycles $T_{STG,max}$ - $T_{STG,min}$	✓	✓	--

1 Based on industrial standard tests for product qualification, as in „Semikron Application Manual“ [1]
2 From ROHM qualification of discrete parts, following JEITA ED-4701.
Table 1: Qualification tests of switches based on silicon and SiC materials.

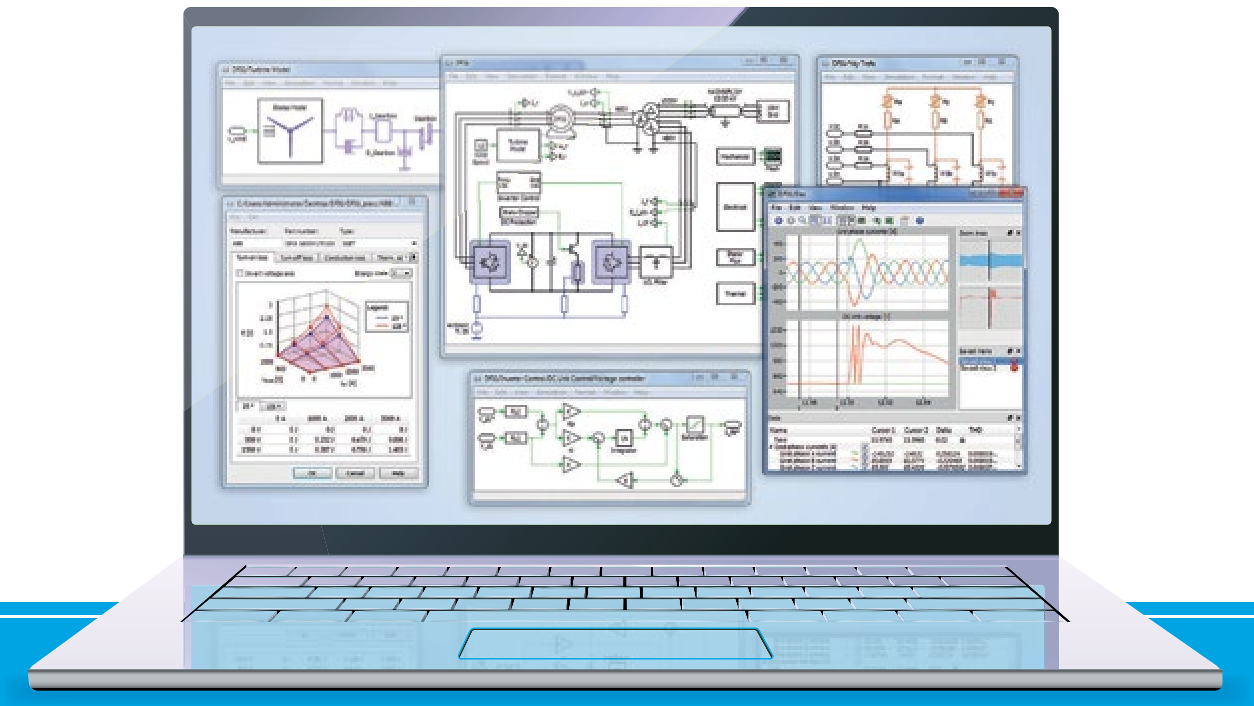

In order to turn the MOSFET on, voltage is applied between gate and source. As consequence, electrical field occurs inside the gate oxide. In order to predict the lifetime of gate oxide, an accelerated test is performed, where higher voltage is applied to the gate. By collecting certain amount of points with different gate voltages, it is possible to extrapolate the gate oxide lifetime when typical gate voltage is used. Figure 3 depicts results from accelerated test of 3rd Gen SiC MOSFET from ROHM. It is possible to see that, for recommended gate values, lifetime of gate oxide is expected to be much longer than typical requirements industrial applications.

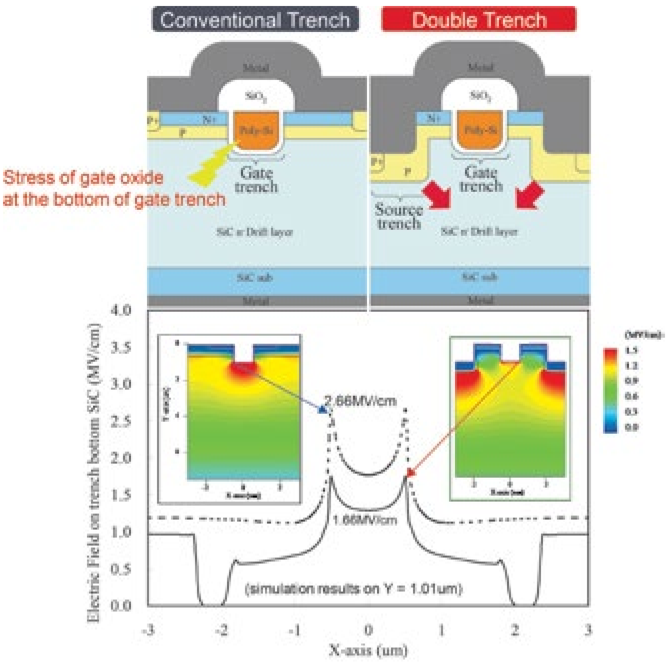

Figure 2: Double trench structure and simulated electrical field, compared to conventional trench

Considering further events, like short-circuit and avalanche, they have been proved through laboratory tests of SiC MOSFETs at ROHM. Definition of parameters like short-circuit withstand time (SCWT) and avalanche energy is now under preparation.

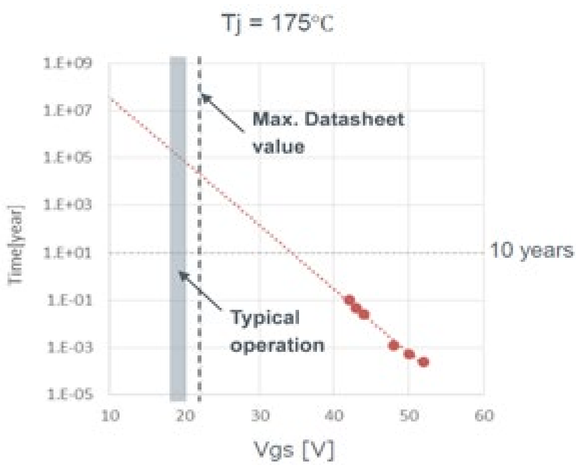

Figure 3 – Accelerated gate oxide lifetime test of 3rd Gen SiC MOSFET from ROHM, at Tj=175 °C.

In the meantime short-circuit and avalanche shall be avoided, or solved in system level. This is already done for instance with silicon IGBTs, that inherently do not have avalanche robustness. Moreover, some ultrafast IGBT devices have also none or very reduced SCWT. Nonetheless, they have been widely used in industrial applications.

Robustness against Cosmic radiation

The phenomenon of cosmic radiation has been well described in literature [3]. It can represent a critical issue, especially for applications which operate at voltage levels very close to the nominal voltage of the switch. This is the case for instance of photovoltaic inverters and UPS systems.

Failures due to cosmic radiation occur randomly during the lifetime of a semiconductor device. In accelerated tests, it is possible to predict the failure in time (FIT) rate of a device. This value is normally increasing exponentially with the blocking voltage, as shown in the test results in Figure 4. It shows the comparison between devices from silicon, namely IGBTs and MOSFETs, and SiC MOSFETs from ROHM semiconductor, all rated for same current and voltage. It is possible to observe that SiC MOSFETs have a FIT rate up to 3 orders of magnitude lower than silicon counterparts.

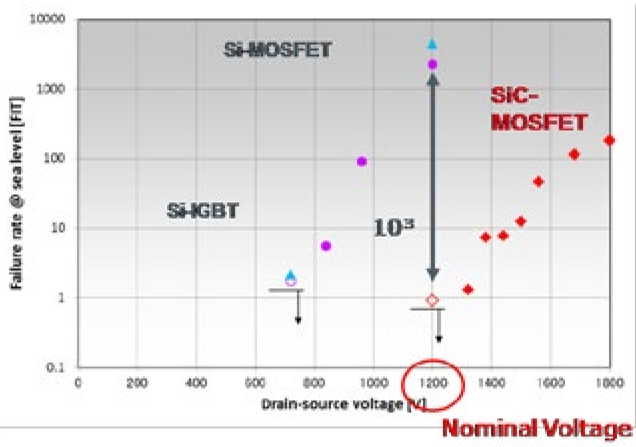

Figure 4 - FIT rate due to cosmic radiation for same current, same voltage rated devices from silicon (IGBTs and MOSFETs) and SiC MOSFETs. [3]

The reason of this huge improvement is due to some characteristics of SiC MOSFETs, which guarantee their robustness against cosmic radiation. Among them there is the smaller chip area of the device for same current rate and the higher margin of electrical field during blocking state, with respect to breakdown field of the material.

Price-performance ratio

It is well known that the production cost of silicon carbide wafers is comparatively higher than those out of silicon. This is related, among other factors, to the energy involved in the growing process. This cost difference is expected to reduce sensitively in next years, driven by factors like:

- Increase of wafer size;
- Reduction of defect density on wafer level and those caused by processes;
- Economy of scale, following the increasing adoption of SiC devices.

Even facing higher price per device, it is already possible to build up systems based on SiC which offer economic advantages. Next section will discuss two examples of systems whose cost can be reduced by introducing SiC switches.

Auxiliary power supply

Industrial systems need an auxiliary power supply, which provides

Fuji Electric's X-Series - 7G IGBT
with improved package technologies

Main features

- Improved switching performance
- Reduced on-state voltage drop
- Enhanced power cycling capability
- Increased output power
- $T_{j(op),max}$=175°C *(except Small IPM=>150°C)*
- Downsizing package
- Expanded current rating

Downsizing package
Example 75A PIM-IGBT

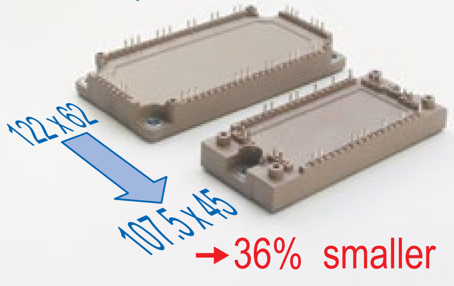

Upgrading current rating
Example 50A PIM-IGBT

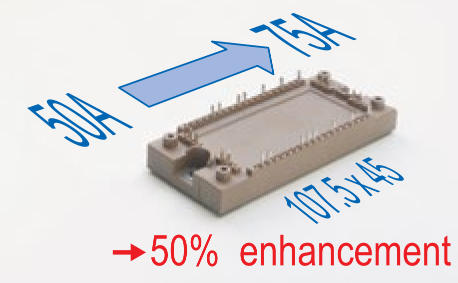

Comparison

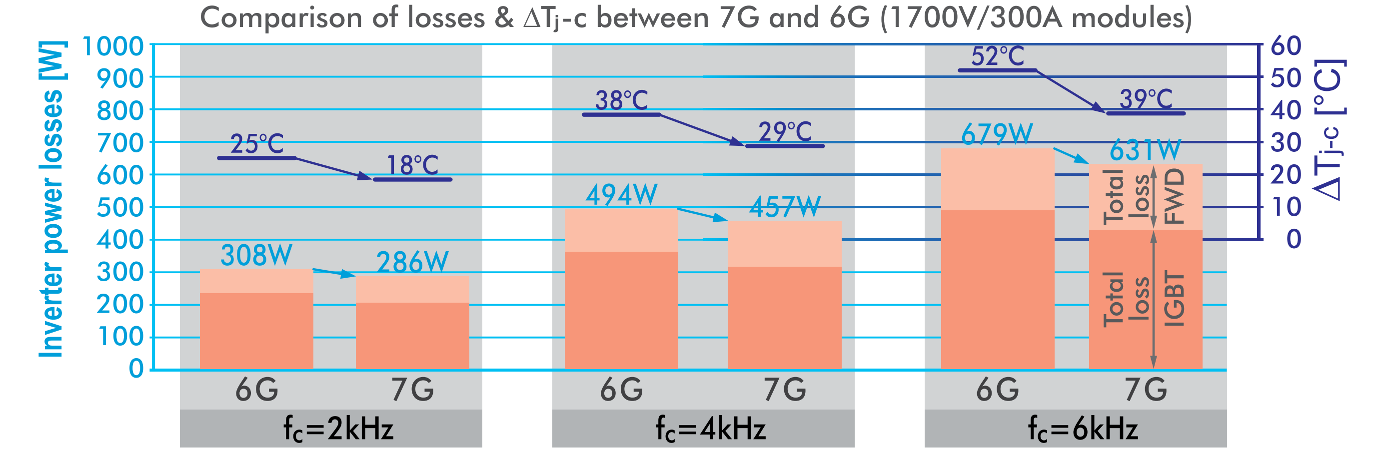

Line-Up

Small IPM

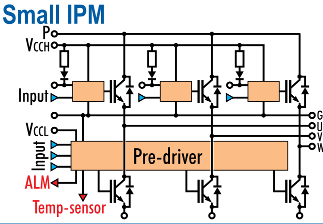

26x43mm
600V: 15-35A

6-Pack

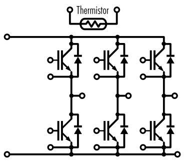

62x122mm
1200V: 100-200A

Dual XT

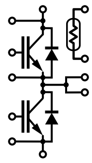

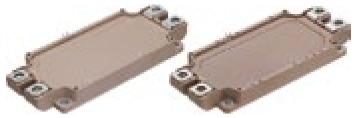

62x150mm
1200V: 225-800A
1700V: 225-600A

Small PIM

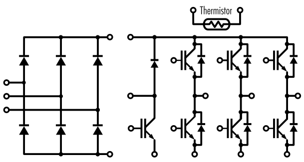

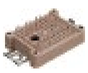

33.8x62.8mm
650V: 10-30A
1200V: 10-25A

56.7x62.8mm
650V: 50A
1200V: 15-35A

PIM

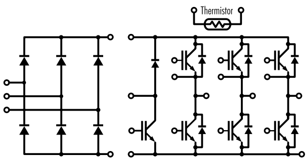

45x107.5mm
650V: 50-100A
1200V: 35-75A

62x122mm
650V: 75-150A
1200V: 75-150A

Standard 2-Pack

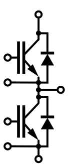

34x94mm
650V: 150-200A
1200V: 100-200A
1700V: 75-150A

45x92mm
650V: 300-400A
1200V: 200-300A

62x108mm
650V: 400-600A
1200V: 300-600A
1700V: 150-400A

80x110mm
650V: 600A
1200V: 450-600A
1700V: 300-400A

High power 2-Pack

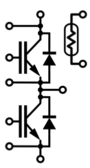

89x172mm
1200V: 900-1200A
1700V: 650-1200A

89x250mm
1200V: 1400-1800A
1700V: 1000-1800A

Fuji Electric
Innovating Energy Technology

Fuji Electric Europe GmbH
Goethering 58
63067 Offenbach/Main-Germany

Fon +49(0)69-66 90 29 0
info.semi@fujielectric-europe.com
www.fujielectric-europe.com

energy required to feed peripheral components, like micro-controller, gate drivers, fans, LCD displays, etc. For this application, Flyback converter is typically used. In 3-phase systems, where the input voltage can reach 480 Vac phase-to-phase, devices with blocking voltages above 1000 V are normally required.

Before availability of SiC switches, auxiliary systems were implemented with silicon MOSFETs and BJTs of up to 1500 V blocking capability. These devices present big chip area and still high on resistance. This results in high static and high dynamic losses, making the use of heat-sinks almost mandatory and increasing system cost.

With the use SiC, 1700 V rated MOSFETs offer on-resistance as low as 1 Ω. In addition, due to small chip size, dynamic losses are sensitively reduced. As a consequence, it is possible to operate at switching frequencies up to 120 kHz - thus reducing transformer size, - and still avoid the use of any heat-sink. This is demonstrated in [4], which also introduces the quasi-resonant controller for Flyback converters from ROHM.

Industrial power supply

Switched mode power supplies (SMPS) are widely used in industry to feed DC loads, like low voltage batteries. These systems are typically composed of two stages: an AC-DC rectifier followed by an isolated DC-DC converter.

Figure 5 shows two industrial power supplies, disposed side by side. The system on the left is based on silicon IGBTs. It operates with switching frequencies of 20 kHz (AC-DC) and 40 kHz (DC-DC). Its achieved efficiency is 83% at the nominal power of 20 kW.

On the right side there is the new system, based on SiC MOSFETs. The much lower dynamic losses of these devices allowed switched frequency increase. The AC-DC stage operates at 40 kHz, and the DC-DC at 150 kHz. Considering all the consequent reduction in magnetic components, total system volume is 40 % smaller than reference system. Furthermore, there was no system cost increase, while the nominal power could be increases 30%, up to 26 kW.

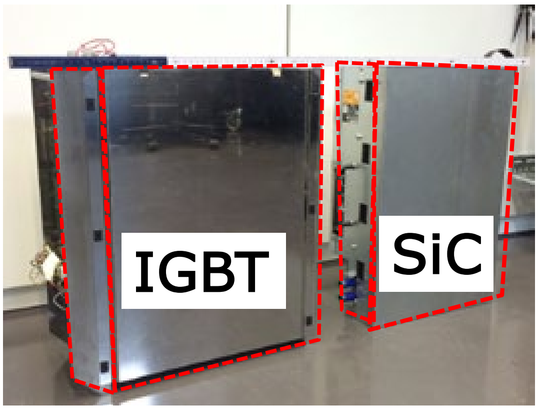

Parameter	Si	SiC	Factor
Frequency AC/DC	20 kHz	40 kHz	2
Frequency DC/DC	50 kHz	150 KHz	3
Power	20 kW	26 kW	1.3
Efficiency	83%	93%	2.5 losses
Cost	100%	100%	1
Volume	100%	60%	0.6

Figure 5 – comparison between SMPSs made out of silicon IGBT (left) and SiC MOSFETS (right). Table aside shows circuit parameters and most important achievements with SiC based system.

Electromagnetic Compatibility

SiC switches is to allow high frequency, high speed switching. This kind of operation results in very low dynamic losses, but can also bring some challenges in accomplishing electromagnetic compatibility (EMC) requirements.

The standard CISPR11, - and specially its "B" version, dedicated to grid connected systems – establishes limits for the electromagnetic interference (EMI) in the frequency range starting from 150 kHz. Frequency range and emission limits in dBμV are depicted in Figure 5.

Let a photovoltaic inverter be considered, operating under 20 kHz, typical frequency for silicon IGBTs above 600 V blocking capability. The squared waveform voltage coming from the inverter needs to be filtered before reaching the grid. This waveform can be described according Fourier transformation as a series of sinusoidal waves, whose frequencies are the fundamental i.e. 20 hHz, and the odd harmonics, i.e. 60 kHz, 100 kHz, and so on. It is possible to demonstrate then, that the first frequency to fall into the regulated range is the 9th harmonic, which is naturally damped by almost 20 dBμV. This has been well depicted in [5], and is reproduced in Figure 6.

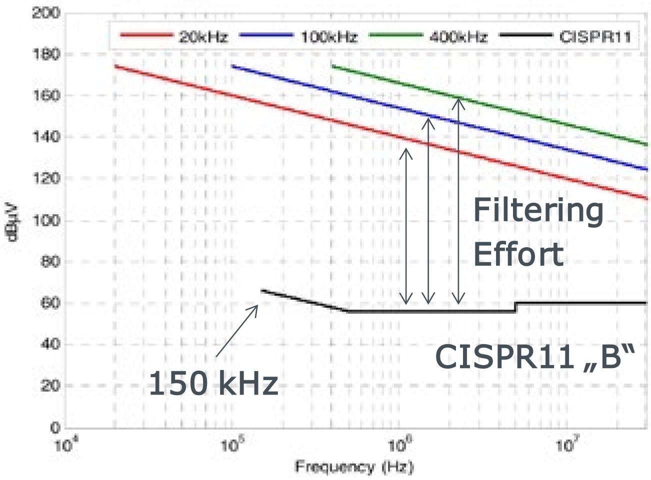

Figure 6 – Filtering effort for a grid-connected photovoltaic inverter, for different switching frequencies. As reference, the standard CISPR11 "B" [5] modified.

If frequency is now increased to f.i. 100 kHz, the 3rd harmonic will already fall into the regulated area. As a result, there will be around 18 dBμV less natural damping, which must be compensated by passive filter. In order to avoid system cost increase due to extra filtering effort, it is recommended to operate at switching frequency just below 50 kHz (3rd harmonic out of regulated range) or still slightly below 150 kHz (1st harmonic out of regulated range).

If higher switching frequency is desired, according to [5] the next sweet spot will fall above 400 kHz. Above this value, the size of the passive filter will be again smaller.

Parasitic elements as stray inductances, capacitances and resistances from the surrounding may block operation at such high frequencies. They may come, for instance, from packaging, isolation foils, capacitor series resistance, PCB design, among others. In order to overcome this issue, resonant topologies maybe an interesting option. Circuits like series resonant LLC [6] avoid hard switching operation, reducing thus the emitted electromagnetic radiation. In addition, switching speed can also be controlled. This makes the voltage waveform more trapezoidal-like, and increases the natural dumping of the high frequency harmonic content.

Conclusion

SiC MOSFETs brings significant technical improvement with respect to equivalent silicon devices. In addition, SiC MOSFET devices have already achieved required quality level for most common industrial applications. This is proven by results of standard qualification process, and accelerated tests of gate oxide lifetime. In addition, SiC MOSFETs have improved robustness against some events, like cosmic radiation.

Economic advantages brought by SiC MOSFETs have also been demonstrated in some applications, even with the price difference as it is today. In near future, factors like wafer increase and economy of scale will decrease price of SiC devices and make it more and more competitive and practically all applications inside electronic industry.

References

[1] „Semikron Application Manual“, 2nd edition, page 117. Available online https://www.semikron.com/dl/service-support/downloads/download/semikron-application-manual-power-semiconductors-english-en-2015

[2] “ROHM Semiconductor shows 3rd Generation SiC MOSFETs with Trench Gate Structure”. Available online http://www.powerguru.org/rohm-semiconductor-shows-3rd-generation-sic-mosfets-with-trench-gate-structure/

[3] Source : H. Asai, I Nashiyama, K Sugimoto, K Shiba, Y Sakaide, Y Ishimaru, Y Okazaki ,K Noguchi, T Morimura “Tolerance Against Terrestrial Neutron-Induced Single-Event Burnout in SiC MOSFETs” IEEE Trans. Nucl. Sci., vol.61, 2014.

[4] Application Note “BD768xFJ-LB series Quasi-Resonant converter Technical Design”. Available online.

[5] A. C. Schittler, D. Pappis, P. Zacharias: “EMI filter design for high switching speed and frequency grid-connected inverters”, EPE 2016.

[6] Y. Nakakohara, et al “Three Phase LLC Series Resonant DC/DC Converter Using SiC MOSFETs to Realize High Voltage and High Frequency Operation”, IEEE Transactions On Industrial Electronics.

Author:

Dr. Vladimir Scarpa

Field Application Engineer-Power

ROHM Semicondcutor GmbH

www.rohm.com

Reverse Conducting IGCT Platform optimized for Modular Multilevel Converters (MMC)

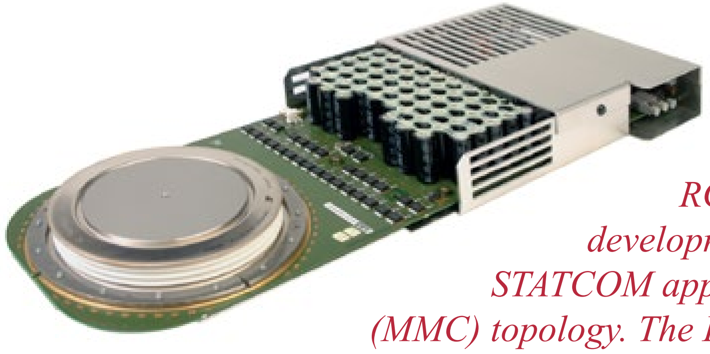

ABB has developed a new Reverse Conducting Integrated Gate Commutated Thyristor (RC-IGCT) platform and recently the first products such as the 4.5kV / 3kA and a 6.5kV / 2.15kA RC-IGCT have reached the production stage. The development was driven by high voltage converters for STATCOM applications with Multi-level Modular Converter (MMC) topology. The IGCT was chosen because of the low switching frequency with subsequent potential for low losses, as well as the straightforward inclusion of redundant cells for continuous operation after faults.

By Tobias Wikström, ABB Switzerland Ltd - Semiconductors

Performance / On-state

In an MMC application with comparably low switching frequency, the on-state losses are crucial for the system's efficiency. This is one of the most important advantages of the IGCT over the IGBT for this type of application.

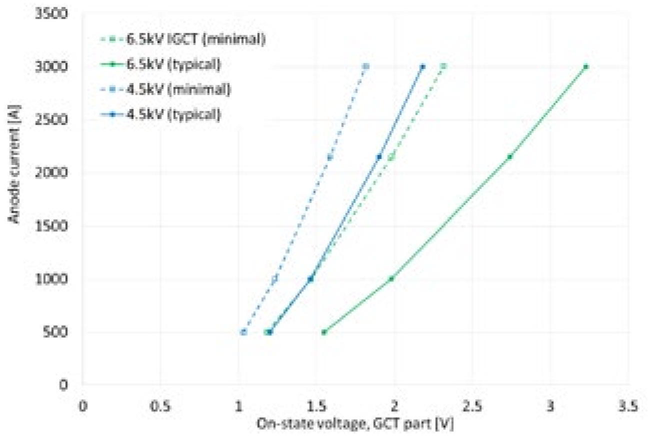

Figure 1: IGCT on-state voltages for the 4.5kV and 6.5kV IGCTs. The "minimal" curves are what can be achieved without reducing the carrier lifetime

Thermal

Figure 2 shows a simulation of the thermal response of the developed RC-IGCT compared to the existing platform, at the same power level and using the same color scale for the temperature. The new housing omits the pole-piece trenches needed for conveying the gate signal, and those that incorporate the gate spring system over the active area. This has a profound effect on the maximal junction temperature and especially on surge-current capability. Additionally, the wafer was shifted from the axial center of the package, closer to the anode thermal contact which reduces RTH for the device in general.

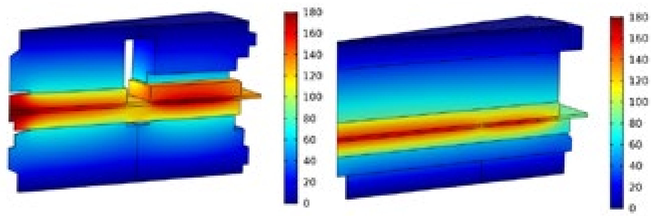

Figure 2: Output of thermal simulations of the existing (left) and new (right) RC-IGCT technology at identical power density in the active parts. The maximal silicon temperature is 30°C lower using the newly developed package. The color scale indicates the temperature in °C. The heated (reddish) parts is the silicon device, stacked with molybdenum disks and copper pole-pieces. The cathode sides are directed upwards. Both devices are stripped of thermally irrelevant features, such as flanges, rubber, plastic and ceramic parts.

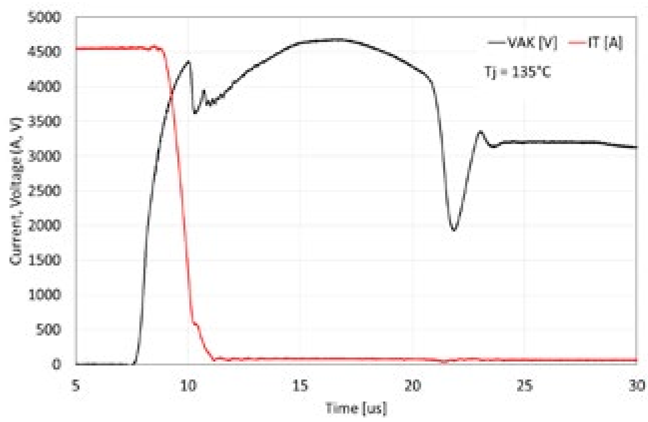

Figure 3: Sample waveforms from a 4.5kV RC-IGCT, switching off above 4500A at 3.2kV DC-Voltage

Maximal controllable current

The HPT$^+$ platform was incorporated in the new RC-IGCT for improving the high-temperature current controllability. Together with the improvements in gate-circuit impedance – it was reduced by more than a factor of three – the current-handling capability of the system could be significantly improved. Both the diode and GCT parts can be switched much beyond the SOA-specification at 135°C as shown in Figure 3. At lower junction temperatures, the maximum controllable current increases to over 6 kA.

The diode is extremely robust. It is governed by the current rate of change during reverse recovery. In IGCT applications, the dI/dt is moderated by dimensioning a reactor together with the maximal cell voltage. For an appropriate selection of cell DC voltage and size of the choke, there is almost no limit to how much forward current the diode can recover from. For these new products, the limit has not even been established exactly, because it so much higher than the specified requirement, that the actual capability is of academic interest only.

Snap-off

A challenging task is to ensure nice behavior at low forward current and high cell voltage over the whole temperature range. The most straight-forward way to improve the switching behavior is to increase the diode thickness, albeit with obvious loss drawbacks. It is particularly important for RC-IGCTs to minimize the diode thickness, due to the integration of both the switch and the diode on the same Silicon wafer. In order to keep snap-off within acceptable limits at a maximal cell voltage of 3.2kV, it was necessary to use a double proton peak for the 4.5kV device. The 6.5kV device prevailed with the single proton peak, with the maximal cell voltage of 4.6kV.

Reliability

As a new device platform, the devices have successfully passed the full range of accelerated reliability testing such as temperature- and load cycling. Hence, ABB is confident that the newly developed technology platform will display the same excellent reliability track-record as its predecessor.

Application

Including an adequately large number of levels in an MMC system leads to a virtual disconnection of the higher-order harmonic output from the switching frequency of the semiconductors. In theory, this can be as low as the output's fundamental frequency, which is 50 or 60 Hz in grid applications. In contrast, for inverter topologies with fewer levels, the harmonic content decreases with increased semiconductor switching frequency. The possibility of low switching frequency favored the selection of the IGCT as the inverter's main switch, thanks to its inherent low on-state voltage compared to the IGBT. Another significant advantage of the hermetic press-pack IGCT is that it can potentially handle large fault currents without rupturing. Hence, choosing the IGCT also facilitated securing the cell integrity, including safety of equipment, at very low extra effort and cost.

Figure 4: The Power-Electronic Building Block containing two MMC cells with four RC-IGCTs each

Design

The existing RC-IGCT platform was developed further as both the size of the diode as well as the current handling capability needed increasing for the intended application. A positive side-effect of platform development is the opportunity to review all design aspects. In that endeavor, it was possible to improve on existing thermal bottlenecks that impede particularly the surge-current capability. One of the basic requirements was maintaining the backwards mechanical compatibility to the existing platform. As a result, the new device is identical on the outside, with the same outer dimensions as its predecessor.

The incorporation of an outer ring gate structure in combination with the integration of HPT$^+$ technology on the RC-IGCT platform addressed both future requirements on current handling capability as well as performance at high junction temperatures. The gate circuit impedance was reduced further by wrapping the gate leads close to the cathode pole-piece. The gate contact was moved to the periphery of the device. The move increases the area consumption of the gate contact infrastructure by necessity, if nothing else is changed. To counteract the loss of active area, the centering tolerance of the gate contact on the wafer was much improved. Thus, despite the new contact has a larger diameter, the space consumption for the gate infrastructure could be reduced. Combined with increasing the maximal device diameter capability of the production facility, the active area could be significantly increased without increasing the size of the raw silicon wafer. All of the active area gain was given to the integrated diode, which almost doubled in size. Nevertheless, the improvements in wafer technology, lowering the gate circuit impedance and removing thermal bottlenecks, the IGCT performance could be improved too, without increasing the size of the IGCT part.

The 4.5kV diode receives local lifetime control in two axial positions; the 6.5kV in just one position, due to the switching behavior at low current and high voltage. The double-position lifetime control has a drawback: it limits the minimal on-state that can be achieved, so it will be a target for future developments to incorporate a different technology, for example FCE, to improve the switching behavior of the 4.5kV device.

Conclusion

A 4.5kV / 3kA and a 6.5kV / 2.15kA RC-IGCT optimized for low frequency applications, such as grid applications employing the MMC topology. In order to fulfil the requirements, a new technology platform for RC-IGCTs was developed. This platform will serve as the base for future technology large area IGCTs from ABB, also for applications with higher switching frequency.

www.abb.com/semiconductors

About the author

Tobias Wikström has developed power semiconductors for ABB since 2001. As a matter of course, he has specialized on IGCT technology, and was the development project manager for the new RC-IGCT platform until its transfer to production.

Digital Telemetry & Programming

3-18V, 12A Regulator with I²C

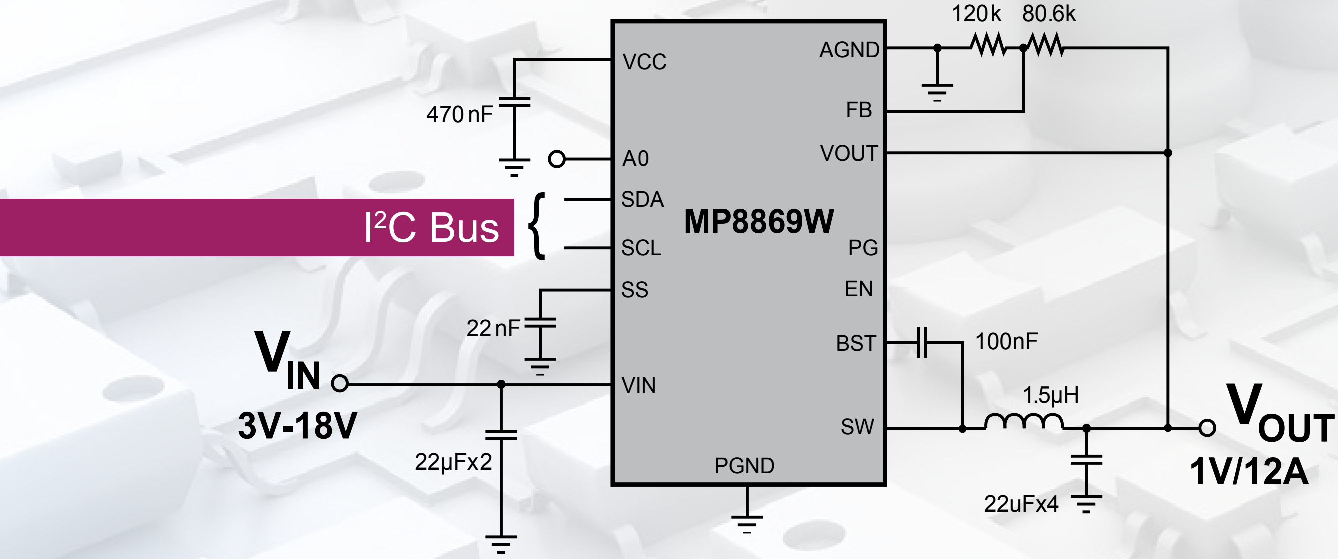

Key Highlights

- 5% Accuracy Output Voltage and Output Current Monitoring
- Programmable Current Limit
- Programmable Frequency
- Selectable PWM/PFM Mode
- 1% Internal Reference Accuracy
- I²C Programmable Output Range from 0.6V

Applications

- Enterprise SSDs
- Networking
- Servers
- Set-Top Boxes
- Smart TVs

MonolithicPower.com

Follow us:

MPS®

Simple, Easy Solutions™

Technology Trends Raising Power-Conversion Efficiency

The latest advances in superjunction MOSFETs and silicon-carbide rectifiers give designers extra freedom to optimise performance and efficiency in cost-sensitive power-conversion applications

By Michael Piela, Toshiba Electronics Europe GmbH

Power Supply Design Demands Efficiency Gains and More
In the drive to continue increasing energy efficiency in switching power-conversion systems such as PFC and switching power supplies, superjunction MOSFETs and wide-bandgap silicon-carbide (SiC) diodes have become favoured solutions for energy-conscious designers. Both technologies have allowed smaller die sizes in relation to key parameters such as MOSFET on-resistance and diode reverse voltage, enabling designers also to reduce circuit size and increase current density. As market adoption of these device technologies continues to grow, new demands are coming to the fore, such as improved noise performance.

Reducing electromagnetic noise emission is desirable in high-end power supplies for equipment such as LCD TV, LED lighting, medical power supply, notebook power adapters and power supplies for tablets. Resonant switching topologies, such as the LLC converter with zero-voltage switching, are popular for these types of applications for their inherently low electromagnetic emissions. Primary-side switching in an LLC circuit as shown in figure 1 (MOSFETs Q1 and Q2), is often now handled by superjunction transistors to achieve a compact and energy-efficient power supply.

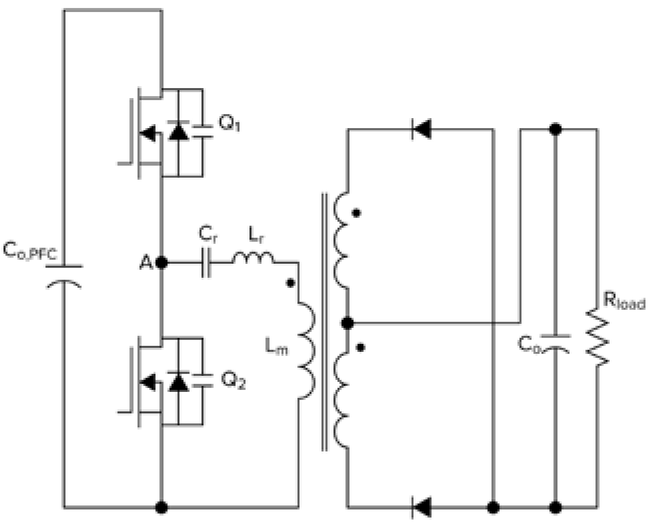

Figure 1: Primary-side superjunction transistors boost the efficiency of high-end LLC-resonant PSUs.

Superjunction Transistor Progress
The superjunction MOSFET has enabled power supply designers to benefit from significantly lower conduction loss for a given die size than is achievable using conventional planar silicon MOSFETs. Because the device architecture also allows low gate charge and capacitance, superjunction MOSFETs also exhibit lower switching losses than conventional silicon transistors.

Figure 2a shows the structure of early superjunction devices, which have traditionally been fabricated using a multi-epitaxial process. Rich doping of the N-region illustrated allows much lower on-resistance than is achievable in conventional planar transistors. The P-type regions bounding the N channel are architected to achieve the desired breakdown voltage.

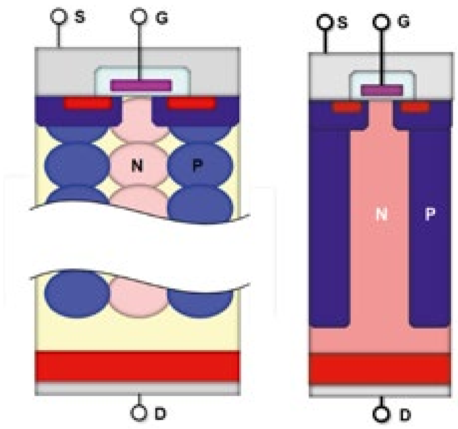

Figure 2a: Multi-epitaxial superjunction MOSFET.

Figure 2b. Single-epitaxial MOSFET.

The N- and P-type structures of these devices have been fabricated using multi-epitaxial processes that have resulted in dimensions that are larger than ideal and have an associated impact on overall device size. The nature of the multi-epitaxial fabrication also restricts engineering of the N-channel to minimise on-resistance.

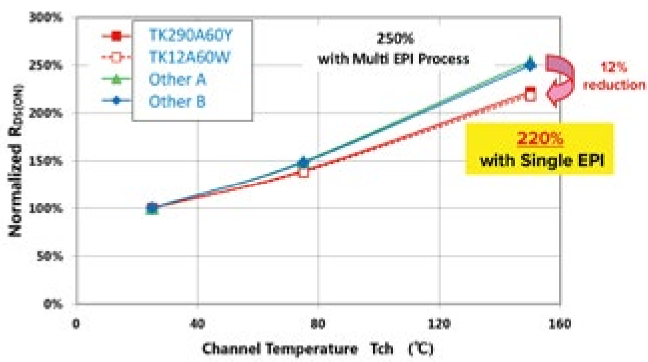

Figure 3: Single-epitaxial fabrication has enabled a flatter on-resistance/temperature characteristic. The TK12A60W represents DTMOS IV and TK290A60Y DTMOS V generation.

Improved fabrication processes, such as deep trench filling that enables single-epitaxial fabrication, now give designers greater freedom to optimise the aspect ratio of N- and P-channels and so further minimise on-resistance while also reducing MOSFET size. Figure 2b illustrates Toshiba's fourth-generation DTMOS IV family, which takes advantage of single epitaxy to achieve a 27% reduction in device pitch at the same time as reducing on-resistance per die area by 30%. Also DTMOS V is based on the deep trench process, with further improvements at cell structure level.

The single-epitaxial process also enables superjunction MOSFETs to deliver more stable performance in relation to temperature change. Ultimately, this helps to counter the typical reduction of efficiency experienced in power converters at higher operating temperatures. Figure 3 shows how the temperature-related change in normalised on-resistance is significantly reduced in devices using the latest-generation technologies, resulting in 12% lower on-resistance at 150°C.

DTMOS V FETs Meet Demands for Lower EMI

With the arrival of fifth-generation DTMOS V devices, designers can now choose superjunction MOSFETs that deliver low-noise performance suitable for use in power converters. DTMOS V FETs also display a well-balanced ratio of lower noise performance and switching performance. This is achieved through a modified gate structure and patterning, which results in increased reverse transfer capacitance seen between the gate and drain (CRSS or CGD).

Emitted noise is comparable to that experienced with competing low-EMI devices, while at the same time the devices deliver the superior on-resistance that characterises superjunction technology. Figure 4 compares the level of EMI emitted by fourth- and fifth-generation N-channel, 0.38mΩ-class 600V devices used in the PFC circuit of a television power supply, showing a significant reduction interference from the later technology.

Rectifier Diodes Toughen Up with SiC Advances

Complementing the high efficiency and current density of deep-trench superjunction power switches, new generations of silicon carbide (SiC) diodes combine inherently superior energy efficiency compared to standard silicon devices with increased current density, higher current ratings and greater robustness, and enhanced cost-performance ratio.

Recap on SiC Advantages

The properties of silicon carbide (SiC) enable SiC Schottky Barrier Diodes (SBDs) to deliver fast and temperature-stable reverse-recovery comparable to that of conventional silicon SBDs, which ensures energy-efficient turn-off performance, without suffering the conventional SBD's relatively high and temperature-dependent leakage current that can result in thermal instability if reverse-voltage derating is not applied. In addition, the wide-bandgap property of SiC allows the device to have a higher voltage rating in relation to die size, enabling 650V and 1200V devices to be housed in industry-standard surface-mount and through-hole packages. This combination of characteristics makes SiC diodes ideal for applications such as power-factor correction when used as shown in figure 5, in conjunction with a high-speed superjunction MOSFET such as a DTMOS IV X-type device.

Figures 6a and 6b illustrate the enhanced architecture of the SiC SBD in comparison with the standard silicon SBD architecture.

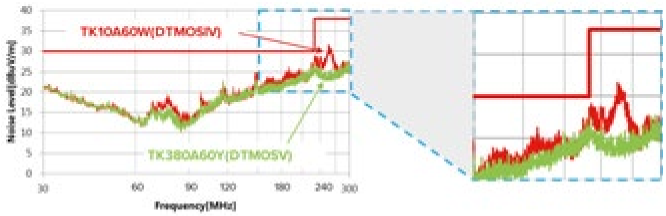

Figure 4: Improved noise performance displayed by fifth-generation superjunction technology

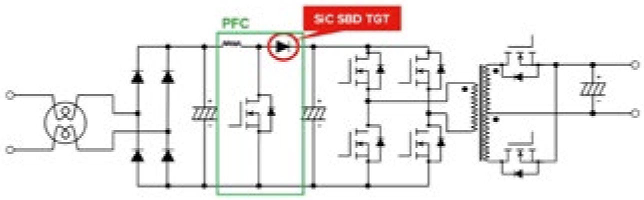

Figure 5. The latest SiC diode technology can be used in conjunction with a high-speed superjunction MOSFET, to boost the efficiency of PFC circuitry.

The Emerging Generation

The key targets for the latest generation of 650V SiC SBDs have been to increase performance in relation to device cost, and to raise the maximum forward-current surge capability and thus deliver more robust devices that are capable of surviving harsh exception conditions.

As with LSI semiconductors, power-semiconductor die size is a key determinant of device cost. Development of the second-generation SiC SBD architecture has focused on reducing the die thickness. The result has been to reduce thickness by two-thirds, bringing an attendant cost saving, while also raising current density by a factor of up to 1.5.

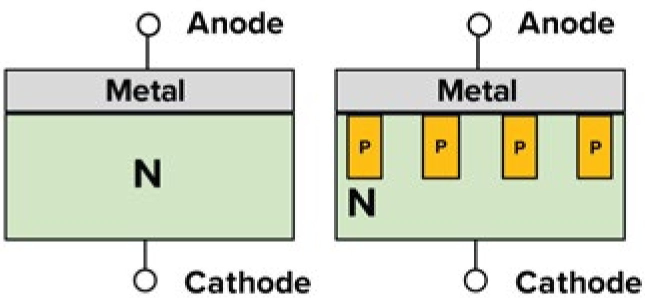

Figure 6a: Basic architecture of standard silicon SBD
Figure 6b: Architecture of SiC SBD

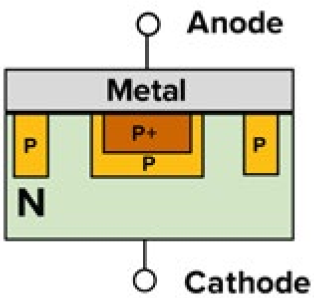

Figure 7: Optimising the SiC P+ region in the second-generation 650V SiC SBD

To increase the surge-current capability and hence deliver more robust devices for power-switching applications, the first-generation architecture has been modified to minimise modulation of the conductivity (as measured using the diode forward-voltage, VF) thereby allowing higher maximum forward surge current, IFSM. Figure 7 shows how this has been achieved by optimising the area of the P+ region.

Changes to the diode architecture have modified the relation between current density and VF, raising the voltage at which conductivity modulation begins to occur, as shown in figure 8. This allows the device to have higher IFSM. As a result, the second-generation architecture permits IFSM to be increased above the reach of first-generation devices.

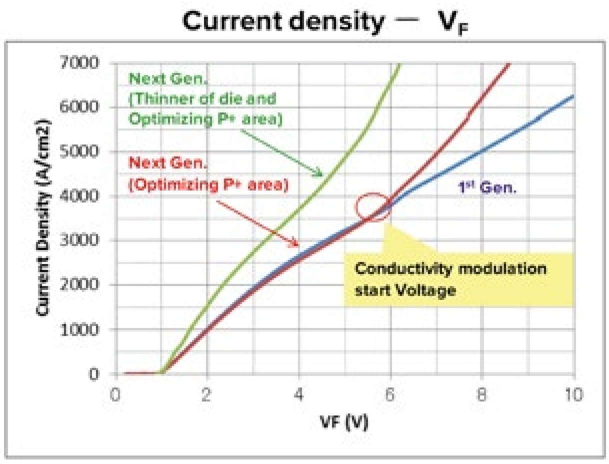

Figure 8: Conductivity modulation starts at a higher VF in second-generation devices

Conclusion

Power supply designers are under pressure to satisfy unrelenting demands for greater energy efficiency, reliability and miniaturisation, within increasingly tight cost constraints. Moreover there is less time available to look at EMI suppression during the design process.

Success depends on taking advantage of the latest power-semiconductor technologies that deliver lower on-resistance and noise performance in the case of power MOSFETs, and reduced leakage with greater temperature stability in the case of rectifier diodes. The latest-generation superjunction MOSFETs and SiC diodes deliver these advances, as well as improved switching performance, greater robustness and reliability, and increased current density, at a price that can make economic sense for cost-sensitive applications.

www.toshiba.semicon-storage.com

Identification of PMSM Motor Parameters with a Power Analyzer

By Kunihisa Kubota, Hajime Yoda, Hiroki Kobayashi, and Shinya Takiguchi
HIOKI E.E. Corporation

1. Introduction
Recent years have seen permanent magnet synchronous motors (PMSMs) and related control technologies rapidly permeate into the advanced power electronics landscape and markets.

These developments reflect the advent of high-performance, high-efficiency designs thanks to progress in permanent magnet materials as well as the advantages of PMSMs relative to other motors in terms of quiet operation and simplicity of maintenance[1]). Recently, PMSMs are being adopted in hybrid and electric vehicles in addition to household electronics and industrial machinery, and their entry into widespread use is expected to accelerate in the future[2]).

In general, PMSM analysis and control are based on the equivalent circuit model for a motor expressed on the d- and q-axes. A variety of high-performance control methods have been proposed for PMSMs, and these control algorithms are based on d-q equivalent circuits, making it extremely important to identify the equivalent circuit constants—in other words, the motor parameters (d-axis and q-axis inductance, L_d and L_q)—with a high degree of precision.

Of these motor parameters, L_q exhibits a particularly high degree of current dependence due to magnetic saturation[3, 4]), making it difficult to implement high-performance control while using low-precision motor parameters measured in a simple manner with an LCR meter or other instrument while the motor is in the stopped state.

This paper introduces a method by which a power analyzer can be used to identify motor parameters easily and with a high degree of precision while the target motor is operating. In addition, it provides results (motor parameters) obtained through the actual use of this method.

2. Method for identifying motor parameters
This chapter provides a brief description of the principles employed to identify PMSM motor parameters using a power analyzer and of a procedure for doing so.

2.1 Principles
If we assume the following with regard to the voltage equation for a PMSM expressed on the *d-q* coordinate axis, we arrive at Eq. (2.1)[3]) .
i) The spatial distribution of magnetic flux in the gap between the stator and rotor takes the form of a sine wave moving along the gap.
ii) The harmonic components of the voltage and current can be ignored.
iii) Core loss can be ignored.

$$\begin{bmatrix} v_d \\ v_q \end{bmatrix} = \begin{bmatrix} R + pL_d & -\omega L_q \\ \omega L_d & R + pL_q \end{bmatrix} \begin{bmatrix} i_d \\ i_q \end{bmatrix} + \begin{bmatrix} 0 \\ \omega \phi_a \end{bmatrix} \tag{2.1}$$

In this equation, v_d and v_q represent the *d*-axis and *q*-axis components of the armature voltage for each phase; i_d and i_q, the *d*-axis and q-axis components of the armature current for each phase; *R*, the armature resistance for each phase; *p*, the differential operator (d/dt); L_d and L_q, the *d*-axis and *q*-axis self-inductance; ω, the rotation angle (electrical angle) speed; and ϕa (=K_e), the RMS value of the permanent magnet's flux linkage with the armature (i.e., the induced voltage constant).

Fig. 2.1 illustrates the result of assuming a stationary state (so that time-derivative terms can be ignored) and expressing Eq. (2.1) as a *d*-axis and *q*-axis vector diagram. In the figure, v_1 and i_1 represent the fundamental components of the phase voltage and phase current, and θv and θi represent the fundamental phase angle of the phase voltage and phase current, respectively. Based on Fig. 2.1, the *d*-axis and *q*-axis voltage equations can be formulated as follows:

$$K_e\omega + Ri_q = v_q - \omega L_d i_d \tag{2.2}$$
$$v_d = Ri_d - \omega L_q i_q. \tag{2.3}$$

Solving these for L_D and L_q yields the following equations:

$$L_d = \frac{v_q - K_e\omega - Ri_q}{\omega i_d} \tag{2.4}$$
$$L_q = \frac{Ri_d - v_d}{\omega i_q}. \tag{2.5}$$

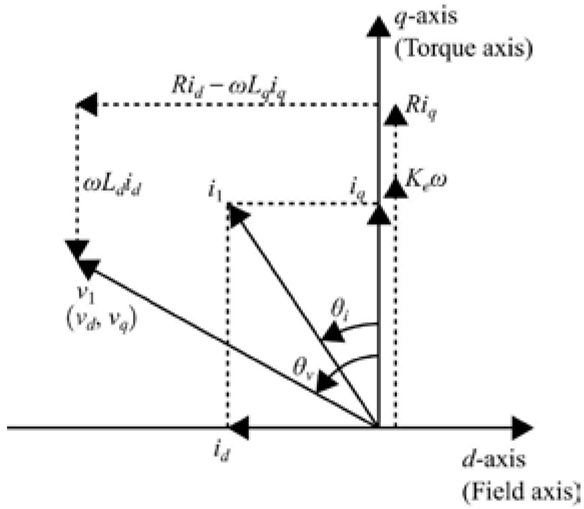

Figure 2.1: PMSM vector diagram

2.2 Identification procedure
This section describes a procedure by means of which a power analyzer can be used to identify motor parameters.

Although this specific procedure uses a Hioki Power Analyzer PW6001, motor parameters can be identified using a similar procedure with any power analyzer that provides an electrical angle measurement function that is equivalent to that offered by the PW6001.

2.2.1 Measuring the armature resistance R for each phase

Measure the armature resistance *R* for each phase using a resistance meter or other suitable instrument in advance.

2.2.2 Performing phase zero-adjustment and identifying the induced voltage constant Ke

After placing the motor terminals of the PMSM being measured in the open state ($i_d = i_q = 0$), connect the motor terminals to the “CH 1”, “CH 2” and “CH 3” voltage inputs of the Power Analyzer PW6001. Additionally, connect the encoder’s A-phase pulse output to “CH B”, its B-phase pulse output to “CH C”, and its Z-phase pulse (origin signal) output to “CH D” (Fig. 2.2).

Configure the Power Analyzer PW6001’s settings by setting the motor analysis operating mode to “Single,” the measurement parameter to “Torque Speed Direction Origin,” and “CH B” input to “Pulse.” In addition, set the wiring connection for “CH 1”, “CH 2” and “CH 3” to “3P3W3M,” the synchronization source to “Ext1,” and Δ conversion to “ON.” Setting the synchronization source to “Ext1” allows the voltage and current phase angles to be measured using the inputted encoder pulse as the reference, and setting Δ conversion to “ON” allows the line voltage to be converted to, and measured as, a phase voltage.

In this state, drive the motor from the load side to generate an induced voltage and perform phase zero-adjustment on the Power Analyzer PW6001. As a result of this step, θ_v and θ_i will represent the phase angle expressed using the phase of the induced voltage generated in the *q*-axis direction as the reference—that is, the electrical angle.

At this time, Eq.(2.4) can be rewritten as follows since the induced voltage v_q is equal to v_1, allowing identification of K_e.

$$K_e = \frac{v_q}{\omega} = \frac{v_1}{2\pi f_1} \qquad (2.6)$$

In this equation, $f_1(=\omega/2\pi)$ represents the frequency of the phase voltage’s fundamental wave.

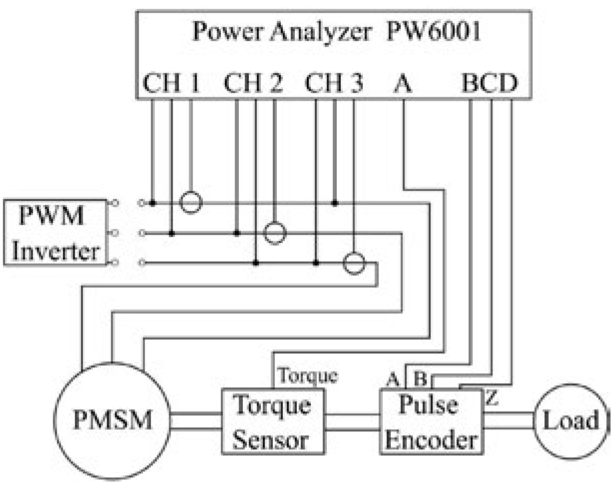

Figure 2.2 Wiring connections when performing phase zero-adjustment and identifying the induced voltage constant Ke

2.2.3 Identifying the motor parameters L_d and L_q with user-defined functions

The *d*-axis and *q*-axis self-inductance L_d and L_q can be identified using *R* as measured in Section 2.2.1 and K_e as identified in Section 2.2.2. First, connect the drive inverter output to the motor terminals that were left open in Section 2.2.2 and operate the motor (Fig. 2.3). At this time, the following equations will obtain based on Fig. 2.1:

$$v_d = -v_1 \sin\theta_v \qquad (2.7)$$

$$v_q = v_1 \cos\theta_v \qquad (2.8)$$

$$i_d = -i_1 \sin\theta_i \qquad (2.9)$$

$$i_q = i_1 \cos\theta_i \qquad (2.10)$$

By configuring the instrument’s user-defined functions (UDFs) with these equations as well as Equations 2.4 and 2.5, it is a simple matter to identify L_d and L_q while monitoring v_d, v_q, i_d, and i_q. See reference[5] for specific examples of settings for the Power Analyzer PW6001’s user-defined functions.

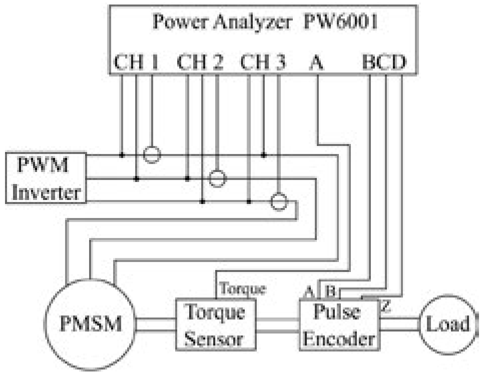

Figure 2.3: Wiring connections when identifying the L_d and L_q motor parameters

3. Measurement example

This section presents the results of using the procedure described in Section 2.2 to actually identify motor parameters.

3.1 Measurement conditions

Tables 1, 2, and 3 describe the specifications of the inverter (Fig. 3.1), drive-side motor, and load-side motor (Fig. 3.2) used in the procedure.

Item	Specifications
Rated output capacity	10.0 kVA
Rated output voltage	400 Vrms AC
Rated output current	14.5 Arms AC
Rated input voltage	700 V DC
Rated input current	15.1 A DC
Maximum input current	18.6 A DC
Input voltage range	0 V DC to 800 V DC
Switching frequency	Up to 200 kHZ
Switching element	SiC MOSFET
Manufacturer	SCH2080KE (ROHM) Myway Plus Corp.

Table 1: Inverter specifications

Table 4 describes the measuring instruments that were used. The Hioki Resistance Meter RM3544 noted in the table was used to measure the armature resistance R of the drive-side motor listed in Table 2 for each phase (Section 2.2.1).

Design & debug your power supply in minutes, not weeks

Digital multiphase power solutions for 10A to 450A applications

Easy-to-use digital multiphase controllers coupled with our smart power stage technology provide scalable solutions from 10A to 450A

- **Full telemetry data, monitoring and control** with PMBus™ 1.3 and AVSBus™ support for smart, energy-efficient systems
- **Patented synthetic current control** tracks phases with zero latency to respond to any load with precise current and voltage positioning, requiring 30% less capacitance than competitive devices
- **PowerNavigator™** GUI software tool allows you to quickly optimize your configuration and easily store it in non-volatile memory

Flexible configurations to meet any rail requirements

Application	Dual Output Device	Compatible Interfaces	Output Phase Configuration
AVSBus	ISL68137	PMBus, AVSBus	X+Y ≤ 7
	ISL68134	PMBus, AVSBus	X+Y ≤ 4
General Purpose	ISL68127	PMBus	X+Y ≤ 7
	ISL68124	PMBus	X+Y ≤ 4
SVI2	ISL69147	PMBus, AMD SVI2	X+Y ≤ 7
	ISL69144	PMBus, AMD SVI2	X+Y ≤ 4
IMVP8	ISL69137	PMBus, IMVP8	X+Y ≤ 7
	ISL69134	PMBus, IMVP8	X+Y ≤ 4
IMVP8 & VR13	ISL69128	PMBus, IMVP8/VR13	X+Y ≤ 7
VR13	ISL69127	PMBus, VR13	6+1
	ISL69125	PMBus, VR13	X+Y ≤ 4
	ISL69124	PMBus, VR13	X+Y ≤ 4

For datasheets, samples, videos and more, visit
intersil.com/digital-multiphase

intersil™

3.2 Identifying the induced voltage constant K_e

The induced voltage constant K_e was identified using the procedure described in Section 2.2.2.

For reference, Fig. 3.3 illustrates the induced voltage (phase voltage) waveforms for the drive-side motor and A/B/Z phase pulse waveforms for the encoder during the identification process.

Item	Specifications
Model	RM86A20-2-E8 DC brush-less motor with encoder
Rated voltage	100 V DC
Rated current	2 A
Rated rpm	2500 rpm
Rated output	120 W
Armature resistance for each phase	0.89768 Ω
Number of poles	8
Number of pulses per rotation	1024

Table 2: Drive-side motor specifications

Item	Specifications
Model	SS60E80-6 DC motor
Rated voltage	100 V DC
Rated current	4.8 A
Rated rpm	2500 rpm
Rated output	350 W

Table 3: Load-side motor specifications

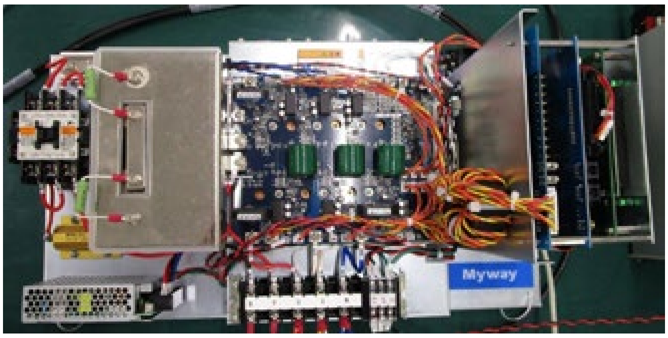

Figure 3.1: Inverter

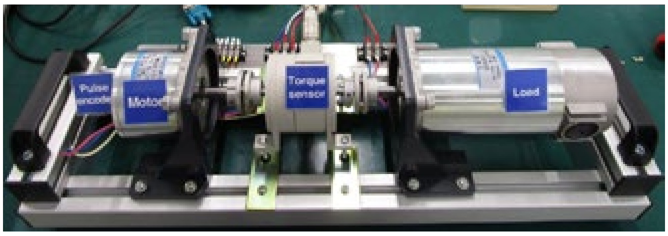

Figure 3.2: Drive-side motor (left) and load-side motor (right)

Instrument	Model	Manufacturer
Power Analyzer	PW6001	HIOKI E.E. CORP.
Current Sensor	CT6841	HIOKI E.E. CORP.
Resistance Meter	RM3544	HIOKI E.E. CORP.

Table 4: Measuring instruments

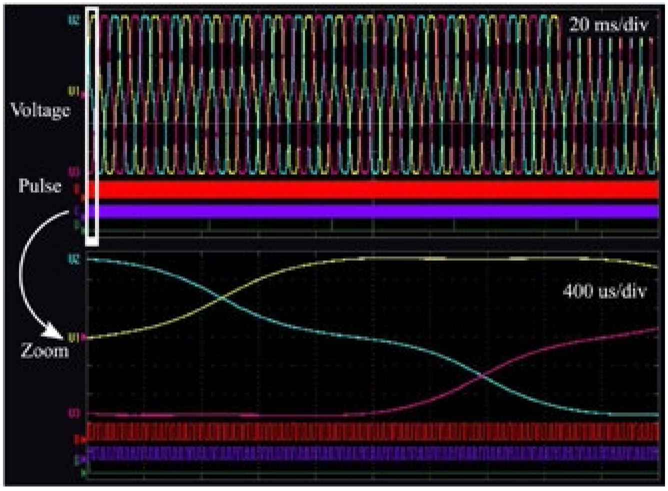

Figure 3.3 Drive-side motor induced (phase) voltage and encoder's A/B/Z phase pulse waveforms during identification of the induced voltage constant Ke

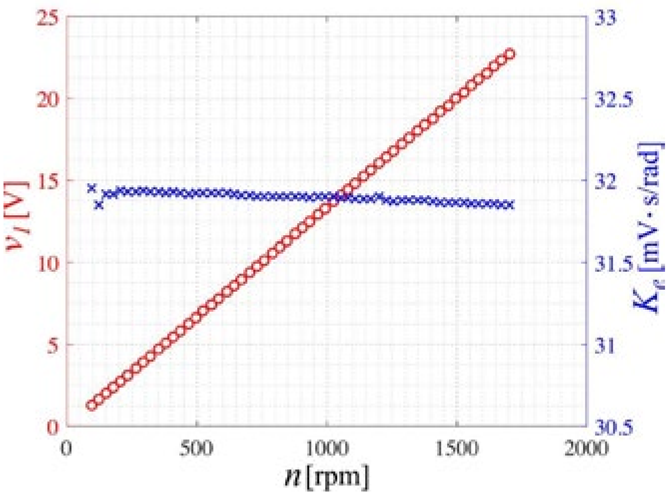

Figure 3.4: Relationships between the motor rpm n, the RMS value v_1 of the fundamental component of the drive-side motor induced (phase) voltage, and the identified induced voltage constant K_e

Fig. 3.4 illustrates the relationships between the motor rpm *n*, the RMS value v_1 of the fundamental component of the drive-side motor induced (phase) voltage, and the identified induced voltage constant K_e. The measured v_1 value varies proportionally with *n*, while the identified K_e value remains roughly constant, without regard to *n*. In this way, the relationships between these three values can be seen to satisfy the relationships described in Eq.(2.6).

K_e exhibits a small amount of variability during low-speed operation due to the more pronounced rotating unbalance of the motor in that operating regime.

3.3 Identifying the L_d and L_q motor parameters

The *d*-axis and *q*-axis self-inductance L_d and L_q were identified using the procedure described in Section 2.2.3. For reference, Fig. 3.5 illustrates the inverter's secondary-side phase voltage and phase current as well as the encoder's A/B/Z phase pulse waveforms during identification.

Fig. 3.6 illustrates the relationships between (a) the *d*-axis current id and the identified *d*-axis self-inductance L_d and (b) the *q*-axis current i_q and the identified *q*-axis self-inductance L_q. L_d remains roughly constant, without regard to i_d. By contrast, L_q exhibits a high degree of current dependency due to magnetic saturation and varies significantly with i_q. These characteristics make it clear that it is not possible to use an LCR meter or similar instrument to identify L_d with a high degree of precision while the motor is in the stopped state. Instead, the value must be identified while the motor is operating.

The variability in the L_d and L_q values when the id and iq values are small is also likely to be caused by rotating unbalance of the motor during low-speed operation.

Fig. 3.6 illustrates the results of identifying the L_d and L_q motor parameters while the motor's rpm is varied while holding the current phase angle constant, showing the current dependence of L_d and L_q. The current phase angle dependence of the motor parameters can also be verified by applying this identification method.

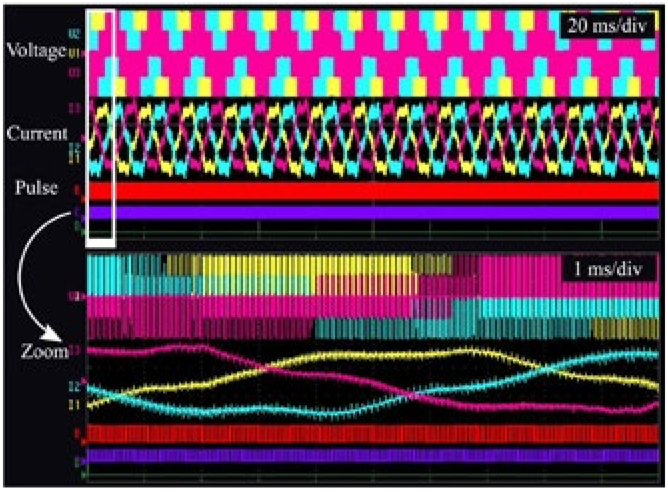

Figure 3.5: Inverter secondary-side phase voltage and phase current and encoder's A/B/Z phase pulse waveforms during identification of the L_d and L_q motor parameters (when driving the motor with the inverter)

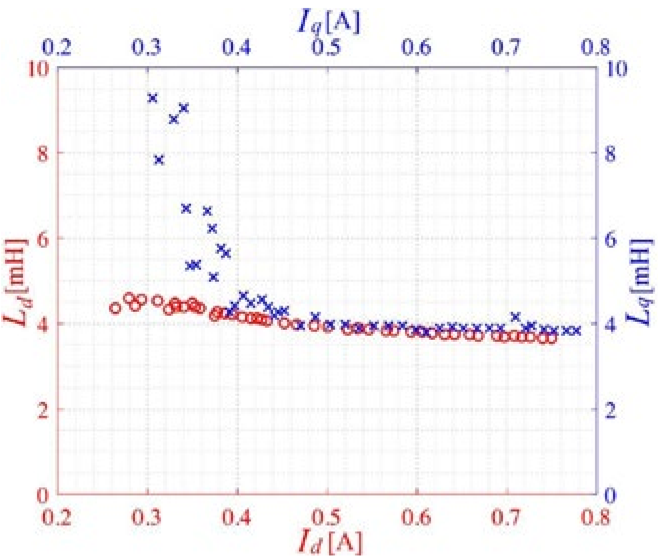

Figure 3.6: Relationships between (a) the d-axis current i_d and the identified d-axis self-inductance L_d (shown in red) and (b) the q-axis current i_q and the identified q-axis self-inductance L_q (shown in blue)

4. Conclusion

This paper has introduced a method for identifying PMSM motor parameters easily and with a high degree of precision using a power analyzer. It also presents the results of using the introduced method along with a Hioki Power Analyzer PW6001 to identify actual motor parameters. It must be noted that the method introduced in this paper presumes the use of an analytical model that posits that core loss can be ignored. That said, by measuring mechanical loss and identifying the equivalent core loss resistance in advance, it would be possible to further develop the described method in order to identify motor parameters while taking into account core loss.

The identification of PMSM motor parameters introduced in this paper is only one example of an application for power analyzers, which can be used effectively in numerous other settings in the power electronics field. The authors look forward in the future to actively introducing other applications in which power analyzers can be effectively.

References

1) Shigeo Morimoto : "Trend of Permanent Magnet Sychronous Machines", IEEJ Trans, Vol.2 (2007), pp.101-108.
2) Investigating R&D Committee on industry applications of PM motors : "Trend in the latest technologies and applications of permanent magnet synchronous motors", IEEJ Technical Report (2009), No.1145 (in Japanese).
3) Shigeo Morimoto, Yoji Takeda, and Takao Hirasa: "Method for Measuring a PM Motor's dq Equivalent Circuit Constants", IEEJ Transactions on Industry Applications, Vol.113-D (1993) No.11, pp.1330-1331 (in Japanese).
4) A. Soualmi, F. Dubas, D. Depernet, A. Randria and C. Espanet : "Inductances estimation in the d-q axis for an interior permanent-magnet synchronous machines with distributed windings", Proc. XX ICEM (2012), pp.308-314.
5) HIOKI E. E. Corp. : "Identification of PMSM Parameters with the Power Analyzer PW6001" (White paper), retrieved from https:// www.hioki.com/ en/ products/ detail/?product key= 5796.

www.hioki.com/ en/

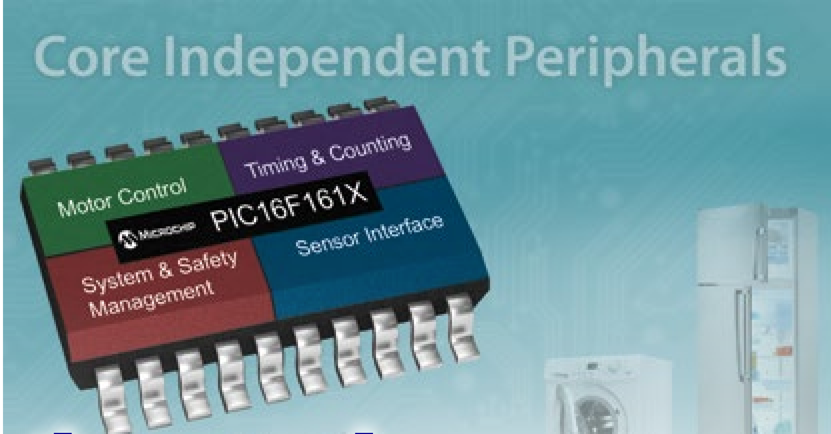

Igniting the spark

The angular timer of a microcontroller can help implement capacitor discharge ignition in an internal combustion engine

By Ashutosh Tiwari, Shailendra Vengurlekar and Namrata Dalvi, Microchip Technology

The capacitor discharge ignition (CDI) system in an internal combustion engine can be implemented on single profile ignition pickup (PIP) systems using standard peripherals on an 8bit microcontroller, but there are challenges associated with such designs.

In an internal combustion engine, the air and fuel chemical mixture is burnt and extreme heat is generated expanding the exhaust gases, which force the cylinder piston to move, causing the camshaft to rotate and create a kinetic energy. This kinetic energy is coupled to the vehicle's wheels by gear trains to convert the angular motion into linear motion.

A four-stroke cycle engine that uses four distinct piston strokes – intake, compression, power and exhaust – to complete one operating cycle is shown in Figure 1.

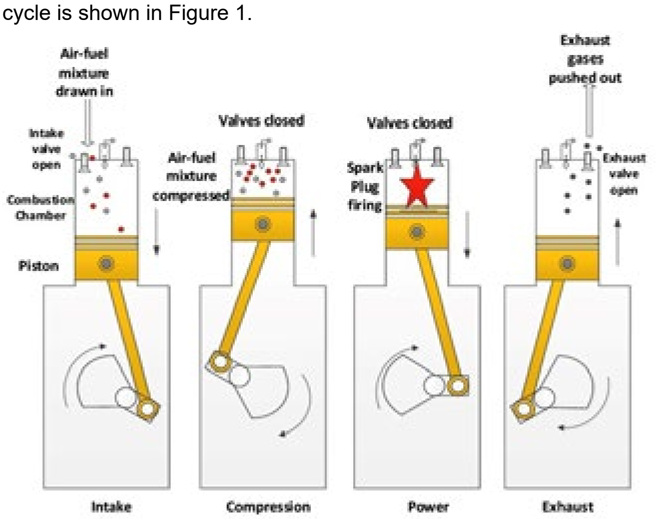

Figure 1: Four stroke engine with engine parts

The top dead centre (TDC) is the highest position of the piston near the spark plug and the bottom dead centre (BDC) is the lowest position near the camshaft. After the spark plug fires into the power stroke, the air-fuel mixture needs time to completely burn; this burning process is progressive in nature in that the mixture at the top burns first and quickly moves towards the bottom.

Therefore, to burn the air-fuel mixture completely and produce the maximum pressure wave, the spark plug should be precisely fired moments before the piston reaches the TDC and at the proper angle, which is determined by the engine piston speed. There are other factors, such as temperature and throttle position that also determine the spark firing angle. To fire the spark correctly and accurately, a separate module known as the ignition control mechanism, is used.

Ignition systems

There are two types of ignition systems: inductive discharge ignition (IDI) or transistor controlled ignition (TCI); and CDI. The CDI system uses high-voltage capacitor discharge current output to fire the spark plug, see Figure 2. It can be implemented using core independent peripherals (CIPs) found on Microchip PIC microcontrollers. These include angular timer (AT), signal measurement timer (SMT), maths accelerator and configurable logic cell (CLC).

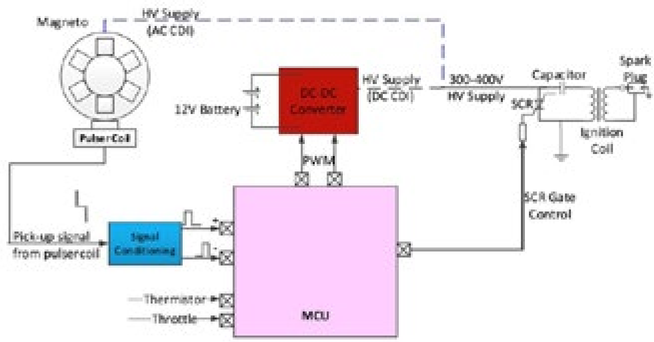

Figure 2: Basic capacitor discharge ignition (CDI) system

There are two types of CDI system – alternating and direct current capacitor discharge ignition, or AC-CDI and DC-CDI. In an AC-CDI system, an alternator or stator (magneto) generates enough power for all electronic systems including the CDI. The capacitor is charged through the rectified output of the magneto AC supply, which is 200 to 400V DC. When the engine is cold (not running), a kick-start is required to rotate both the engine and the magneto. This does not generate sufficient power from the magneto to charge the capacitor completely for a high-voltage spark. For very low RPM, the firing angle is always constant. Hence, analogue firing is used to fire at negative PIP output from the magneto-flywheel pulser coil without calculating the RPM.

In a DC-CDI system, a constant 12V DC power is always available from the battery. It requires an additional DC-DC converter to raise the 12V DC to 200-400V DC. This additional circuitry makes the CDI module slightly larger than an AC-CDI system. When the engine is not running, it can be started easily at a precisely calculated firing angle, as the input DC supply is always available.

To create the high-voltage spark in the spark plug, a high-voltage capacitor with a high-charge capacity is charged using either the output of the DC-DC converter (DC-CDI) or using the output of the magneto, an AC alternator (AC-CDI). The capacitor is charged to a high-voltage supply, usually 200 to 400V.

The capacitor is connected to an ignition coil or step-up pulse transformer, which produces a very high voltage, in the range of 40kV or more.

The switch connects the capacitor to the primary of the ignition coil. The switch is fired when the microcontroller gives a pulse at the gate of the switch. The sudden rush of current in the primary of the coil produces a very high voltage in the secondary, which generates the spark to ignite the air-fuel mixture. Thus, the microcontroller controls the firing angle of the switch for generating the spark.

A silicon-controlled rectifier (SCR) is most commonly used as a high-power switch in CDI. It is highly durable due to the higher operating voltages and current ranges with moderate frequency response. The disadvantage of the SCR is it is a one-sided switch in that the switch can only be on. It will automatically go to off when the input is less than the lower operating threshold.

An IGBT and MOSFET are used in modern CDI designs due to their ability to switch on and off, as well as having better frequency response at higher operating ranges.

The pulser coil – or pick-up and timing coil – is responsible for providing the timing signal to the ignition control system.

A magnet is mounted on a flywheel, which is mounted on the magneto shaft. When the flywheel rotates, the magnet passes near the pulse coil producing a timing pulse. There is one pulse per pole. Hence, for each magnet there are two outputs, one positive pulse followed by a negative pulse, generating one alternating pulse pair. For a single PIP system, there is only one pair. For multi-pulse systems there are multiple pulse pairs, based on the number of magnets on the flywheel. The alternating pulses are at a fixed angle with respect to the TDC piston position in the engine for each rotation. The period of the pulses triggers the rotation of the engine.

Based on the number of alternating pulses from the pick-up, per engine rotation, the pulser coil system can be either a single or multiple PIP system.

In a single PIP system, the pulser coil provides one positive pulse followed by a negative reference pulse. The angle between the pulses and the angle between the negative pulse and the TDC are fixed. The firing of the spark should be at a specific angle based on the engine operating temperature, the throttle position and the RPM. This angle is usually between the positive and negative pulses.

The negative pulse is a reference point for firing the spark at very low RPM. The firing angle changes to an angle between the pulses for higher RPM.

In a multiple PIP system, the pulser coil provides more than one alternating pulse. The second negative pulse is the reference point before the TDC. This is the minimum firing angle at which the spark should be generated for engine speeds below a lower speed threshold.

The first positive and negative pulses can be used for calculating the engine RPM. The second positive pulse can be a reference point for deciding the firing angle for higher speeds.

The pulser coil generates the timing signals that contain positive and negative pulses. These pulses are in the range of ±3 to ±90V, depending on the magnetic field strength of the magnet mounted on the flywheel.

A signal conditioning circuit inverts the negative pulse and limits the pulses to 0 to 5V. It is also used to filter spurious noise. The signal conditioning circuit will provide two positive outputs, one corresponding to positive pulses and another for negative pulses. Output of the signal conditioning circuit is connected to the microcontroller.

Microcontroller

In a digital CDI system, the microcontroller has two major functions: deciding the advance firing angle by reading input from the sensors, such as the pulser coil, thermistor and throttle position, then producing the firing pulse; and setting the duty cycle of pulse-width modulation (PWM) for the DC-DC converter.

The advance angle required for getting optimum performance from the engine is mainly dependent on the RPM. Hence, the system must be aware of the current RPM, temperature and throttle position. Look-up tables called maps are stored in the programme memory of the microcontroller, which give the appropriate advance angles with respect to the RPM.

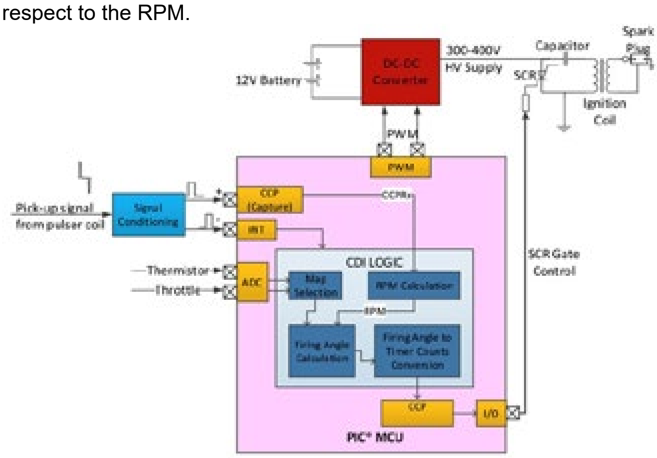

Figure 3: Conventional method for CDI implementation

Multiple maps are stored based on different throttle positions and for different temperature ranges. Once the controller calculates the RPM, it can then look up the appropriate advance angle from the map.

Peripherals on PIC MCUs, such as capture compare or PWM (CCP) and ADC, together with the interrupt pin INT can be used to determine the firing angle control in CDI.

The output for the positive PIP signal of the signal conditioning circuit is given to the capture module. The capture module measures the time between two positive pulses, which is the period of the pulser coil output. The period of the pulses gives the RPM of the engine.

An analogue-digital converter (ADC) can be used to determine the engine temperature and the throttle position if it is analogue; the throttle position input can be either analogue or digital. In the case of a digital throttle, the position for the wide open throttle (WOT) is one state and the partially open throttle (POT) another. There are distinct firing maps for different throttle positions and different temperature ranges. Figure

3 shows the conventional method for the CDI implementation.

The conventional method of RPM calculation uses a 16bit timer along with capture peripheral. For lower RPM values, less than 60 (corresponding to 1Hz frequency), the 16bit timer will overflow if the timer clock frequency is 1MHz. The timer overflow bit should be taken into account for RPM calculations.

conventional method or by using CIPs, such as AT, CLC, SMT, maths accelerator and complementary waveform generator (CWG). However, using the CIPs greatly improve the overall performance and implementation of CDI.

The AT successfully divides the input signal to angular division without CPU intervention, which helps to boost performance by removing the need for firing angle conversion from degree to equivalent time. These angular divisions are also very accurate and constant throughout the input signal range.

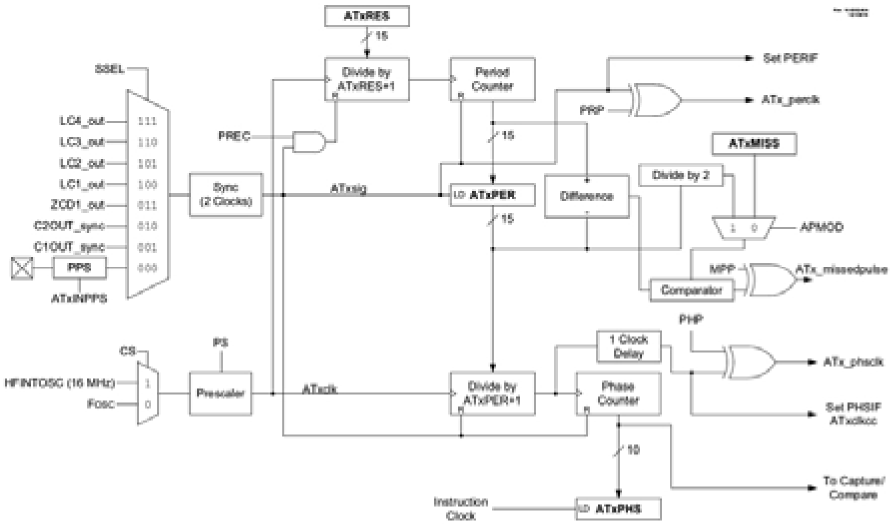

Figure 4: AT block diagram in single-pulse mode

Peripherals

The PIC16F161X 8bit microcontroller has a Core Independent Peripheral (CIP) called the angular timer (AT), which can be used in internal combustion engines to fire the spark at the exact firing angle with very little CPU intervention. As shown in Fig. 4, the periodic pulse input to the AT can be selected either from the internal core independent peripherals or from the external pin.

The CIPs of PIC microcontrollers, such as CLC, AT, SMT and maths accelerator, are used for the firing angle control in CDI.

For the RPM calculation, a 24bit SMT is used. The SMT is configured in windowed measurement mode with the window input set to AT period pulse. Whenever the AT gives a period pulse, the SMT captures the timer value into a register, resets its timer count and restarts counting. The timer capture into the register generates a captured period interrupt.

The maths accelerator peripheral, also called a PID module, is used to calculate the firing angle for the current RPM.

Conclusion

CDI systems can be implemented using PIC16F microcontrollers either through the

The performance of the CDI system can be greatly enhanced using the AT, with significant CPU bandwidth remaining for other calculations. In addition, with the use of the maths accelerator, the calculations are now more accurate and faster. The SMT with its inherent high-bit resolution helps in tracking low engine RPM and taking necessary action, without the need for large computations.

A similar implementation technique can be extended to other systems, such as inductive discharge ignition, that use the same CIPs.

www.microchip.com

Ashutosh Tiwari is Senior Application Engineer at Microchip Technology

Shailendra Vengurlekar is Manager Automotive Applications at Microchip Technology

Namrata Dalvi is Senior Application Engineer at Microchip Technology

A Fast Track to Complex Power System Designs

Innovative power conversion architectures, taking advantage of evolving power semiconductor technologies, have risen to the challenge, especially in terms of the high performance modular solutions now available.

By Arthur Jordan - Applications Engineer, Vicor Corporation

Recent developments in power system components have enabled the designer to configure power supply systems of vastly greater performance than was possible only a short time ago. This has been driven in part by an acute need; today's systems are built around microprocessors and FPGAs that demand ever-higher currents at an unprecedented variety of lower voltages. The circuit boards on which those components reside require multiple power rails, of high stability, at high power levels, and often with complex sequencing constraints. Scale up to the rack and system view, and the problem becomes infinitely more complex.

Innovative power conversion architectures, taking advantage of evolving power semiconductor technologies, have risen to the challenge, especially in terms of the high performance modular solutions now available. The designer's task has not, however, been made any simpler because those same advances in technology have expanded the options available with which to configure a system, and to meet any given specification. The range of modules available today have made a change that appears subtle, but can be radical in its impact. They have separated out the basic functions of a power supply, such as voltage level conversion, regulation, and isolation. With the freedom to place these functions as-needed through a power supply chain, comes the need to explore many more options to find the optimum layout.

More choices mean more flexibility to optimize

Innovative devices such as Vicor's BCM provide an example of how design choices are expanded. A BCM is a low-voltage DC-DC bus converter module; using Vicor's Sine Amplitude Conversion technology, it provides bi-directional fixed-ratio conversion at very high efficiency. Packaged in the IC-style ChiP, or the easy-to-use VIA packaging technology, the BCM gives the power engineer an isolated DC-DC conversion function. Regulation can be done upstream of the BCM; feed it a stable 48V and it will directly supply a low-voltage rail on a PCB with no further regulation required. Or, it can down-convert a rail that has less precise regulation to a low voltage, leaving individual point-of-load (PoL) regulators to supply power to what might be a multiplicity of on-board rails.

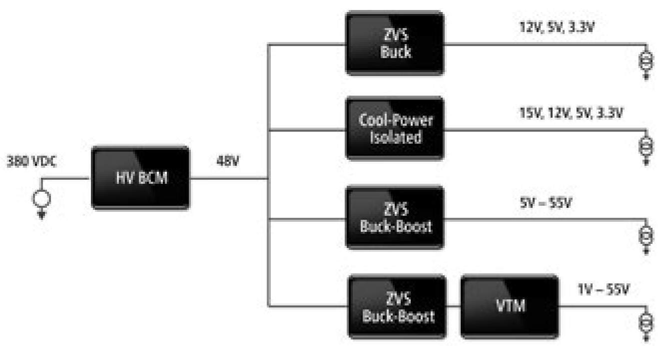

Figure 1: A Typical BCM Application

The BCM takes its place in a large portfolio of power components, such as the VTM, a point-of-load current multiplier (again, fixed-ratio conversion); PRM, a regulator for use in Factorized Power architecture, that would feed a VTM to generate PoL voltages; and the DCM, an isolated, regulated DC-DC converter. These examples are part of a broad portfolio of regulated and non-regulated, isolated or non-isolated, functional blocks that can be assembled in a virtually limitless number of ways.

For the power engineer, the question becomes less, "can I achieve the necessary power provision?" and much more, "how do I determine the optimal solution for my power design, given the comprehensive array of options?"

In the past, design choices were often rapidly narrowed by product performance and by accepted practice. For example, a 48V distribution rail is frequently a standard feature of a power distribution scheme. However, with earlier generations of buck converters, conversion efficiency would typically decline sharply at high conversion ratios (from 48V to single-figure voltages). Therefore, and with PCBs demanding more and more rails at voltages down to – or lower than – 1V, a further distribution level of, perhaps 12V might be interposed.

What is the cost of optimization?

With Vicor's power components, however, converting from 48V direct to PoL is not only feasible, it can be the most efficient option when the losses associated with generating an intermediate bus are eliminated. It does not take a great leap of imagination to observe that the 'universe' of feasible solutions has expanded enormously. It has become an optimisation problem; one with many dimensions and, in all likelihood, multiple candidate solutions.

To achieve optimal efficiency, the power engineer has had no option but to turn to the data sheets. Every data sheet presents page after page of charts showing operating parameters and performance of its particular device. Having decided on a suitable power system topology, the designer has to work through it, establishing the operating point of each module, look up their conversion efficiencies and losses, sum them by pencil-and-paper or by spreadsheet – and then repeat the exercise for every alternative configuration that looks like a realistic option.

If standby power is a consideration: repeat the process using the quiescent power figures for every block. The option, noted above, to place the fundamental functions of power conversion at-will along the conversion chain offers a further degree of freedom. To a certain extent, and given that some losses/heat dissipation are inevitable, the engineer may adjust the supply topology to have those losses concentrated where they are most easily dealt with.

When all of that is completed, the designer will only have explored efficiency and losses. Other constraints may very well apply, not least, cost. Alternative configurations that perform to specification in electrical terms may be significantly different in bill-of-materials terms. Another aspect of power supply design that has hardly changed over many generations is that power provisioning may be left to fit in the cabinet or rack space remaining when design of every other aspect is complete. Therefore, physical footprint can become critical; not only of major blocks such as off-line AC-DC conversion, but of point-of-load regulators and any associated passives in their footprints, distributed around PCBs.

A better Way to design power systems
It was against this background that Vicor created its online Power System Designer software package, designed to allow an engineer to create a power system in minutes. The Power System Designer is a simple-to-use, parametric-input tool that leverages Vicor's Power Component Design Methodology and delivers optimized power fast. Using Vicor's high-performance power components, the tool asks the designer to define a system in the simplest terms; input and outputs. Using that data, it automatically generates a complete power supply configuration, together with all relevant operating parameters.

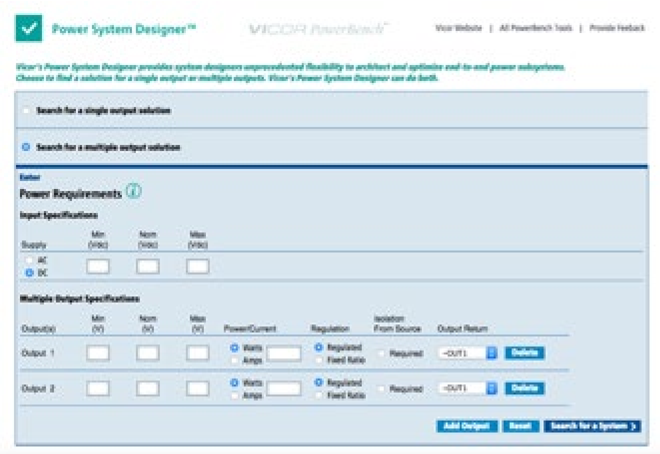

Figure 2: Power System Designer

No other tool provides such simplicity of use nor the same complete end-to-end (Source to PoL) coverage. Although the Power System Designer is not a full circuit simulator, it is backed by comprehensive and detailed simulation of every Vicor power component. It is closer to a behavioural model-based approach, where the detailed circuit operation of every component and module has been simulated and/or measured in real-world operation and tabulated, in a form the tool can rapidly access.

Added to that is a degree of rule-based behaviour; in the broad span of solutions available with Vicor's power components, there are some choices that are inevitably more productive than others, and that knowledge is built into the software. Due its mode of operation, the Power System Designer is fast and precise, delivering results instantaneously. When the time comes to verify a solution with a more detailed parametric analysis, the package acts as a "front-end" to Vicor's fully-editable Whiteboard tool.

Customize your solution based on you key figures of merit
Given AC or DC input source and operating range, together with required output voltages and respective power (or current), regulation and isolation specifications, the software automatically identifies not only a "best" solution, but presents a range of alternative solutions, each one accompanied by a spread of figures-of-merit. Efficiency is presented not only as an overall conversion efficiency, but broken out into front-end and PoL efficiencies. Other parameters include:

- lowest component count
- lowest cost (cost is presented for 1-off and 500-unit volumes)
- smallest footprint
- recommended best fit.

Once again, the designer can consider options for "moving" footprint (physical area) along the power conversion chain as the tool returns total, front-end and PoL footprint figures for each solution. For any selected design, the Power System Designer can display a visual representation of the mechanical layout of the system and generate a complete Bill-of-Materials along with ordering and pricing information.

A more holistic, faster approach to designing your power system
The Power System Designer also reports the power utilization of the front-end and of each PoL output – that is, how much of the capacity of each component specified in the chosen solution, is actually being used. The engineer thereby gains a detailed view of both design margin and capacity utilization of a given design. For more detailed analysis, launching Vicor Whiteboard is only a single-click away.

Figure 3: A Typical Output

The Power System Designer is a significant advance over simulators and design aids that have been offered up until now, in that it takes a holistic view of the power provision function from input to output, rather than focussing on front-end parameters or point-of-load performance in isolation. Allowing exploration of the full range of solutions possible with Vicor's comprehensive families of field-proven, high density modular power components, that are capable of addressing virtually any front end or power train requirement, fast-tracks the route to superior power density and quicker time-to-market, while minimizing design risks.

http://www.vicorpower.com/

Advanced and Broad Power Management Portfolio

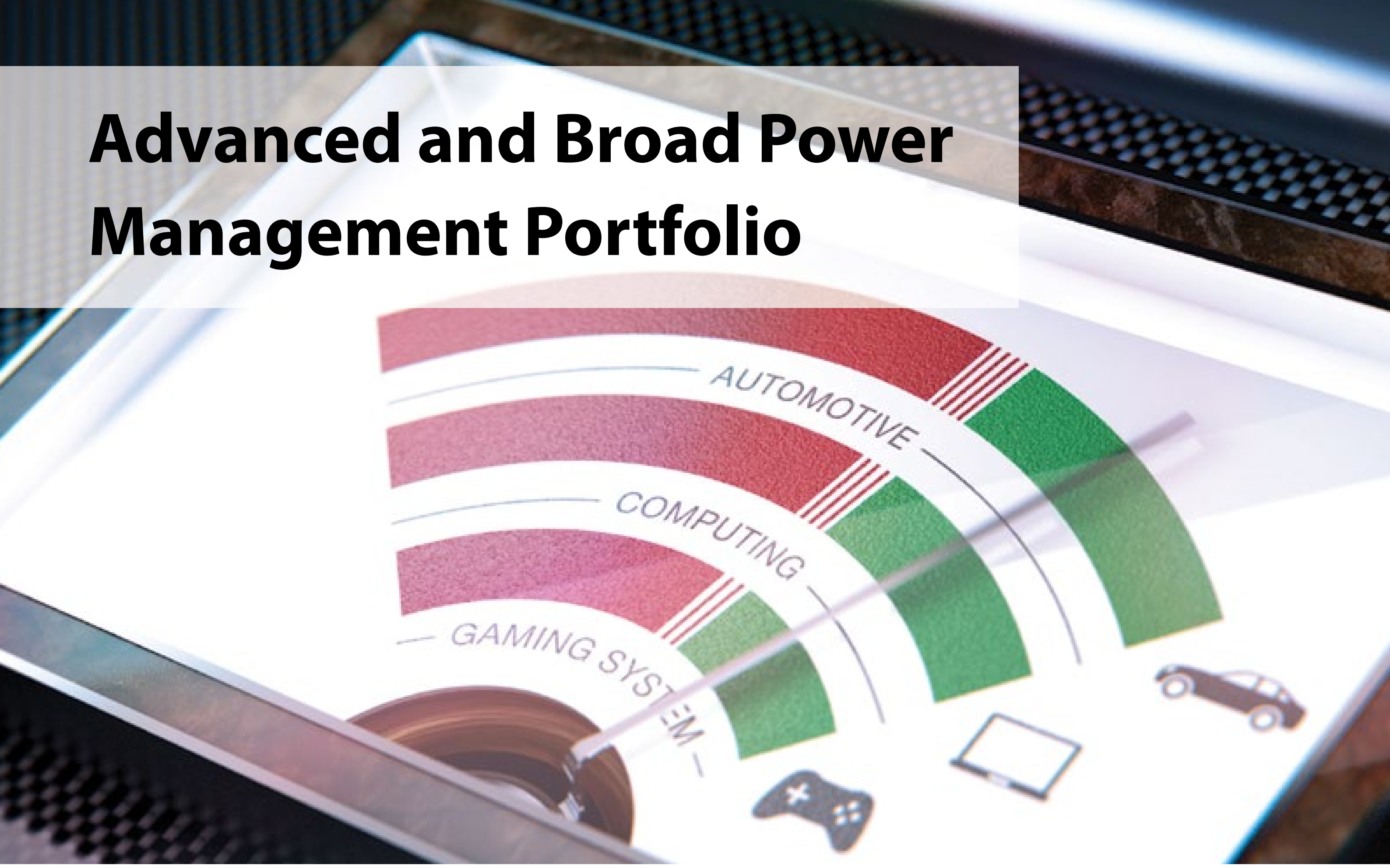

Microchip Technology has an expansive offering of power management solutions to fit virtually every type of design criteria. From the smallest form factor needed for mobile devices to complex industrial power management designs to automotive standards, you are sure to find a highly integrated solution to meet your needs. If you are looking for greater flexibility in your design, Microchip's digitally enhanced power analog devices integrate a microcontroller (MCU) or digital signal controller (DSC) for a fully programmable and flexible solution.

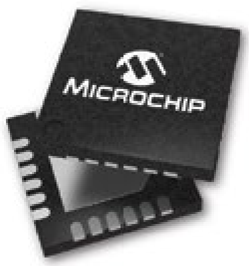

Applications:

- LDO and switching regulators
- Charge pump DC/DC converters
- Power MOSFET drivers
- Digitally enhanced and PWM controllers
- System supervisors
- Voltage detectors
- Voltage references
- Li-Ion/Li-Polymer battery chargers
- Power MOSFETs

Embedded Designs Drive Tomorrow's Solutions

Embedded drive solutions for motion control simplify integration, enhance performance and speed up time-to-market. Vincotech's power modules lineup represents the best fit for highly reliable, low-cost motor controls that deliver higher performance in a smaller footprint.

By Michele Portico, Product Marketing Manager, Vincotech GmbH, Unterhaching

Embedded drive solutions for Industrial motion control
Discrete drives are standard solutions designed to control a wide range of motion applications. Nevertheless, higher integration and more complex subsystems are some of the current trends in the Industrial market and more and more Companies provide embedded drive systems with different level of customization.

Embedded drive systems integrate drives and electric motor to reduce the space occupancy thanks to their compact and hermetical design. Since they are dedicated to specific applications, design engineers can optimize them to reduce the size and cost of the final product and increase the reliability and performance.

Discrete drives feature filters, connectors, and cables to be assembled and tested for UL and /or CE certifications. This increases the assembly time and the overall cost of the system. On the other hand, in embedded drives the overall system's size, cost, and time to market can be slashed by considerably increasing the level of integration. Mass-produced embedded drive systems benefit considerably from economies of scale.

Vincotech's product portfolio for embedded drives
Space is tight in embedded drive systems, and their compact, hermetical design makes it difficult to dissipate the heat generated by so many electronic components.

Vincotech's power module portfolio for embedded drives features 600 V and 1200 V intelligent power modules (IPMs) as well as power integrated modules integrating PFC circuit (PIM+PFC) and achieves the highest level of integration of any power module available on the market today, representing the best solution for such space-constrained mechanical environments.

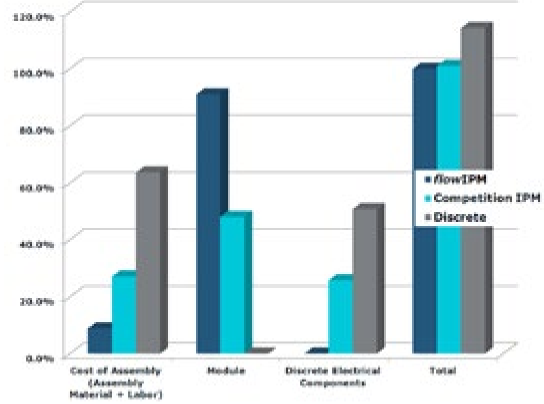

Figure 1: Cost analysis – flowIPM vs. discrete and competing IPM

The overall system's size, cost, and time to market can be slashed by integrating all of a motor drive's functional blocks, apart from the input filter, DC capacitor and microcontroller (see Fig. 1).

Protection circuitry is tuned to match the power device's capability and factory-tested to improve the system's reliability.

A lot of space is saved with highly integrated components and bare power chips to achieve a much smaller footprint than that of discrete designs.

Motor drive assembly is streamlined and simplified with fewer external components and smart isolation techniques.

The ceramic sheet used in thick-film technology improves the module's thermal performance by providing the best possible direct cooling for power components.

Vincotech's power modules for embedded drives come into very compact housings eventually equipped with Press-fit pins (see Fig.2). Press-fit technology reduces PCB assembly time and effort considerably by eliminating the need for soldering. This cuts process time and costs and boosts production output.

Figure 2: Press-fit pins for solder-less mounting

The module's creepage and clearance distances fulfill the applicable industrial standards. There are no special requirements regarding the shape of the heat sink.

The thermal interconnection between the power module and the heat sink is vastly improved by pre-applying phase-change material (see Fig. 3). Vincotech's in-house screen-printing process deposits the material with great precision, achieving the proper thickness. The material can be optimized for maximum heat transfer capability.

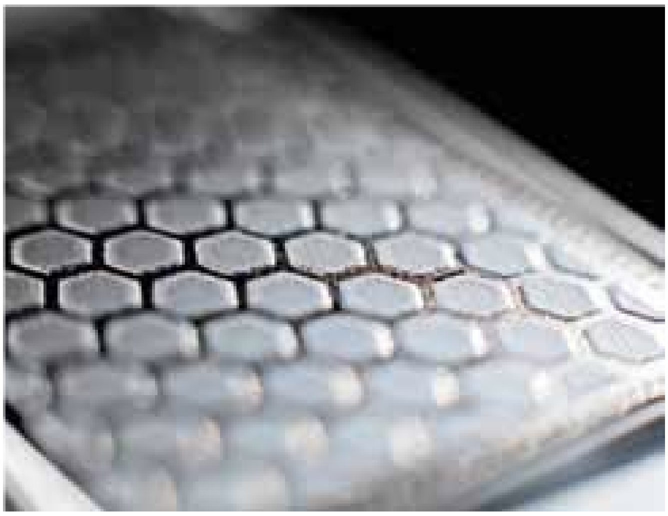

Fig. 3: Phase-change-material

Conclusion

Vincotech's product portfolio provides the functional integration and power density that engineers need to design embedded drive systems. The outstanding level of integration achieved by Vincotech's intelligent power modules enables system engineers to come up with more compact designs and to take advantage of a proven combination of power components and gate drive circuits, which happen to be the most critical elements in the inverter's design. This mitigates the risk associated with circuit design, speeds up development, and dramatically reduces time to market.

www.vincotech.com

Innovative Integrated Magnetics for Hybrid and Electrical Vehicles Onboard Battery Chargers

How to lower the volume of magnetics in ZVS or LLC converters by integrating the insulating transformer and its resonant chokes together on the same core.

By Patrick Fouassier, PhD.-Eng., Inductive Components R&D Manager, PREMO Group

Introduction

Nowadays, the market of hybrid and electrical vehicles is growing quite fast. These are alternative solutions to common thermal engine cars to reduce the global pollution, especially in terms of rejected CO_2 or other NO_x pollutants as well as toxic-for-health thin particles. Such new models require more and more power electronics inside, not only for the electrical motor supply with speed and torque control, but also for high-voltage battery chargers and stable in-car continuous low-voltage power supplies.

New SUV cars become plug-in hybrids too

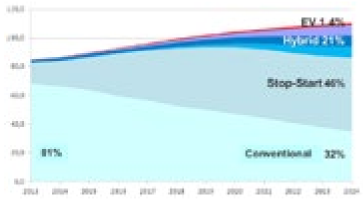

Trend in HEVs on 2013-2024

For 200-450V battery chargers, different power electronic topologies like quasi- or resonant half- or full-bridge can be used. They enable the development of high efficiency converters (> 90%) with a switching frequency commonly in the 70-350kHz range. A power of 3.5kW enables a complete charge of the batteries during one night (around 6-8 hours through a 10/16Arms domestic plug) whereas 7kW reduces the duration to approx half-a-day charging (32Arms plug). The power can be increased from 11-22kW (AC 3-phase network) to 50kW (DC network) for ultra-fast charging in 30-60 minutes but it requires dedicated charging stations to be installed through the cities. For modularity concept, 3.5kW bricks can be connected together with the selection of 1-phase 3.5 or 7kW or 3-phase 11kW charging configurations.

Thus 3-4kW HF transformers are required in the charging operation both for voltage level adaptation from the rectified mains to the battery voltage and for the by circuits physical separation between the AC and DC. As the component belongs to a switch-mode power supply

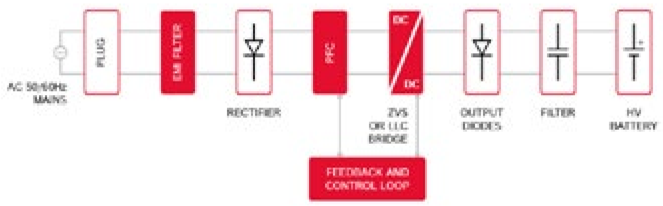

Common battery charger SMPS schematics

it is often associated to inductors for benefit in soft-switching, better control and EMI reduction.

LLC topology

The first possible and most efficient used topology is the LLC resonant bridge. It can be formed from 2 switching transistors (half-bridge structure, figure 1) to 4 transistors (full-bridge operation). The transistors in series form legs connected to the DC-bus (input voltage Uin). The transformer and its related resonant tank are connected between these legs. At the secondary side we find a rectifier module made of 2 (center-tap transformer) or 4 diodes (single secondary winding transformer) and a filtering capacitor.

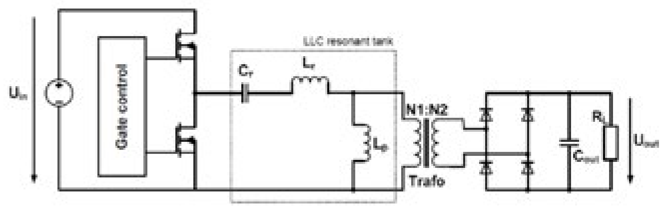

Figure 1: Half-bridge resonant LLC converter topology

The resonant tank associates to the transformer a parallel inductor (Lp) and a serial additional inductor (Lr) as well as a serial capacitor (Cr). These 3 passive components are usually discrete components that require space in the application. They can show losses and possible related heating at additional costs. The idea here is to integrate the Lp and Lr components inside a single magnetic set around the transformer. The set of values is defined to fix the operating frequency range according to the Uout/Uin ratio to achieve. The turn-ratio of the transformer is another parameter linked to the resonant tank values. Example for a 3.5kW LLC full-bridge converter from 220-420Vdc to 200-450Vdc in the 70-200kHz range : Ns/Np = 1, Lp = 130µH, Lr = 22µH and Cr = 100nF (all at +/-5% tolerance).

This resonant topology is preferred in kW battery charging devices since the control in power is only made by frequency adjustment. According to the required output voltage-current needs (following the batteries charging load-chart), the control-loop and associated microprocessor calculate the switching frequency to apply to have the corresponding Uout/Uin ratio. Even if the voltage that is applied to the transformer is of a symmetrical bipolar wave-shape, the current shows a quasi-sinusoidal waveform which is a great advantage for higher efficiency by soft switching as well as for EMI reduction.

ZVS topology

The second possible topology is the ZVS phase-shift full-bridge which is a quasi-resonant structure to also reduce the losses in the semiconductors at switching instants (figure 2). In this, the control of the transistor legs is shifted between both diagonal of MOSFET or IGBT transistors and the applied duty-cycle reflects the calculated compensation to get the required output voltage Vout at a given Vin point. The ZVS inductor in series with the transformer is used to create the zero-voltage-switching condition with the self capacitance of each MOSFET transistor.

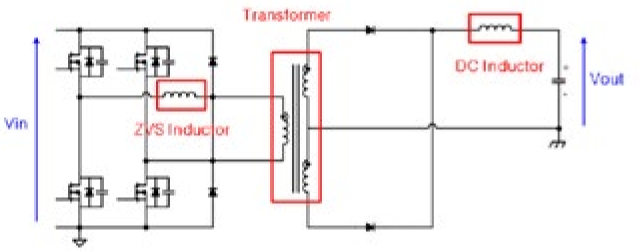

Figure 2: ZVS phase-shift full-bridge converter topology

Even if it is often requested to use the leakage inductance value of the transformer, this practice is not without any effect in the self heating of the transformer. As a matter of fact, a value from 5 to 15µH is normally necessary to create the ZVS condition with MOSFETs showing some 1-5nF of parasitic capacitance value. It cannot correspond to the self leakage inductance of the transformer without a bad coupling (k < 0.995) which generally leads to additional high frequency losses inside the windings which are crossed by the energy not stored inside the magnetic core. That's why a discrete additional inductor in series with the primary of the transformer is normally found (figure 3).

Figure 3 : ZVS transformer and its related serial resonant choke

In some cases it can be better to introduce also a thin gap in the transformer core to make its behavior more linear in case of any possible dissymmetry that can appear secondary side due to the rectifier bridge or any difference in the cabling length or contact resistance between the two polarities of the secondary. Thus the magnetizing inductance value of the transformer is of a slightly lower value but with a more accurate tolerance on it. Example for a 3.5kW ZVS phase-shift full-bridge converter at 100kHz : Lmag = 800µH+/-20%, Lzvs = 7µH+/-10%.

The integrated magnetic set

The idea is to focus on a magnetic set that provides all these alternatives at once in a single component. The main advantages are the size and weight reduction at a more competitive price. In terms of cost, one has to consider not only the cost reduction because one or two physical components less but also in terms of assembling process of the converter where less connections have to be made. Some interconnections can be also directly replaced by special techniques at the proposed magnetic set level.

Thus the result is a kind of magnetic set (figure 4) where we find a common transformer, showing or not an air-gap, and an additional choke in series with the primary winding. The magnetic core of both serial components is shared together at one side. The choke is the serial inductor Lr or Lzvs depending on the topology (LLC or ZVS). The transformer can include the Lp value if the center leg is cut to set the magnetizing inductance value at Lp.

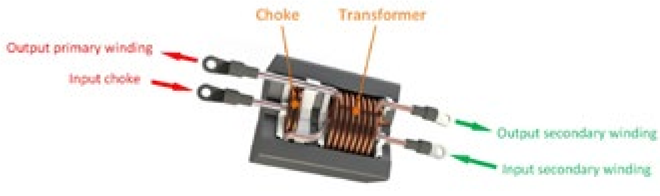

The magnetic set integrates both a transformer and a couple of resonant inductors

The use of low-losses high thermal stability ferrite cores as well as thin stranded and twisted conductors in parallel for the winding participate to the optimization of the losses versus temperature, input voltage range and current consumption according to the charging level of the battery.

The use of special isolated conductors is followed to fulfill the isolation and creepage distance as required by many electrical safety standards (UL-2202, IEC-61558…). As a matter of fact, the isolation requirements does not only include a high dielectric strength (typically 2.5-4kV) but also construction criteria like creepage distance, clearance and distance through the insulation to guarantee the reliability of the insulating system provided.

Conclusion

The size reduction of magnetic components embedded in battery chargers for the increasing demand of HEVs goes through the integration of the switching transformer and its associated resonant chokes on the same core while providing a reliable insulation and an efficient cooling capability. This 3-in-1 concept (1 transformer + up to 2 chokes) enables not only a volume and weight reduction but also a big cost saving because less materials and also a reduced connecting system (chokes and transformer partially linked internally) are used.

The work is not finished at that point and PREMO R&D has been already developing an innovative 3Dpower™ concept which will soon enable to design more compact solutions for the benefit of automotive SMPS. However the new BCIM Series (Battery Chargers Integrated Magnetics) is already presented as available standard products from PREMO catalogue.

PREMO is a Spain-based company engaged in the development, manufacture and sales of electronic components with a special focus on the growing market of HEV, smart metering and market segments including automotive, telecommunications and industrial electronics. Our product portfolio includes NFC and RFID antennas, power transformers, inductors and chokes, current sensors, EMC filters, PLC components and accessories. In addition to our broad range of standard components, off-the-shelf products, PREMO designs custom solutions to fit customer requirements.

www.grupopremo.com

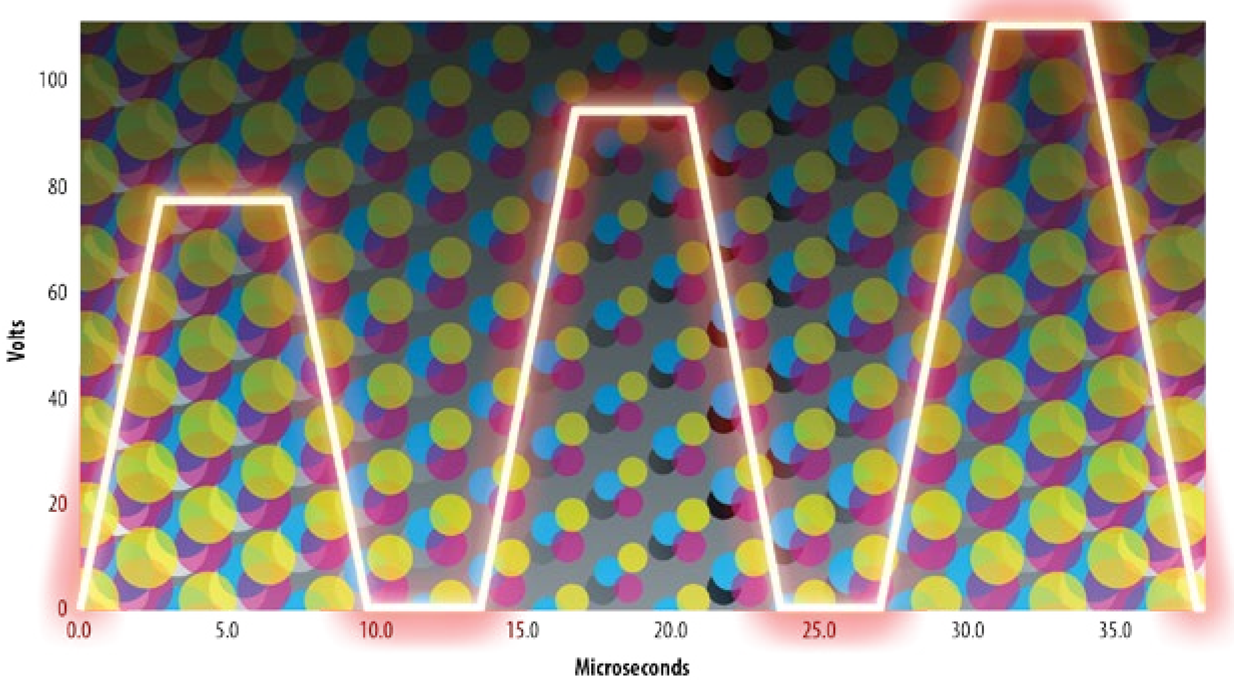

Drive Smart.

Generate Multi-Pulse Waveforms for Driving Multiple Inkjet Nozzles using the MP113 Digital Dual Channel Printer Driver

FIRMWARE MAKES DRIVING PRINT JET NOZZLES “EASY”

The Apex MP113 combines the simplicity of a digital interface with the high voltage, high current and high speed of a dual channel power operational amplifier. The onboard firmware supports user-defined, multi-pulse waveforms required for industrial inkjet printing applications. The MP113 solves the challenges of generating precisely timed, nozzle head data streams, and high fidelity fire pulses when driving a changing number of print nozzles. This comprehensive solution incorporates the digital control and system interface with a dual power amplifier rated at >10A PEAK per channel, 180V supply operation and provides output voltages up to 135V referenced to ground. Use this module to upgrade an existing drive system to grayscale printing, or as the integrated solution for an entirely new design while expanding the capabilities to print higher quality images by changing droplet sizes for greater color intensity.

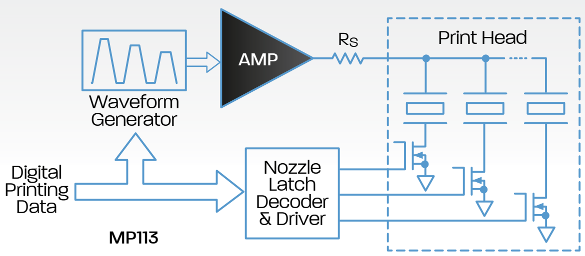

CARD EDGE CONNECTOR MODULE PACKAGE STYLE NC

Open Frame Product Technology
Footprint 110.5mm x 104.5mm

Power up at apexmic.ro/bodosMP113

apexmic.ro/bodosMP113

APEX MICROTECHNOLOGY

The Flyback Dc-Dc Converter

The best bet for most SMPS"

The Flyback converter combines lowest cost with best performance and is the optimum choice for offline SMPS up to more than 250 W. The simplicity of the circuit diagram is deceptive, it is highly complex. This article is a practical guide to optimum designs and lists the pitfalls.

By Dr.-Ing. Artur Seibt, Vienna

... Continue from October 2016 page 59:

5.5 RMS currents, winding losses.

The losses in the windings and all other resistances depend on the rms values; the rms value of a trapezoid is between a sawtooth and a square wave.

$I_{rms} = I_{av} \times {}^2 \times \sqrt{\tau} \times \sqrt{(k2 + k + 1)/[3(1 + k)^2]}$
$= i_{p,max} \times 0.577 \times \sqrt{\tau} \times \sqrt{(k^2 + k + 1)}$

k = 0 = sawtooth: $0.577 \times i_{peak} \times \sqrt{\tau}$ k = 1 = square wave: $i_{peak} \times \sqrt{\tau}$

For k = 0.5 it follows: I_{rms}, CM $= 0.76 \times i_{p,max} \times \sqrt{\tau} = 0.51 \times i_{p,DCM} \times \sqrt{\tau}$

I_{rms}, DCM $= 0.577 \times i_{p,peak, DCM} \times \sqrt{\tau}$.

CM rms current is thus only lower by 0.51/0.577 = 0.87 or 13 %.
On one side it is true that all losses proportional to the rms current squared are lower, but the number of turns and the winding resistance are 73 % higher. Assumed the wire size and τ remain the same, and the DCM values are considered for reference 1:

$P_{Cu, DCM} = 1$ $P_{Cu, CM} = 0.757 \times 1.73 = 1.31$

Hence the losses are higher by 31 %. Whether the assumption of equal τ is justified, would have to be checked in each case, because τ is much more modulated in DCM. The current density in the wires would be reduced only by 13 %, this is hardly a justification for selecting a thinner wire which would cause higher losses. Nor does this suffice to compensate for the increased winding space.
Note that the rms currents in FB's with several output voltages are interdependent and can have varying waveforms. Therefore it is mandatory to measure all rms currents in all relevant load combinations, otherwise windings, diodes and electrolytics may be overstressed!

5.6 Voltage stresses on the semiconductors.

An increase of the primary number of turns by 1.4 to 1.73 means that, the number of secondary turns unchanged, N will be increased and the reflected voltages by the same factor. Remember that the numbers of turns have no bearing to the voltages. Example: $V_{out} = 24$ V, N = 10, VB = 360 V. With DCM, the reflected voltage on the primary would be 240 V, with CM it would increase to 336 resp. 415 V. While with DCM the stress would be 600 V, it would rise to 700 resp. 775 V with CM and rule a 650 V Coolmos out. There are 800 V Coolmos, but they are more expensive and the Rdson is higher. Also emi would become worse. The factor 3 for the Lp increase would not be realizable because 775 V is much to close to 800 V. N could be reduced by increasing the number of secondary turns, but this would require still more winding space and cause higher losses.

5.7 Losses, efficiency.

Efficiency eventually has become the catchword, norms require > 87 % even at low loads, very low standby power etc. Although these figures do not yet apply to all offline SMPS, this will follow in due course. Quite independent of these regulations, the very compact supplies do not allow high losses. Comparisons of total losses will, in most cases, be in favor of DCM. The smaller and less expensive transformer also counts. In particular:

Winding losses:

These were treated above. In addition to the resistive losses of CM the larger winding adds higher capacitances and dielectric losses.

Losses in the active components.

Even if Schottky diodes are used in the secondaries, the higher turn-on switch losses remain. With standard Si ultrafast diodes there will be higher losses in the diodes and the switch. With DCM, there are only losses by the discharge of capacitances, but switching-off losses may be higher.

Losses in the magnetic circuit.

DCM suffers from higher AC drive and the higher peak current. With CM, the drive is lower, but on a high ip,min pedestal, i.e. in an area of higher core losses. The higher amplitude DCM sawtooth will not necessarily cause higher core losses, this must be checked in each case.

Summary of the comparisons.

DCM advantages: 1. The transformer is smaller und less expensive. 2. Simple regulation. 3. Fastest converter. 4. Uncritical, less expensive secondary diodes. 5. The switching transistor turns on at zero current. 6. Lower peak voltages on the semiconductors, lower emi.

Disadvantages: 1. Higher peak currents, because the inductances are lower, the average currents are identical. 2. AC core drive level higher, not necessarily higher core losses. 3. Higher ripple currents in all active and passive components, larger capacitors. 4. Without a regulation loop or a defective one it is a constant-power resp. constant-current generator, without a sufficient load the output voltage will rise to destructive levels.

Advantages CM: 1. Constant-voltage generator. 2. Lower peak currents. 3. Lower AC currents, lower ripple current loads.

Disadvantages: 1. Bigger and more expensive transformer. 2. Higher switch and diode losses. 3. Higher winding losses. 4. Regulation loop design more complex. 5. Slower.

Whether DCM or CM is best has to be studied in each design because of the very many parameters and interdependencies

6. Transformer design.

FB transformers are by far the most difficult ones in SMPS design, especially for offline SMPS, because, apart from technical viewpoints, safety and emi norms have to be observed in addition; transformer manufacturers have to use one of the acknowledged insulation systems. These items can not be treated within the scope of this article, the reader is referred to the pertinent literature. Also, the reader is kindly requested to refer to the article "The Focus is on Passive Components ..." in Bodo's Power Oct. and Nov. 2015 which treats winding and insulation materials, the skin and proximity effects and their influences on transformer design. The knowledge of the basic equations for magnetic circuits and the catalogs of major ferrite and transformer materials (like coil formers etc.) manufacturers like Ferroxcube or Epcos are indispensible.

With special regard to young engineers, the practical procedure is explained step by step. This is not a chore for a young engineer. "... even a novice can ...", no, he can not! Nor is it "child's play".

New designs require iterations because so many parameters which are partly interdependent, partly contradicting, have to be reconciled. There is no direct route to the optimum transformer, the allegations of diverse software programs are arrogant and misleading. It was explained that even grossly wrongly designed FB transformers often function. The designers of such software claim that their program contained "the experience of decades". How come that they did not learn in decades, e.g., that such important parameters like diode blocking voltages exist and must be observed. During the design iterations the designer has to take repeated decisions before continuing which no software can take. The design task is expressly to create an optimum and not just any transformer, not only for cost reasons, this chapter will show that the transformer has the overwhelming influence on the operating mode, the stresses on components, the efficiency, so only an optimum design will ensure best performance and reliability. Today optimum efficiency is asked for, so also dielectric losses have to be considered. If several outputs are needed it depends entirely on the transformer design how well those will be stabilized under variable load conditions; a poorly designed transformer will require postregulators which add cost, need space and generate losses; a professionally designed one can hold output variations within a few percent.

Fixed-frequency, hard-switched operation with CMC is assumed which is most appropriate, reliable and gets away with the smallest transformer. As long as there is yet no transformer, windings and their resistances are unknown, losses are disregarded, they are introduced in the last step. At the present state-of-the-art of power switches, Coolmos and especially cascodes, high performance ferrites and winding materials, FB's own the territory to beyond 250 W. With SiC cascodes higher output powers are possible. However, for higher powers than 250 W it is advisable to partition the load among two or more FB's driven by a multiphase clock.

6.1 1st step: Core selection.

The first step is the selection of the type and size of a magnetically satisfactory core, it is essential to realize that this means just that, it does not ensure that a transformer with that core will provide enough winding space! This is a separate condition to be fulfilled; if it turns out in the course of the design that a bigger size will be required, all calculations of the magnetic circuit will have to be redone which will again lead to reduced numbers of turns and less winding space needed. Right here it becomes obvious that the design consists of a series of iterations.

In Europe, the US and other countries there are standardized core types and sizes, listed in the catalogs resp. on the home pages of the ferrite manufacturers. The European types are based on the metric system and should be preferred; in the last years many US types based on the inch system were added which mostly differ little and offer no advantages. The selection criteria are:

1. Dimensions. 2. Cost. 3. Second sources.
4. Performance. 5. Other criteria like stray fields.

Dimensions come first because the transformer is the biggest component in a power supply, the designer may, e.g., be forced to select one of the special low-profile core types. Planar transformers are the lowest-profile types, but their design should be left to specialized firms. In higher power SMPS, the electrolytics may be the tallest; unless absolutely unavoidable, low-profile electrolytics should be shunned, because their life expectancy is lowest. After a first selection of those core types which come into consideration, the next step is to select the one best for the application. Single-source components are an absolute no-no, they must be considered as non-existent. Some manufacturers created non-standard types and their own ferrites in order to lure customers into a single-source trap; even if such a nonstandard type would fit, it must be rejected. If a designer chooses a single-source component, his purchasing department is not only forced to nod to any price the supplier will ask for, but if he can not deliver for some reason or other, production will stop. Most control ic's these days are single-source, requiring a redesign or a new design of the SMPS if not available. This is dangerous, because in the past there were fairly few control ic's which were standards and multiple-sourced; today, a single manufacturer offers dozens and hundreds of such ic's, products will be cancelled very fast if the expected volume or profit was not realized. As the transformer is always the most expensive component in a SMPS, it is wise to share the final decision of core type and manufacturer(s) with the purchasing department which has its own viewpoints on suppliers. The purpose is to create a winding prescription for the purchasing department which it can distribute to several transformer manufacturers. If transformer design is farmed out to a manufacturer, the design would be his, so competition would be excluded.

There are magnetically superior types like the pot cores (RM, PM etc.) which also do not radiate, there are types like the ETD cores which are designed especially for low leakage. Traditionally the E- resp. EE cores are the lowest cost types which were derived from 50 Hz iron core transformers, but differ somewhat for ferrite cores! Cores and coil formers are simple and available from a host of suppliers. However, their strong stray fields increase the leakage and can couple into the circuit and cause severe malfunctions and false measurements. Before triple-insulated wires were available, many types like pot cores were not eligible for offline SMPS because the 8 mm clearance was impossible. E cores and their derivatives were preferred, on both sides of the layers 4 mm were left free; a poor solution, especially for small transformers, because this not only costs winding space, but increases leakage. Triple-insulated wires allowed down-sized and magnetically improved transformers.

The decision to take: if the dimensions of EE cores are acceptable, will they fulfill the other requirements or is a better type required. The problem is that any influence of the stray fields will show up very late in the SMPS design phase. By proper orientation and clever component placement as well as correct routing of critical conductors it can be handled.

Starting point: Energy content.
The core type settled, which size is the next question; in the following it is assumed that E cores are selected, they range from tiny to sizes good enough for several hundred watts. Where to start? In general, nearly quadratic core types are preferable, this is the reason for the versions of one type with different core thicknesses. Hence, before going up in size it is better to choose the version with the thicker core.

The solution is based on the fact that the transformer is a storage choke, capable of storing the amount of charge necessary to supply the load and all losses at the operating frequency. This amount of charge will be transferred - NOT transformed - f times per second to the output. Starting from the basic specifications Pmax, VB,min and assuming a partition of 50 % - 50 % for charge and discharge as a reasonable starting point, the following equations from chapters 3 to 5 apply in this case:

$P_{out} = 0.5 \times L_p \times i_{p,\,peak}{}^2 \times f$ $\qquad L_{p,max} <= V_{B,min}{}^2/8Pf$

$L_{s,max} =<= V_s{}^2 /8Pf$

They are strictly only valid for fixed frequency DCM, but yield satisfactory first approximations. The frequency is assumed 100 ... 140 KHz. Below 100 KHz has been the state-of-the-art 30 years ago; 150 KHz is a practical limit, because EMI norms begin to become strict, they are strictest from 0.5 to 5 MHz, so the 3rd harmonic of the clock frequency should also stay < 500 KHz. If the increased expense for emi suppression and the higher losses are accepted, up to 250 KHz are possible; this depends mainly on the ferrite, see below. The control ic must already be selected and its built-in duty cycle limit, e.g. 50 % known, because the transformer must guarantee that under worst circumstances the duty cycle stays below. Design for 40/60 % will be a reasonable choice. The necessary storage capacity is given by

Energy content $E = I^2 L = 2P/f$ (Joule) by rearranging the basic equation.

The two factors can in principle be interchanged. The energy is stored in the air gap, which reduces L which allows the current to reach higher levels in a shorter time, but first decreases P. The equations show there are limits to L_p and L_s if DCM shall be ensured. For the determination of an approximately satisfactory core size, first only L_p needs to be considered. $L_{p,max}$ can be calculated with the formula above. $i_{p,peak} = \sqrt{i_{p,peak}{}^2}$. The current rises with a speed given by di/dt = V/L; if it can not attain the necessary ip,peak within the 40 % assumed, the desired P can not be achieved. So L must then be reduced and $i_{p,peak}{}^2$ raised until the product E can be realized If, e.g., L is reduced to ¼, the number of turns n to 1/2 , $i_{p,peak}$ has to rise by a factor of 2. The $\Theta = I \times n$ remains constant.

Magnetic relationships..
From Θ follows the field strength $H = I \times n/l_{core}$. The crucial parameter is however the flux density $B = \mu_0\, \mu_{rel} \times H = \Phi/A_{core}$, where Φ is the magnetic flux. For the selection of a core and final checks these forms of the equation are most handy:

$B = 1.26$ Gcm/A $\times\, \mu_{eff} \times I \times n/l_{core}$
[I in A, l_{core} in cm. Result in G. 1 G = 10^{-4} T = 10^{-8} Vs/cm^2]

$B = A_L \times n \times i_{peak} /A_{core}$

A_L is the inductance factor of a coil or winding,
$L = A_L \times n^2$ resp. $n = \sqrt{L/A_L}$

μ_{eff} is a dimensionless factor for a specific core with a specific air gap for a given ferrite, to be taken from the catalog data as well as A_L . $l_{gap} = \delta$ is not needed for any calculation because it is implied in A_L resp. μeff . Some ferrite manufacturers specify their core series by A_L, some by δ. This is why the first equation above is most appropriate.

► Only cores those cores are adequate which allow an operating $B_{peak,100}$ at 100 C.

Ferrite considerations
The higher the operating $B_{peak,100}$, the more power can be moved through a transformer; in a given winding, B_{peak} is proportional to i_{peak} , $P \sim i_{peak}{}^2 \sim B_{peak}{}^2$, a better ferrite allows a smaller transformer and lower losses, but it is more expensive; on the other hand the smaller core and the smaller coil former cost less. A smaller transformer offers more benefits: 1. The smaller the transformer, the


Can you engineer Power Electronic solutions of tomorrow?
Danfoss Silicon Power is growing!
We are looking for bright individuals to join us on our exciting journey.
Are you our new colleague?
Are you ready to engineer tomorrow´s power electronics for automotive, industrial and renewables applications?
Interested? Discover more at www.danfoss.com/career
www.siliconpower.danfoss.com
ENGINEERING TOMORROW
Danfoss

larger the specific surface for heat radiation. 2. Winding resistances and losses are lower. 3. Also the ferrite losses depend on the volume. 4. Capacitances will mostly be lower. As the only "penalty" is the price of the ferrite, it will turn out eventually that the higher price for a premium ferrite pays off; it is justified because extremely pure iron oxides have to be used, and the final heat treatment which belongs to the trade secrets, is more complicated. There is much black art in ferrite production, so there are only a few manufacturers in the world which can deliver these qualities. Ferrites for SMPS use are made of MnZn, useful to about 2 MHz. But high B's can only be used up to about 250 KHz, above the B's have to be drastically reduced as the losses rise steeply.

f x B_{max} is called the Performance Factor. Fig. 6 depicts f x B_{max} of some Ferroxcube ferrites ; it shows how much the modern ferrites like 3C96 surpass the older materials like 3C90 or 94. It also proves that the optimum frequency extends to about 250 KHz. This picture does not yet include the flat-temperature materials 3C95 nor the extended saturation materials like 3C92 or the materials for higher operating temperatures.

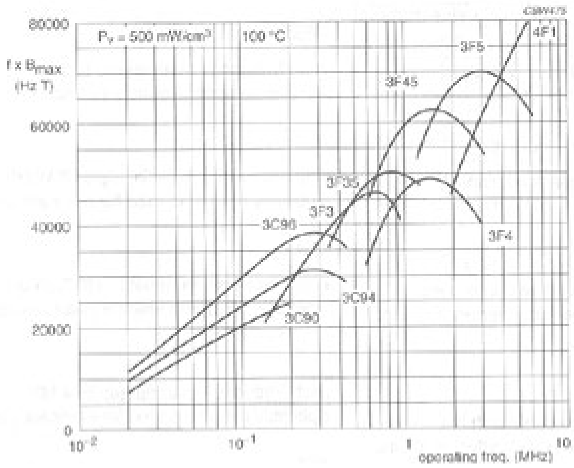

Fig. 6. The performance factor f x Bmax of some Ferroxcube ferrites.

All power ferrites except these new materials show loss curves vs. temperature which fall towards a minimum around 100 C; the "95" type materials have a flat curve. There are special types with the loss minimum at 60 C and such for up to 140 C. Beyond the respective minimum, the curves rise steeply towards the Curie temperature around 220 C.

The other major manufacturers have equivalent materials so second sourcing is assured, but the designations all differ. The topic "ferrites" far exceeds the scope of this article and will be deferred to a future one. Important in this context are these items:

1. All 25 C specs are for the birds and have no practical meaning whatsoever! No power supply remains at 25 C in operation. The internal air temperature is rather between 60 to 85 C, and the transformer must heat up more in order to get rid of its heat. And the parts of the core which are inside the coil heat up most. Therefore only the 100 C values are of practical use.

2. Do not mix up the B values in the socalled "materials specifications" with practically usable ones, they are always higher and illusory. Many core types suffer from deficiencies like unequal areas and flux concentrations, consequently only a lower value of B_{max},100 is permissible, this value is not always given in the data; in these cases, it is safe to derate the material's spec by 20 to 25 %.

Size selection method 1: With some experience.

The route to core size selection is now clear: after picking a size which might suffice one picks a gap length which might be right, reads the 2 parameters from the data sheet and, inserts them in first equation for B above; if the B calculated is below the B_{peak}, 100 of the selected core, heureka. If not, a larger gap is tried, if that does not lead to a solution, the next bigger core is picked and so forth. There are several routes to core selection, manufacturers have their preferences and differ in the data they offer for that purpose.

If there is already some experience, this is the fast route. Example: the core estimated to be satisfactory is an E 42/15; the data sheet delivers the following table:

AL	μ_{eff}	air gap/mm
100	43	4
160	69	2
250	108	1.5
315	137	0.85
400	173	0.63

The A_L values are standardized.

Air gaps of 2 mm are rather uncommon with such a small core, because δ/l_{core} must remain within reasonable limits, from experience it is known that A_L 's mostly range between 250 to 400. So 1.5 mm is first chosen. The number of turns for the $L_{p,max}$ calculated in the beginning follows from n = $\sqrt{L_{p,max}/A_L}$. Now n, l_{core} , i_{peak} from above and μ_{eff} for 1.5 mm are entered into the formula for B and checked whether this value is below a reasonable operating $B_{max,100}$ for the ferrite selected. 3C96 assumed, in the material's spec, the saturation flux density at 100 C is 0.44 T. From the hysteresis curve it follows that one should stay clear of 0.35 T. The diagram for the losses as a function of B with the frequency as the parameter and the spec of 300 KW/m3 at 0.2 T indicate that one should rather stop at 0.3 T. This is still based on the materials spec. In the core's specs, there is none for a Bpeak,100, only a spec for the losses at 100 KHz, 0.2 T for the similar 3C92 as a guidance. $B_{peak,100}$ should hence be limited to 0.25T. The waveform has a strong influence, all the catalog data are taken with sine waves while the sawtooth or trapezoids cause different losses. It is therefore possible to let the peaks of the waveform go up to 0.28 .. 0.3 T. There is no other way as to pick such a reasonabe value and to proceed with transformer design. In any case, it will be necessary to measure the inner core temperature in the actual worst case operation, it must not extend into the steep part of the losses' curve above 100 C.

If this first assumption resulted in too high a B, A_L = 160 can be tried. If in the first test B was much below 0.23 T, A_L = 400 can be tried. Nonstandard air gaps are possible if ungapped cores are bought, there are companies specializing in core gapping. The formulas follow.

Bear in mind that this calculation only proved that this core size is magnetically ok, whether the windings will fit is indeterminate at this point. If it should turn out later that they will not fit, a bigger size has to be selected, the determination of the optimum air gap would then have to be repeated and yield a higher A_L and thus a lower number of turns.

The special high Bmax grades like 3C92 deserve attention; they are destined for all applications where the core is driven far towards saturation. This applies in the first place to all such chokes where a fairly low AC ripple is ontop a high DC bias. It is the material of prime choice for PFC chokes. In transformer applications, losses are somewhat higher than with standard premium power ferrites like 3C96, Experience shows that one should always perform the calculations also for 3C92 and build test samples; in many cases 3C92 will turn out to be superior, because the higher Bmax allows higher power resp. a smaller and less expensive transformer!

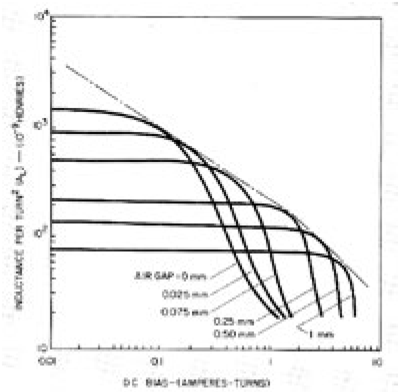

Fig. 7. Inductance per turns squared of a material. These curves look alike for all materials. The designation "DC bias" on the abscissa is misleading, because only the peak Θ = ipeak x n counts. If it is known, the necessary air gap can be read from the graph. However, if the temperature is unknown for which the curve is valid, it can give only a rough indication.

Size selection method 2: via the curves A_L vs. i_{peak} with the air gap δ as parameter.
Some manufacturers provide such curves like Fig. 7.

Size selection method 3: Hanna curves.
The Hanna curves were published 1927 and show the energy content E = L x ipeak2   per volume in cm3 of a given core vs. the field strength H in Oe with the relative air gap δ/lcore as the parameter. They yield the air gap and the number of turns for the desired L.

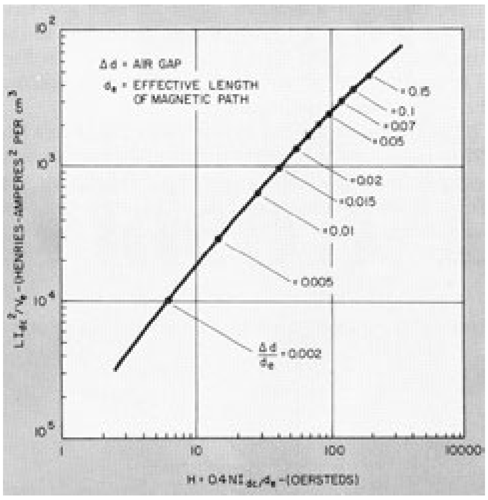

Fig. 8. An example of Hanna curves.

There is a curve for each core. Their use requires some caution; lower points may already be close to saturation! Procedure:

1. First calculate $L_{desired}$ x $i_{peak}{}^2$ / V.
2. Now the curve is entered, preferably in the center region, also there, some points may already be close to saturation, and one does not know whether the saturation level on which the curve is based is the 25 C or 100 C. Ferroxcube specifies for 25 C. Hence Hanna curves should be used with care and the values obtained checked by calculations. But they give at least an approximation.
3. Determination of the air gap: from the value calculated above on the vertical scale move to the right and read δ/l_{core} (in the picture called "$\Delta d/d_e$ "): δ = δ/l x l.
4. Determination of the number of turns: Read the corresponding value of H (Oe) on the abscissa. 1 Oe = 0.8 A/cm. H = 0.4 x n x i_{peak} /l_{core} [Oe]. n = H (Oe) x l_{core} /0.4 i_{peak} .
5. Final check of B whether it is below the permissible $B_{peak,100}$.

There is a more practical version of the Hanna curves (Philips) : P x f/ f_{ref} on the abscissa, A_L resp. $\sqrt{A_L}$ on the Y axis and a set of straight lines from top left to right below for the various standard sizes of a core type, completed by a set of straight lines from left below to top right with the ampere x turns. This diagram is based on the formulas:

$0.5\,LI^2 = k_1 \times n \times I + k_2$ $\qquad$ $P = 0.5\,LI^2\,f$ $\qquad$ $AL = L/n^2$

The first formula should provide an approximate linear relationship for the non-saturating portions of the Hanna curves. The procedure for using this diagram is this: determine P x f/f_{ref} , draw a vertical line from this value to the abscissa, this will intersect the curves for the core sizes at those values of A_L which correspond to saturation (probably 25 C). As A_L is only available in those standard values, one has to choose whether to pick the value at the point or a higher value of a bigger core.

Size selection method 4: via curves AL vs. δ with the core sizes as the parameter.

Some manufacturers provide curves like Fig. 9 which shows an example for pot cores. Here, A_L is shown vs. δ with the sizes as the parameter. The curves show that often several sizes are eligible; it is preferable to select the bigger one and directly check Bmax with the above formula.

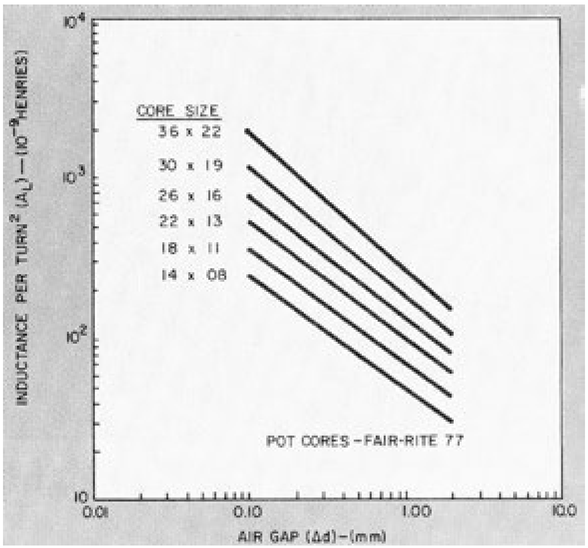

Fig. 9. Core selection by AL vs. δ

Size selection method 4: I2 L curves vs. δ

Most manufacturers offer curves which only require to calculate I2 L, the volume is already taken into account by showing all sizes of a core type as the parameter. This is the most practical and popular method. Fig. 10 shows these curves for E cores.

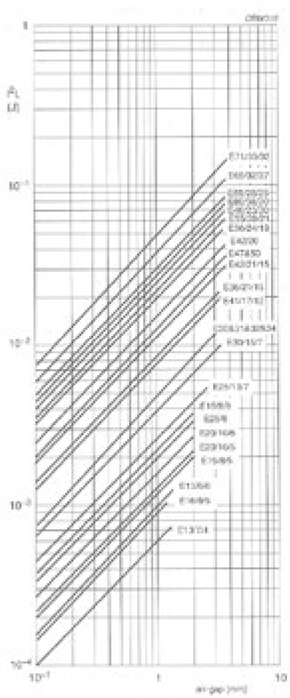

Fig. 10. I^2 L vs. δ curves for E cores (Ferroxcube).

To the right of the I^2 L value on the ordinate all core sizes and the appropriate air gaps are shown which would fit. As these curves are provided for all core types, it is easy to see which core sizes would fit in the various types. Ferroxcube states that all specs pertain to 25 C. It is therefore wise to directly select one size bigger than indicated and remain rather in the middle, i.e. small air gaps and very wide ones should be disregarded.

► Remember that, irrespective of the method used, $B_{max,100}$ eventually has to be checked, using the data sheet values and the formula given above.

This completes this step, the result is a core size only commensurate with the requirements from the viewpoint of the magnetics. Whether the windings will fit, will be a different story.

6.2: 2nd step: Primary winding and transformer size determination. Simple case: choke.

The procedure for determining the primary winding is in principle identical to that for designing storage chokes, e.g. PFC chokes. In such cases there is a fairly small AC ripple ontop a high DC bias (in case of PFC chokes those are the peaks of the 100 Hz half-sine). Therefore it is admissible to use a higher $B_{peak,100}$; the true rms value causes winding losses, the AC part core losses. Note that the current consists of the 100 Hz half-sine and the high frequency sawtooth ripple which is typically 20 %; this applies to the high-quality PFC, the inferior PFC types have a high frequency ripple of twice the average line current, so their chokes are far bigger, lossier and more expensive. The popularity of the inferior PFCs is due to the misconception that a cheap control ic also means a cheap PFC. Comparing complete designs resp. BOM's counts.

Transformer size selection.

In transformer winding design only the total height counts, calculations based on the winding volume are too inaccurate; this is especially true in case of offline transformers which require a lot of insulation. In most cases it is standard to split the primary in two halves, one at the bottom, one on top, so there are two insulation barriers. Also, as will be seen in the following chapters, the secondary winding construction can be very complicated.

At this point it is important to note that the designer may well have decided to operate in CM and with a 20/80% partition, but no final calculations can be performed because there is still no transformer, only a core! The assumptions taken in step 1, i.e. a 50/50 % partitioning and DCM are reasonable starting values; if eventually CM is desired, it is clear from the outset that the transformer will become bigger.

With the formulas from step 1 resp. chapters 2 and 3 L_p can be calculated:
$P_{out} = 0.5 \times L_p \times i_{p, peak}{}^2 \times f$ $L_{p,max} <= V_{B,min}{}^2/8Pf$
$L_{s,max}$ =<= $V_s{}^2$ /8Pf

$n = \sqrt{L/A_L}$ yields the number of turns; the rms current follows from the general equation:
$I_{rms, DCM} = 0.577 \times i_{p,peak, DCM} \times \sqrt{\tau}$. for 50/50 %: = 0.4 x i_{peak}

For each transformer type and size there exists a maximum current density which depends on the size (smaller sizes have a better surface-to-volume ratio and allow more). Please refer to the article "The Focus is on Passive Components" for an explanation of wires and insulation materials. PFC chokes as well as primary windings use hf litz. For a start, one can take current density values from the same size 50 Hz transformers' norms' data sheets for magnet wires. The copper area follows from: $A_{Cu} = I_{rms}$ /S (current density), the outer diameter is taken from a table of hf litz. There are insulation materials like Teflon which allow much higher temperatures than the enamel on copper wires. But the current density figures given for the specific transformer sizes are based on definite copper losses which heat the transformer to a definite temperature. Even if high temperature materials are used, one can not allow the winding to get too hot, because the standard power ferrites show sharply increasing losses above 100 C and would run away! In order for the ferrite to get rid of its heat and stay below 100 C, a temperature difference to its surroundings must be maintained. A thermal run-away towards the Curie point would result in loss of permeability and destruction of the switching transistor with ensuing burning of the transformer. If this should happen, for verification clip a DC/AC current probe around a primary conductor of a new sample with temperature sensors within the winding close to the core and on the core inside the coil former and watch. The onset of thermal runaway resp. saturation is very fast. This is why the finished transformer must be thoroughly tested, for temperatures and electrically.

The hf litz type which provides the necessary copper area selected, the winding width is divided by the litz' maximum outer diameter which yields the number of turns per layer. Dividing the total number of turns by this number gives the number of layers. This figure multiplied by the litz' maximum outer diameter gives the height of the winding. In case of the primary the 4 KVrms insulation must be added for each half. A 10 % reserve should be provided.

This check of the winding height for the primary will show how much is left for the secondary, if less than half is left, choose the next bigger size core und iterate, until half the height is available. Each time a bigger size is selected, A_L will be increased, np decreased, due to greater winding width the number of layers and the height will be reduced further; but the wire size may have to be increased, because the current density permissible will be lower. The interdepence of all parameters is obvious. The necessary barrier for 4 KVrms test voltage is achieved, if either P or S are wound with triple-insulated approved litz. However, Furukawa litz is only available with 7 strands, so, for higher power transformers, several wires have to be wound in parallel which wastes winding space. Rubadue can provide hf litz with hundreds of strands, also Teflon-insulated for lowest dielectric losses. In most cases it is the primary which uses the triple-insulated litz, especially if there are several secondaries.

The transformer size thus defined, with a half empty coil former, will be close to the final one if DCM or "mild" CM operation is used. For "deeper" CM operation the primary winding should already here be increased; repeating from the foregoing chapters it is not advisable to exceed Lp,CM = 2 x Lp, DCM which requires an increase of np by a factor of 1.4. Remember that CM is not only defined by Lp but also by Ls which is still unknown. This will in most cases require a bigger transformer.

Although the primary of an offline transformer will practically always have a much higher number of turns than the secondary, also here rules the strict requirement that only full layers are allowed! So one must play with n and the wire size to realize full layers. It this should not be possible, the last layer must be evenly distributed over the whole winding width. In order to minimize the voltage between layers, Z winding should be preferred which also helps to alleviate the dielectric stress. The beginning of this half, on the bottom of the coil former, is the hot end and is connected to the drain of the switching mosfet which has to be placed so that this connection is as short as possible. The end of the winding is thus almost cold, and here the low voltage auxiliary winding for feeding the primary side control circuitry is placed and distributed

Another problem arises if the core has an overly large air gap: the stray field will be strong and induce additional losses in the windings directly above; in such cases there should be no turns above the air gap at least in the two bottom layers.

Last, by far not least: the insulation barriers between the primaries and the secondaries must conform to the safety norms. However, in the author's opinion, the usual materials are not good enough. Most triple-insulated wires and litz use low-cost thermoplastic materials like polyester, nylon etc. which melt beyond their maximum operating temperatures, so does polyester as a barrier. The insulation properties of these thermoplastic materials deteriorrate drastically with rising temperature! A burning winding can reach much higher temperatures. What about the primary fuse? The typical failure is a destroyed switching transistor, this places the primary directly across the line, i.e. up to 254 Vrms ,maybe only 90 V. The fuse must be rated for the highest current at low line, i.e. 90 V, and it must withstand the current surge at turn-on at 360 Vpeak without fatigue. Fuses are frequently rated for a much higher current than in normal operation. The author has seen 4 A fuses in a 75 W SMPS made by a big concern. A fuse must withstand 1.5 rated current for at least one hour, in that case 254 V x 6 A = 1.5 KW can flow into this SMPS for one hour. To make a long story short: it is highly recommended to use barriers of twice Kapton; this material takes 400 C and disintegrates at 800 C without obnoxious gases. Kapton is expensive, but in those small transformers very little is needed.

6.3. 3rd step: Turns ratio(s)

Lp and the number of turns for the core selected sofar are known, all on the assumption of a 50/50 % or 40/60 % partition of a period. The paragraph above described how to arrive at the winding height of the primary. Keeping to the step-by-step procedure, the turns ratio has to determined.

► Remember that the numbers of turns and the turns ratios of a FB transformer have nothing to do with the primary and secondary voltages.

► Contrary to most texts there is not one turns ratio, but a range.

The turns ratios N are determined first of all by the permissible peak voltages on the switching mosfet and the secondary diode! Regarding the reflected voltages, the transformer indeed acts as one. Whether a PFC precedes the FB converter or not: the maximum input voltage VB,max = 360 V. This pertains to a well designed PFC, others need output voltages up to 420 V. The switch will be a Coolmos or a cascode with an upper mosfet. Please refer to the former articles in Bodo's Power for details. The standard Coolmos takes 650 V, there are 800 V types, but they are unnecessary for offline SMPS. Beyond this voltage the part will enter a nondestructive avalanche breakdown; the energy in this mode will be dissipated, the part will survive as long as it is not overheated. Principally, the part could break down in each period, but this is not advisable, because avalanching is a stochastic process which generates output ripple and emi. Note that only individual mosfet's have a rating, the high voltage transistors on one-chip ic's will be destroyed by any overvoltage! Samsung invented the two-chip components which comprise a standard mosfet chip and a control ic on the same leadframe, these are available from several manufacturers, the best combine a Coolmos and a CMC control chip, e.g. from Infineon.

Behind the reflected voltages there are "hard", i.e. low impedance voltage sources: the primary and secondary capacitors, the transformer is low impedance and low leakage; it is therefore of vital importance to ensure that the sums of the reflected and the primary resp. secondary voltages do not exceed the blocking voltages of the switch resp. the diode(s), because this would destroy them. With a 650V Coolmos and a V_B = 360 V, the maximum permissible reflected voltage would be < 290 V, so < 250 V would establish a reasonable design margin. Spikes of some ten ns can be allowed.

In the following example it is assumed that there is one output voltage V_{out} = 5 V and that the blocking voltage of the diode is 45 V, typical of a low voltage Si Schottky. A 30 % margin would allow 32 V. Note that Schottkies can not absorb overvoltages resp. very little. Spikes have to be damped by RC's.

In order to stay below the maximum voltage across the mosfet
$V_{max} <= V_{B,max} + V_{refl,S-P}$. or
$V_{refl.S-P} = V_{max} - V_{B,max} = V_{out} \times N$.

It follows that
$N_{max} < (V_{mosfet,max} - V_{B,max})/ V_{out} = 250/5.6 = 45$. Note the 5.6 V.

A high N is good for the diode, but if it is too small, the diode will be endangered. $V_{D,max} = V_{out} + V_{refl,P-S}$; $V_{refl,P-S} = V_{B,max}$ /N.

A lower limit for N follows:
$N_{min} > V_{B,max} /(V_{D,max} - V_{out}) = 360/27 = 13$

A low N is good for the mosfet.

► Permissible N range: Nmax > N > Nmin

In the course of all iterations N must be kept within this range. For a start, it is reasonable to choose the average value

$N_{av} = (N_{max} + N_{min})/2 = 58/2 = 29$

Of course, the final value may differ, but it is mandatory to stay within this range which incorporates safety margins. Note that these days there are no reserves in the specs, i.e. if a 100 V mosfet measures 101 V in final test, it will be delivered.

6.4. 4th step: One secondary winding resp. output.
The design of the secondary winding(s) is the most difficult task in FB transformer design. Note in the first place, that all secondaries must have the opposite polarity of the primary, if those are connected wrongly, the SMPS will "kind of" function, namely as a forward converter which may or may not be noticed, mostly high losses and overheating will point to this. The regulation loop always tries to bring the output up to the programmed voltage.

In chapter 6.2 the - still preliminary - size of the transformer and its AL were defined. Because N will have to be limited to the range Nmax to Nmin it is now necessary to know np which follows from np = $\sqrt{L_{p,max}}$ /AL . In order to set up an example, it is assumed A_L = 250, P = 100 W, it is further assumed that this FB is fed by a preceding PFC with 360 V, so this is $V_{B,min}$ = 360 V.

$L_{p,max} = V_{B,min}^2$ /8Pf = 360^2 V^2 /(8 x 100 W x 100 KHz) =
1,6 x 10^{-3} V^2 /VA x s^{-1} = 1.6 x 10^{-3} Vs/A = 1.6 mH.

$n_p = \sqrt{L/A_L} = \sqrt{1.6\ \text{mH}/250\ \text{nH}} = 125$

n_s may thus only vary between 125/45 = 3 and 125/13 = 10. Remember that these N limits stem from the specifications of the semiconductors and are rock-solid resp. any change would require other semiconductors. If, e.g., the 45 V of the Schottky diode is considered too low, an ultrafast Si diode would offer 200 V before becoming too slow, but would have somewhat higher losses. As mentioned 600 V SiC diodes outperform Si ultrafast down to appr. 24 V output, so this would offer considerable leeway.

With N_{av} = 29 n_s = 125/29 = 4

Disregarding the other secondary parameters for a while, but remembering that low leakage = tight coupling is absolutely essential for a FB transformer, it is evident that 4 secondary turns spell miserable coupling, this is totally unacceptable! Nor is 10 turns any better. The transformer E 42/15 which can easily handle 150 W, the example in a preceding chapter, e.g., has a winding width of 26 mm, spreading the 4 turns over the 26 mm would improve the coupling but waste winding space. Also, the 20 A_{av} would cause an I_{rms} = 1.64 x I_{av} = 33 A. A single litz good for carrying 33 A would be quite thick which would hurt the leakage again and waste still more space. This is no way to go.

A copper foil must not be thicker than twice the depth of penetration at 100 KHz, i.e. 0.25 mm, not good enough for 33 A. Using two such foils in parallel would be disastrous, why is explained in the article "The Focus is ...". The current would only flow in the lower one. No way either.

The solution is multifilar winding: The copper area necessary for 33 A at a current density acceptable for an E 42/15 has to be calculated, this area distributed to as many thin litz as are necessary to fill one or more layers fully, with the stress on "fully". n_s may vary from 3 to 10, this is helpful in fulfilling the condition. Ten parallel wires resp, litz are not uncommon.

But: it is by far not that simple: each time ns is changed, so does Ls which influences t2 resp. the t1/t2 %. E.g., if a higher n_s is used to fulfill the foregoing condition, the increased Ls may shift the converter operation from DCM into CM. Consequently, each time any of these parameters is changed, the consequences must be calculated! If CM operation is desired, L_s resp. n_s may have to be increased, so n_s may run against the stop given by N_{max} or Nmin !

6.5. 5th step: Several secondary windings resp. outputs. Cross regulation.
Matters become considerably more complicated as soon as several outputs are required. The outputs are coupled by true transformer action, that means that their relations are equal to their respective n's, including the diode forward voltages, this imposes additional restrictions. Example:

The $V_{out's}$ desired may be: 3.3 - 5 - 12 - 24 V. It will be quickly evident that higher numbers of turns are necessary in order to realize the relations: 3.9 : 5.6 : 12.6 : 24.6 V. As the currents remain unchanged, higher numbers of turns may require a bigger transformer, apart from higher losses and the possible undesired transition from DCM into CM or from an intended mild into a deep CM. Example: Assumed 1 turn for 3.8 V would mean 3.8 V/turn. 5.5 V would require 1.45 turns, impossible. 2 turns for 3.8 V equals 1.9 V/turn, now 2.9 turns would be required for 5.5 V. The error if 3 turns are used would be 3.6 %; this might be tolerable, also because the diode forward voltages are temperature-dependent. For 12 V it should be 6.3 turns, the error is already 11 %. For 24 V it should be 12.6 turns, the error is 3.2 %. These errors can only be reduced by again increasing all windings with the consequences.

The main output, as the rule that with the highest power, is the one with the pick-off of the regulation loop, its output voltage (at the pick-off point, the first capacitor, downstream the resistances of filter coils will cause voltage drops) is typically extremely stable and recovers from large load steps within a few ten microseconds. However, the main output may be 3.3 V, although FB's are a poor choice for low voltages at high currents. In such a case one would take another output as the reference and stick a linear FET postregulator to the 3.3 V output which requires only a few ten millivolts for proper operation. As mentioned earlier, the best solution for low voltages at high currents with a FB is to design it for 24 V and add a simple buck.
The temperature drift in the other outputs can, at least partly, be compensated if the same type of diode is used in all. The drift in the diode of the reference output wil, however, be multiplied by the ratios of the voltages.

Cross regulation.
The term Cross Regulation denotes the interdependence of several outputs under varying load conditions. This depends extremely on the winding structure. Winding the secondaries as was used with 50 Hz transformers, i.e. one after the other, would result in pretty poor performance. This is the way to go: all secondaries are combined in one multifilar structure, that means that first the lengths of litz for each secondary will be cut to size, then the beginnings of all will be soldered to the respective pins of the coil former. Then the bundle of wires will be wound by carefully keeping them side by side, i.e. they should not overlap. The wire belonging to the regulated output in the middle. Still better performance can be realized if the winding of the regulated output is split into several wires such that the wires as they lie side by side are ordered like this: unreg. output 1 - reg. output - unreg. output 2 - reg. output and so forth. This must be done very orderly. Of course it holds what was said about one output: only full layers are acceptable. Therefore one must play with number of turns, wire sizes, numbers of parallel wires until this is fulfilled. A professional design like this will allow the unreg. outputs to stay within a few percent. Cross regulation must be tested by changing the load on one in turn and looking at the others. The most critical situations are: maximum load on the regulated output, no loads on the others and minimum load on the regulated output and maximum loads on all others. Note: a minimum load must be assured on all unreg. outputs,

because the diodes will rectify spikes, so that unloaded outputs will rise in voltage which will endanger the electrolytics and also the load.

If that was not enough complexity: the secondary rms currents, necessary for the determination of wire sizes, diodes and capacitors, are interdependent, i.e. they change their waveforms any time a load on one or more outputs changes and so also their rms values. Therefore they must be determined by accurate measurements.

6.6 Final adjustments

After all windings are fixed so that the desired operating mode is ensured, now also the winding resistances are known, so their losses can be calculated with the respective rms currents. The core losses can be taken from the respective curves in the ferrite manufacturers' data sheets, bearing in mind, that the curves are based mostly on sine waves. The calculations should then be iterated and the losses considered. A modern offline SMPS by itself, i.e. without a PFC, attains efficiencies of 90 to 95 % at 230 V. A modern wide-range PFC has an efficiency of 97 to 98 % at 230 V, the combination achieves close to 90 % with a transformer loaded to its limits; if the transformer is allowed a bigger size, this can be improved. The losses in the electrolytics are considerable, due to the dual high rms load by the transformer and load currents, the latter is often overlooked; even if the load is straight DC, in phase 2, the discharge phase, it will be supplied solely out of the capacitor. The stress on the capacitor is far higher than e.g. in a converter where there is a fairly continuous stream of current, e.g. in a buck in CM; here, the capacitor sees only the hf ripple. The placement of the transformer and the electrolytics is most critical, the author has seen many SMPS where all electrolytics were placed around the transformer, a worse case is inconceivable. This is a matter of FB circuit design which may be covered in a future article.

6.7. Test and fine adjustments.

Electrical stresses on the semiconductors, the semiconductor, transformer winding and ferrite temperatures and especially the temperatures of the electrolytics under worst case conditions are a minimum of final design tests. The emi tests are so special that they require a separate description.

7. Selection of the switching transistor.

There are quite some requirements on a FB switch; it is not sufficient if the voltage, current and wattage ratings are met for the intended load. A SMPS does not only know normal operation, but there are also overload situations like turn-on. At turn-on all capacitors on the secondary are still empty and present almost a short. Regulation is mostly from the secondary, at turn-on there is no secondary voltage so the loop does not yet function. In order for the supply to reliably start under full load, the primary must be designed for a much higher maximum load than during regular operation; the supply thus starts with this maximum power and runs the secondary voltage up until the regulation circuit is powered up and senses that the desired voltage is reached and, e.g. via an optocoupler, causes the primary control circuit to reduce the charge per period to the actual level required by the load. This must function with maximum load, at the highest ambient temperature and after all components reached their maximum temperatures. Si power mosfet's profit from several decades of improvement, most notably they can withstand enormous overloads by going into a nondestructive avalanche mode; the overload is converted into heat, and the part will survive as long as its maximum Tj is not exceeded.

For some time to come, Coolmos (Infineon designation, other firms use the term "superjunction") switching mosfet's remain the best choice. Coolmos mosfet's combine lowest on resistance with low capacities, and they switch extremely fast, especially in cascode, in offline SMPS down to 5 ns. Too fast rise and fall times resp. dv/dt's cause excessive emi and dielectric stresses and are undesirable. In other words: Si Coolmos is already faster than needed.

The latest Coolmos families also have their drawbacks which are, understandably, not pointed out by the firms. A most important parameter is the R_{thj-c} . The low capacities and fast switching came about by drastically shrinking the chips; this has a deleterious effect on the heat transfer which can go so far that these chips get much hotter inspite of lower losses and come closer to destruction under overload! This is a stern warning: in general the power transistors which were designed in can not simply be replaced by a newer family without prior checking everything thoroughly! Some firms shrunk the chips but left the data sheet unchanged... Comparable SiC and GaN chips are much smaller than Si chips, so their Rth is much worse!

This is why the older families of Coolmos like C2 or 3 are still being made, because their chips are larger and more robust. In cascode they are as fast as the newer ones and to be preferred if at all possible. Note that in a cascode, it is the lower transistor which dictates the performance, this is why older and sturdier chips are not outmoded. For offline SMPS up to some ten watts, the best solution are two-chip components as they are available from several manufacturers, invented some years ago by Samsung; the best contain a Coolmos and a bipolar control chip with CMC. Such parts which switch operating modes back and forth are only useful for known, constant loads.

Do not fall for the shrilly siren tunes from GaN and SiC manufacturers! Extensive tests have shown that in FB SMPS neither SiC nor GaN outperform Si Coolmos, see the article "Performance comparisons ... " in Bodo's Power.There is no reason to go out on a limb and replace proven Si Coolmos by any of the new components which are no better in the first place, unproven, more expensive, especially the composite parts, without second sources. The boisterous, mostly ridiculous claims of the manufacturers are directed mainly to their investors who are no engineers and must be convinced that Si will be replaced by their products so fast that gigantic profits are to be expected. In particular, since many years over and over, they tout that Si will disappear within 2 years. Serious drawbacks are not mentioned, e.g. only one firm openly admitted that their GaN transistors can not take any overload but will be destroyed on the spot, this applies to all. Also SiC transistors have no avalanche spec sofar.

8. Selection of the rectifier diodes.

In general, ultrafast Si diodes are the types of choice. Hyperfast diodes trade speed for increased forward voltage such that they can only be used for high output voltages e.g. in PFC's. Si Schottky diodes make only sense for low voltage outputs; there are types up to 200 V available, but they offer no advantage vs. ultrafast types. Too often their very high capacitances are overlooked. For PFC's SiC Schottky diodes became standard, because their losses are lower than those of UF diodes, and due to their fast recovery the losses in the switching transistor are drastically reduced. Funny enough, their manufacturers never realized that these 600 V diodes are also superior to Si UF diodes for all secondary rectification purposes down to about 24 V. The property of SiC comes to bear that the losses do not increase with temperature. Modern SiC diodes differ from the first ones by the integration of a junction diode in parallel which takes over at higher currents, alleviating the sensitivity to overload. Nevertheless SiC diodes have to conservatively derated!

9. The art of correct measurements within SMPS.

Correct measurements inside SMPS require solid knowledge and appropriate measuring instruments. 1. A high quality oscilloscope with a bandwidth of at least 200 MHz. 2. Passive probes 100:1 and 10:1. 3. A DC/AC current probe with a bandwidth of at least 50 MHz and a sensitivity range of 1 mA/cm to at least 1 A/cm. 4. A power analyzer.

Scopes: Lucky is the owner of a high performance analog scope like a Tektronix 7000 series model, but there are only Digital Storage Osciloscopes (DSO's) on the market. While analog scopes show the signal itself and are absolutely reliable, hence need no explanations, this is not so with DSO's. They do not show the signal, but only a more or less correct reconstruction which can be grossly distorted and bear no resemblance to the original! Even a superficial listing of their problems would require some 30 pages, here just a few important hints. The bandwidth of DSO's is not constant, but depends solely on the memory length and the time scale selected, totally irrespective of the maximum values. All manufacturers lie about the fact that the bandwidth is dependent upon the actual sampling rate and advertise e.g.: "Max. sampling rate 5 GS/s, bandwidth 500 MHz". This is factually wrong, because it should run: "Max. bandwidth". The bulk of DSO's in use are low and medium-priced instruments with memories between 1 and 10 KB because they employ cheap, noisy and rather poor socalled MOS CCD's. Such scopes have no place in a SMPS lab! Example: the current in the choke of a PFC shall be measured; in order to see a full cycle of 50 Hz, the sweep rate must be set to e.g. 10 ms/cm. With a memory length of 1 to 10 KB the maximum sampling rate can not be upheld because of memory overflow; the scope must hence reduce the actual sampling rate from e.g. 5 GS/s to 50 KS/s. The actual sampling rate is not displayed, but concealed somewhere deep in the menus. The bandwidth is 1/10 of the sampling rate, i.e. 5 KHz, not 500 MHz! The PFC converter's 100 KHz sawtooth riding on top of the 100 Hz half-sine will be suppressed resp. all kinds of aliases will be shown if anything. In SMPS labs DSO's with at least 1 MB are required. Another example: DSO manufacturers advertise an "improved resolution" function. Yes, 3 more bits of vertical resolution can be obtained, what they do not say: at a price, and this price is a most drastic bandwidth reduction because this function does nothing else but averaging which is the same as low-pass filtering!

If a lab still has an analog scope it should be kept and always used as the reference when DSO displays are doubtful.

Probes: In SMPS the preferred probes should be 100 : 1. 10:1 probes seldomly can take more than 400 Vp, also the loading is much less and ground connection problems are not as critical. Probes contain an enormous knowhow, it is highly recommended to use only probes from the few renowned manufacturers, others may show grossly distorted high amplitude signals. In order to precisely measure the peak voltages in SMPS, the probes must be carefully adjusted to the specific scope input which includes the adjustment elements in the compensation box, a pulse generator with a rise time of < 0.5 ns and a perfect top is required, the calibrator output of the scope is not good enough. For these adjustments a special 50 Ohm connector with a probe soocket is necessary like the Tektronix type 017-0088-00.

Even with 100: 1 probes the use of the probe's ground strip should be avoided. Most SMPS use E cores and similar types for cost reasons. These have intense stray fields which couple into the loop of the ground strip and cause grossly erroneous measurements. Especially output ripple measurements are thus corrupted. Reliable results can only be obtained by installing the special Tektronix probe connectors in the circuit und inserting the probe with the ground strip removed! However, these don't fit the 100:1 probes.

RMS measurements: The importance of rms current measurements was already mentioned. Because all components are soldered to the board, it will be necessary to unsolder the part to be tested. For this purpose take a 20 cm length of Teflon stranded wire, fold and twist it, leaving a small loop for the current probe. This is then soldered between one wire of the part and the board. This will even work between the drain of the switching transistor and the transformer. Any DSO can calculate the rms value from the waveform. The current probe amplifier output can also be connected to a true rms instrument. Warning: only DC/AC current probes may be used, no AC probes, they would saturate and display nonsense.

Dr. Arthur Seibt
Lagergasse 2/6; A 1030 Wien, Austria
Tel. +43-1-505.8186 email: dr.seibt@aon.at
http://members.aon.at/aseibt

1200W - 1500W Modular Power Supply Series has Lowest Acoustic Noise

TDK Corporation announces the introduction of the QM series of AC-DC power supplies; the first 1200W to 1500W rated modular series to have full MoPPs isolation, with the lowest acoustic noise available on the market at that power level. This product is the latest in a 37-year heritage of modular power supplies, beginning with the invention of the ML series - a world first in 1979. Having both medical and industrial safety certifications, the QM is suitable for a wide range of applications, including BF rated medical equipment, test and measurement, broadcast, communications and renewable energy applications.

Product definition is made extremely easy with an online configurator, giving an optimised module selection with a choice

of signals, leakage current and standby voltages. Once the desired output voltages and currents have been entered, the configurator will automatically produce a unique 8-digit code for easy order placement.

With a wide range 90-264Vac, 47-440Hz input the QM can deliver 1200W, and 1500W with a 150-264Vac input. Up to 16 outputs can be provided, with voltages ranging from 2.8V to 52.8V, with additional higher voltages later. Module power ratings start with a low power 35W, with single or dual outputs, all the way to a powerful 1200W single output. The units will operate in ambient temperatures of -20 to +70°C, derating output power and output current by 2.5% per °C above 50°C. Overall case dimensions are a compact 176 x 63.3 x 270mm (W x H x D), and the weight is between 2.6 and 3.1kg, depending on the module configuration. The QM is covered by an industry-leading seven-year warranty.

www.de.tdk-lambda.com

External Ac-Dc Power Supplies Now Meet EU's CoC Tier 2 Efficiency Standards

CUI announced that the majority of its line of external ac-dc power supplies now meet the European Union's (EU) Code of Conduct (CoC) Tier 1 and CoC Tier 2 efficiency standards.

The European Union's CoC Tier 1 effectively harmonizes the EU with US DoE Level VI and became effective as a voluntary requirement from January 2014, two years ahead of Level VI. Its adoption as an EU Ecodesign rule is currently under review to become law with an implementation date of January 2017. The more stringent CoC Tier 2 requirement became effective on a voluntary basis from January 2016 and is similarly under review to become law as an Ecodesign rule from January 2018.

The key difference between the CoC requirements and Level VI is the new 10% load measure, which imposes efficiency requirements under a low-load condition where historically most types of power supplies have been notoriously inefficient. While CoC Tier 1 includes the new 10% load measure, its no-load and active mode limits are less

stringent than DoE Level VI. CoC Tier 2 further tightens the no-load and active mode power consumption limits for key classes of power adapters enacted by Level VI and covers both standard voltage and low voltage adapters.

www.cui.com

Hermetically Sealed Aluminum Electrolytic Capacitor Line Expands to Higher Voltages

Cornell Dubilier Electronics, Inc. has announced significantly higher voltage values for its MLSH Slimpack series of hermetically sealed aluminum electrolytic capacitors. These unique components feature a true glass-to-metal seal that prevents dry-out of the capacitor electrolyte. As a result, they provide extraordinarily long life (5,000 hours) to more than meet the most demanding applications for military and aerospace. With the line expansion just announced, they are now available in nine values, from 120 µF to 3,200 µF, with ratings up to 250 Vdc.

The hermetic Slimpack is an offshoot of the well-established non-hermetic Flatpack series. The new MLSH Slimpack can be used as a replacement for parallel and series banks of wet tantalum capacitors for both new and existing designs. This change is especially beneficial where bulk storage is paramount. MLSH Slimpack devices measure 1.0" x 1.5" x 0.5", weigh less and have more capacitance than a parallel bank of three or more wet tantalum capacitors. High rated capacitance is maintained at temperatures as low as -55 °C, a key requirement for power supplies used in military and aerospace applications. Top-end temperature rating is 125 °C.

All devices in the MLSH Slimpack series feature rugged stainless steel cases with a vibration rating of 80g. In most applications, there are significant cost and space savings vs. a comparably rated bank of wet tantalum capacitors. The new high-voltage MLSH Slimpacks eliminate the need for series banking.

Since its founding in 1909, CDE has been dedicated to advancing capacitor technology for new applications. The company combines innovative products with engineering expertise to provide reliable component solutions for inverters, wind and solar power, electric vehicles, power supplies, motor drives, HVAC, motors, welding, aerospace, telecom, medical equipment and UPS systems.

www.cde.com/MLSHSlimpack

200 Degree Celsius High Voltage Capacitor Products

KEMET Corporation announced the addition of EIA 2824, 3040, 3640, and 4540 case sizes to the HV-HT surface mount multilayer ceramic capacitor product line. These added case sizes allow for up to 150 nF of temperature-stable capacitance in 200 degree Celsius environments.

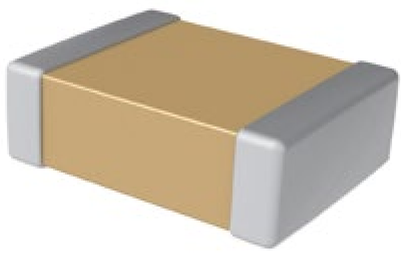

HV-HT capacitors are specifically designed to withstand the demands of harsh industrial environments such as oil exploration and automotive/avionics engine compartment circuitry. In addition, with the growing trend of increased voltage, frequency, and temperature in Wide Band Gap semiconductors (SiC, GaN) technology, KEMET's HV-HT capacitors are ideal for realizing design goals such as maximum power density and efficiency.

Typical applications include critical timing, tuning, circuits requiring low loss, circuits with pulse, high current, switch mode power supplies, high voltage coupling, DC blocking, and voltage multiplier circuits in extreme environments such as down-hole exploration, aerospace engine compartments, and geophysical probes.

HV-HT capacitors were developed under KEMET's patented 200°C high reliability base metal electrode (BME) dielectric platform which is 100% Pb-free, RoHS and REACH compliant without exemptions. In addition to a low profile and aspect ratio, these devices exhibit low inductance and ESR with respect to application frequency, allowing for very high ripple current capability.

www.kemet.com/Hi-Temp-Ceramic

WT1800E Precision Power Analyser

Yokogawa Europe announced the launch of the WT1800E power analyser. This instrument introduces new standards of accuracy and flexibility in power measurement across a broad range of applications.

Today's energy conscious world is driving efficiently. Renewable energy markets like photovoltaic and wind power are growing and we are seeing accelerated development of environment-friendly vehicles and energy-efficient home and industrial appliances.

Developing these technologies requires

engineers towards an ever-increasing focus on energy conservation, energy efficiency and renewable energy. Engineers seeking to improve their product through better energy management therefore need more accurate power measurement.

To curb global warming, greater efforts are being made to generate and use power more accurate measurements of electric parameters like voltage, current and power to validate even the smallest changes in energy consumption. In the WT1800E high performance power analyser, engineers have the ideal tool to accurately measure power, its quality and efficiency.

http://tmi.yokogawa.com/products/digital-power-analyzers/


Messe München
Connecting Global Competence
Planet e:
Where the
future begins.
Electronics of tomorrow.
Today.
Tickets & Registration:
electronica.de/en/tickets
World's Leading Trade Fair for Electronic Components,
Systems and Applications
Messe München I November 8–11, 2016 I electronica.de
electronica 2016
inside tomorrow

Bussmann™ Series Fuses Meet Higher Power Requirements

Power management company Eaton announced the Bussmann™ series 1025HC high current fast-acting surface mount (SMD) fuses designed for the power requirements of new generation telecommunications and computing systems.

The compact footprint of the new series allows developers to utilize less circuit board space with a higher current rating, higher voltage rating and improved performance. The increased current squared time (I2t) ratings in the 1025HC are ideal for power systems that are used in next generation server and desktop computers, gaming consoles, industrial and consumer electronics, storage systems, base stations, test equipment and LED lighting.

“Our goal is to bring new technology that adds value to our customers’ designs,” said Matt Joiner, global product manager, Eaton’s Electronics Division. “This line of fuses offers high-current-carrying capability in a very compact, surface-mount package saving customers space in their advanced high-power designs.”

The 1025HC offers one of the industry-leading I2t ratings from 25 to 600 amperes squared seconds (A2s). It provides a superior solution to power system designers who require performance and technical advancement in demanding operating environments. The 1025HC fuse delivers excellent protection during in-rush currents on start-up helping to eliminate nuisance fuse openings. The compact size of the 1025HC, 10 mm in length by 3.15 mm in height by 1.7 mm in width, helps designers utilize board space efficiently.

www.eaton.com/electronics

Digital LED Driver ICs with Flicker Free Control and Low Stand-by Power

Modern LED technology offers many advanced possibilities for lighting applications. With the XDPL8220, Infineon Technologies

AG extends its product portfolio of digital and configurable LED driver ICs. The IC enables the lighting industry to realize essential features for smart lighting and increases the benefits for both, end user and manufacturers. The primary side control of this device saves extra components, reducing cost on the one hand and increasing reliability on the other.

The XDPL8220 offers a modern two stage architecture, significantly easing the implementation of up and coming flicker standards. This was made possible by eliminating the low frequency variation from the mains supply and guaranteeing a stable output. Aiming at high energy efficiency, the low stand-by power facilitates permanent operation of the Electronic Control Gear (ECG). With a stand-by power of less than 70 mW, the XDPL8220 reduces power consumption in the non-active mode while still reacting to external events or user requests.

www.infineon.com/xdp

3-5 Cell Li-Ion/Li-Polymer Battery Protection Analog Front-End IC

Ricoh Europe (Netherlands) B.V. Semiconductor Support Centre has launched a Analog Front-End (AFE) Integrated Circuit (IC), the R5601. The new addition to Ricoh's battery management ICs portfolio is designed for Lithium-ion or Lithium-polymer battery packs of three up to five cells in series. Applications include cordless power tools, robot vacuum cleaners, lawn mowers, and electrical bikes.

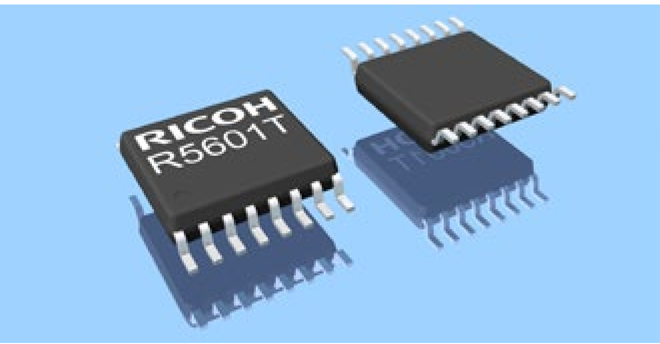

Traditional stand-alone protection ICs have internally fixed hardware settings for various monitoring thresholds that decide to interrupt the charge or discharge process and control the external dual MOSFET. The advantage of an AFE IC versus a stand-alone protection IC is the flexible concept enabling short time to the market. An AFE IC is a measurement device of which the results are forwarded to a MCU (microcontroller unit). The fact that all threshold settings are saved within the software of the MCU and software settings are easily adaptable means a significant advantage. Therefore, an AFE IC is more convenient to use as a standard measurement IC for various battery pack designs.

www.e-devices.ricoh.co.jp/en/products/product_power/bmu/r5601/

LED Drivers for Integrated Lighting

RECOM DC current (RACD04) and DC voltage (RACV04) LED drivers have been designed for cost-sensitive applications. Safety extra low voltage or SELV terminals are ideal for supplying power to integrated LED lighting.

RECOM LED drivers can be built into furniture, hidden under shelving, or integrated into applications with extremely space available due to their their compact design, including cable connections. The RACD04 series is aimed at LED spotlights, reading lamps and accent lighting, whereas the RACV04 series is ideal for LED strips, background and wall lighting, and furniture and cabinet illumination. Each 4W AC/DC LED power supply in IEC protection class II packed into a compact casing measuring 38 x 27 x 21 mm at a weight of just 40g. The RACD04 series has 350, 500 and 700 mA DC current terminals, whereas the RACV04 has 12 and 24V DC current terminals. The isolation voltage in either case is 3.5 kV AC/1 minute. These LED drivers are classified to IP65, and are therefore suitable for damp areas such as kitchens and bathrooms, or covered garden or outdoor facilities. The drivers provide complete protection against short circuit, overvoltage, overload and overheating, and are certified according to CE, DB, CSA and UL8750 standards and comply with the RoHS2.1 and ErP directives. Both series have a three-year guarantee. RECOM RACD04 and RACV04 are now available from the RECOM distribution network.

www.recom-power.com

TVS Diodes Suited to High-Speed Interfaces

The continuous growth of data traffic - driven by smartphones, wearables and applications such as virtual reality and the Internet of Things (IoT) - leads to increasing numbers of high-speed interfaces that typically require protection against ESD events. To address this demand, Toshiba Electronics Europe has released ESD protection diodes based on its 4th generation ESD diode array process (EAP-IV), which uses Toshiba's proprietary snapback technology.

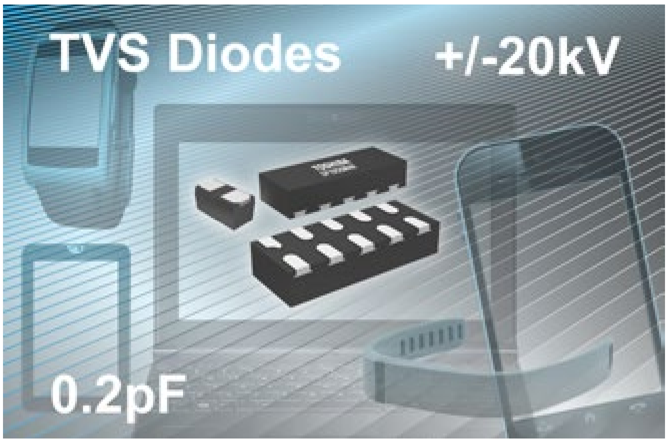

The DF2B5M4SL, DF2B6M4SL, DF10G5M4N and DF10G6M4N offer protection for high-speed interfaces including USB 3.1 applications. A choice of operating voltages (3.6V and 5.5V) and packages (SOD962 and DFN10) provides flexible options for realizing ESD protection in a variety of designs.

Thanks to Toshiba's new process, the four devices simultaneously deliver low capacitance, low dynamic resistance and high ESD endurance. Minimum signal distortion of high-speed data signals is guaranteed by the ultra-low capacitance of 0.2pF, while a typical dynamic resistance of RDYN=0.5 Ω ensures low clamping voltages. High ESD protection levels are supported as electrostatic discharge voltages of at least ±20 kV according to IEC61000-4-2 are guaranteed.

www.toshiba.semicon-storage.com

16bit ‘Tough’ MCUs Optimized for Rechargeable NiMH Applications

LAPIS Semiconductor, a member of the ROHM group, has announced the development of the ML620130 family of 16bit low power MCUs, optimized for compact industrial equipment requiring battery drive in noisy environments, featuring superior processing capability with low power consumption.
In addition to clearing the ±30kV noise measurement limit, operating voltage has been successfully reduced to 1.6V. Optimizing the operating voltage to an integral multiple of standard nickel metal hydride batteries (NiMH, 0.8V× 2=1.6V) ensures efficient use without wasting battery charge. This contributes to decreased battery consumption, prolonging battery life in portables and battery-equipped industrial equipment. The ML620130 family consists of 9 models offered in a variety of memory capacities, pin counts, and other characteristics that make it possible for users to select the ideal solution to fit set needs.

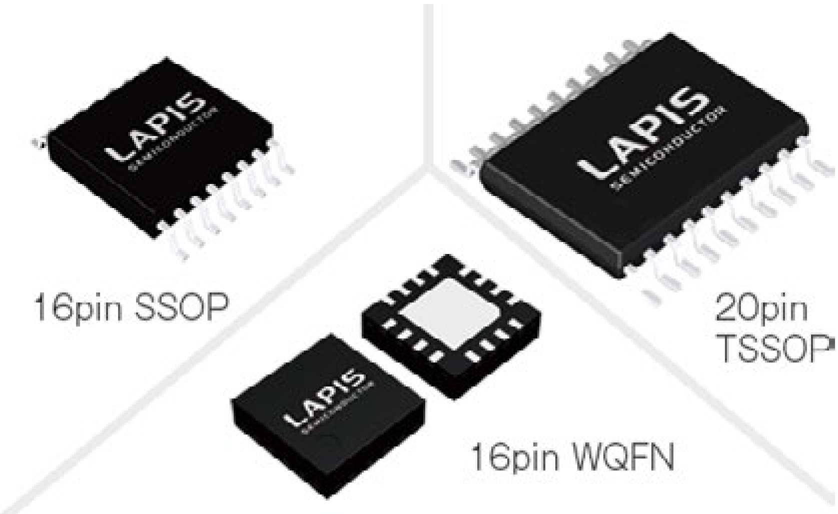

To provide increased miniaturization and lower costs, many applications are opting to eliminate noise and/or thermal countermeasures. However, this makes it difficult to balance the conflicting demands for increased environmental resistance while maintaining safety utilizing fewer external parts. In addition, reducing the size of the battery mounted in the module while also increasing battery life requires that the power consumption (voltage and current) be optimized for each application.
To meet these disparate needs, LAPIS Semiconductor has expanded its lineup of market-proven 16bit low power microcontrollers to include the ML620130 family of ‘tough‘ MCUs that incorporate multiple functions optimized for battery drive operation.

www.rohm.com/eu

CALL FOR PAPERS

EPE'17 ECCE EUROPE

19th European Conference on Power Electronics and Applications

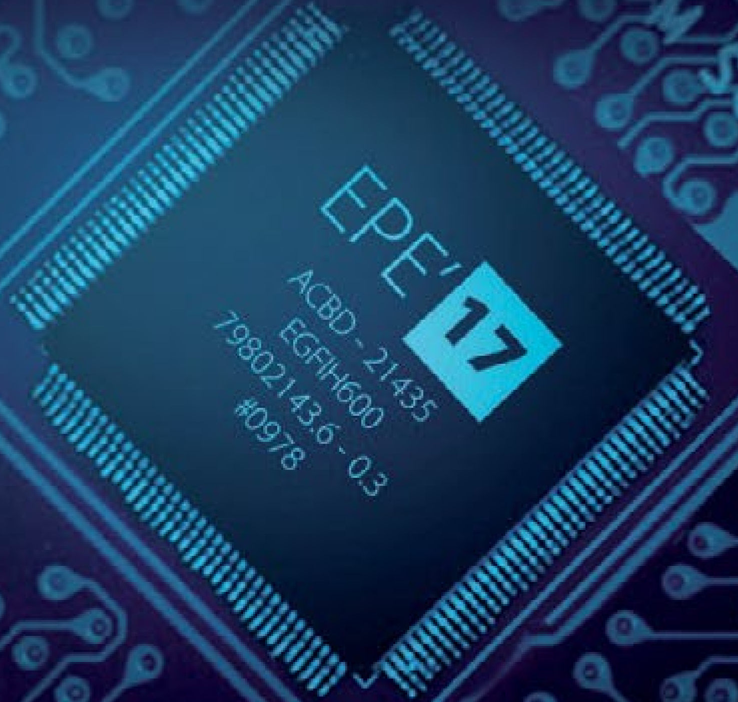

September 11–14, 2017

Warsaw, Poland, www.EPE2017.com

November 14th, 2016
Abstract submission deadline

March 1st, 2017
Notification of provisional acceptance

June 5th, 2017
Final submission deadline

IEEE

pels

EPE

ECCE

Warsaw University of Technology

Solid State Relay with a 170mA Load Current Rating

IXYS Integrated Circuits Division, Inc., a wholly owned subsidiary of IXYS Corporation, announced the immediate availability of the CPC1010N, 250V, single-pole, normally open (1-Form-A) Solid State Relay (SSR) with a 170mA load current rating. The CPC1010N is specially designed to provide the best combination of performance, size and price.

Packaged in a 4-pin SOP, the CPC1010N employs optically coupled MOSFET technology to provide 1500Vrms of input to output isolation. The efficient MOSFET switches and isolated driver IC use IXYS ICD's patented OptoMOS architecture and technology.

IXYS ICD's advanced molded vertical construction makes the CPC1010N one of the world's smallest relays and offers board space savings over the competitor's larger 4-pin SOP relay. Additional features include low drive power requirements, high reliability, arc-free with no snubbing circuits, and no EMI/RFI generation. The CPC1010N is designed to replace, and offers superior reliability over, electromechanical relays.

The 250 volt load voltage rating, 170mA load current rating and 11.5 ohms of on-resistance makes this device suitable for industrial applications, instrumentation, multiplexers, data acquisition, and electronic switching.

Approvals include: UL Recognized Component: File E76270, CSA Certified Component: Certificate 1172007, EN/IEC 60950-1 Certified Component: TUV Certificate B 13 12 82667 003.

www.ixysic.com

High Isolation DC-DC Converter for High Power

Power electronics specialist, Amantys Power Electronics Limited, has announced the launch of a high isolation DC-DC converter to power high voltage gate drives for 4500V and 6500V IGBT modules. The DC-DC converter is designed to comply with international standards including EN 50155 for railway applications and IEC 61800-5-1 for variable speed motor drives.

The DC-DC converter can accept a 15V or 24V input voltage and has an output power of up to 15W making it suitable for driving several gate drives in parallel. It features low quiescent current of 50mA and a maximum current output of 1100mA. The DC-DC converter provides a minimum of 12kVrms working voltage isolation, making it suitable for two level and three level converter topologies.

The robust design can operate from -40ºC to +85ºC and has protection features for: input reverse polarity; input overvoltage; output short circuit; and output overload. The protection features are complemented by status LEDs that indicate DC-DC operation and fault conditions.

The isolated DC-DC converter will be used in applications such as railway traction, HVDC infrastructure and medium voltage motor drives. The DC-DC converter is available for sample orders in Q4 2016.

www.amantys.com

High Performance, Compact, Medium and High Voltage Transducers for Traction

LEM introduces the DVM series for insulated nominal voltage measurements in traction applications. This family of devices spans the range from 600-4200 VRMS and incorporates LEM's proven and patented insulating technology. Despite achieving very high levels of isolation with a safety insulation voltage of 12 kV, the DVM transducer is compact, measuring only 138 x 63.4 x 69 mm.

It is fully compatible and out-performs the previous generation of transducers in terms of functions and performance with new improved levels of accuracy and temperature stability, thus greatly simplifying retrofits.

DVM is also suitable for base mounting, but with slightly different outline dimensions to take into consideration for primary and secondary connections locations for example. The DVM is 30% smaller in height, occupies 25% less volume and is 56% lighter! The reduction in size does not compromise the DVM's high immunity against the external surrounding perturbations or against the high voltage variations. The new size is also an advantage when confronted with size constraints in modern railway propulsion converters.

LEM developed the DVM to be fully compliant with the International Railway Industry Standards (IRIS), providing engineers in the railway industry, who are working with both rolling stock and sub-stations, with a versatile transducer that is equally applicable to measuring network voltages, or the main converter DC link on-board trains.

www.lem.com

Miniaturization with High-Temperature Surface-Mount Silicon Controlled Rectifiers

STMicroelectronics has introduced the industry's first 800V surface-mount Silicon Controlled Rectifiers (SCR, or thyristor) specified for operation at temperatures up to 150°C without derating, giving freedom to miniaturize power modules for applications that demand high reliability in harsh conditions.

With its 80A current rating, the new TM8050H-8 SCR, housed in the High-Voltage D3PAK (TO-268-HV), enables mid-power applications in the 1-10kW range to leverage surface-mount assembly efficiencies and reduce PCB and heatsink sizes, lowering system cost. The package has very low junction-to-case thermal resistance of 0.25°C/W, ensuring efficient heat dissipation, and a large pin-to-tab creepage distance of 5.6mm that gives a large safety margin in the presence of high applied voltages. A TO-247 package option is also available.

The TM8050H-8 is the latest addition to ST's family of SCRs that all bring state-of-the-art device and package technologies to automotive and industrial power control. Spanning current ratings from 12A to 80A, the devices enable designers to create extremely compact and reliable car or motorcycle voltage regulators, induction motor starters, soft starters, industrial heater or cooker controls, Solid-State Relays (SSRs), uninterruptible power supplies (UPS), and AC-line conditioners.

With low dynamic resistance (RD) and on-state voltage (VTO) of 5.5 mΩ (TJ = 150°C) and 0.85V respectively, and leakage current of 20µA max (at 800V, Tj = 25°C), the TM8050H-8 ensures extremely high energy efficiency under all operating conditions.
www.st.com/tm8050h-d3pak-nb

www.toshiba.semicon-storage.com

Optical PHY leadership with New Generation of Gearbox Products

Broadcom Limited announced a generation of gearbox PHY IC devices, the BCM82332, BCM82793 and BCM82864, designed for data center and enterprise networking applications.

With the general availability of switch chips that have flexible multi-speed port interfaces supporting 10G, 40G, 100G and emerging Ethernet speeds, new gearbox PHY solutions are needed to ensure robust signal integrity and optimize port adaption. The latest Broadcom gearbox PHY devices extend the capabilities of switches by providing flexible port interface andnmaximizing the electrical link distance to optical interface while consuming minimal power. The BCM82793 and BCM82332 are application-optimized, cost-effective 100G gearbox devices that support IEEE802.3bj Clause 73 Auto-negotiation, Clause 91 FEC and Clause 92 & 93 transmit training.

www.broadcom.com

Record-Breaking Low Profile Product Series

Power, leading designer, manufacturer and seller of high efficiency and small size Power Supplies, will present its new Ultra Low Profile (ULP) series of Medical and Commercial, High Efficiency, High Power Density AC/DC power supplies at the Electronica 2016 in Munich. The new (M)ULP 180 & 250 Watt Series have power densities which reach 30 watts per cubic Inch with maximum height profiles of 0.75 Inches (19.05mm).

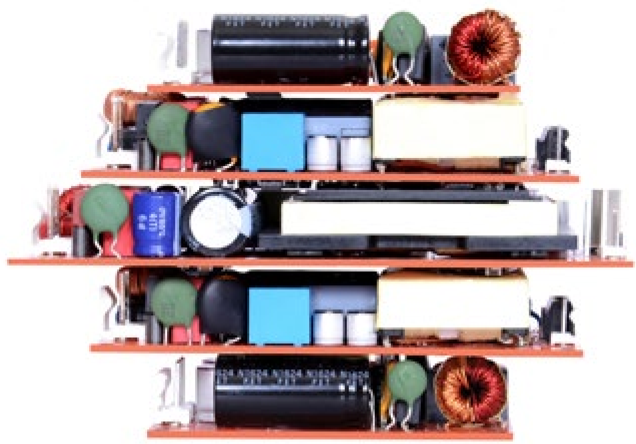

The (M)ULP40, 180 Watt Series offer existing and new customers the possibility of using standard 2 x 4 and 3 x 5 inch open frame medical and commercial grade power solutions in height restricted environments without having to change mechanical footprints while increasing efficiencies. The 0.75 Inch (19.05mm) height profile is a market first in this AC/DC open frame power range which expands even further the options available to EOS Power customers and their applications. The MWLP225 and MWLP350 series of medical open frame products released last year by EOS Power have been a global success due to their power densities and market leading specifications. To further enhance the appeal of these medical products to our medical customers EOS Power is now offering extended warranty option on both the 225 and 350 MWLP product series. See EOS at electronica, Hall A2/475.

www.eospower.com

Reference Design adds Wi-Fi Capability to Electric Vehicle Charging Stations

Texas Instruments introduced the first reference design that adds Wi-Fi connectivity to an electric vehicle (EV) charging station. EV owners will now be able to remotely monitor and control the charging of their vehicles from just about anywhere with Wi-Fi, presenting dozens of potential use cases from home automation to checking the availability of nearby public charge points. Download the new EV Charging Station with Wi-Fi reference design.

Battery technology advancements and government regulations have resulted in a growing number of new electric vehicles around the world. But EV makers still need more charging stations to make it easier for drivers to charge their vehicles. The new reference design uses TI's SimpleLink™ Wi-Fi wireless microcontroller (MCU) technology that allows design engineers to create stations that intelligently charge at non-peak times or detect and communicate when a charging station is available.
One barrier to widespread EV charging station adoption is the amount of time it takes to charge a vehicle. The reference design supports Level 1 charging, which is compatible with household outlets, as well as Level 2 EV charging, which helps vehicle owners tap into higher current (15A to 30A and higher) connections available in commercial office buildings. Level 2 chargers typically take up to eight hours to fully charge the vehicle if the owner wants to plug it in while at work.
Later this year TI plans to introduce a Level 3 EV direct-current charger reference design scalable to 600V and 400A that cuts charging time down to only 20-30 minutes – enough time to stop at a Wi-Fi enabled restaurant that has a charging station and charge the vehicle during lunch. Read the blog post, Electric vehicle charging stations are getting smarter and charging faster.

www.ti.com

High-Speed, Small Footprint RS-485 Receivers for Industrial Applications

Exar Corporation announced a family of high-speed RS-485/RS-422 receivers that accommodate the complex demands of next generation high-speed serial communications designs. The XR33180, XR33181, XR33183, and XR33184 occupy a 3mm x 3mm footprint and feature 52Mbps data rates, fast 15ns propagation delay and 2ns maximum receiver skew. This family is best suited for high performance industrial applications such as multi-drop clock distribution, telecom networking, robotic control, process automation and local area network applications.

The XR33180/81/83/84 (XR3318x) operate from either a 3.3V or 5V supply and are available in tiny 5-pin and 6-pin TSOT23 packages, ideal for high-speed point-to-point RS-485 applications where space is a concern. The XR33184 includes a low voltage logic pin that eliminates the need for a level shifter when interfacing to MCUs or FPGAs that run off of lower supply voltages.

All devices feature ±15kV ESD protection on the receiver inputs and exceed the highest ESD rating of IEC 61000-4-2 and operate over an extended temperature range of -40°C to +125°C.

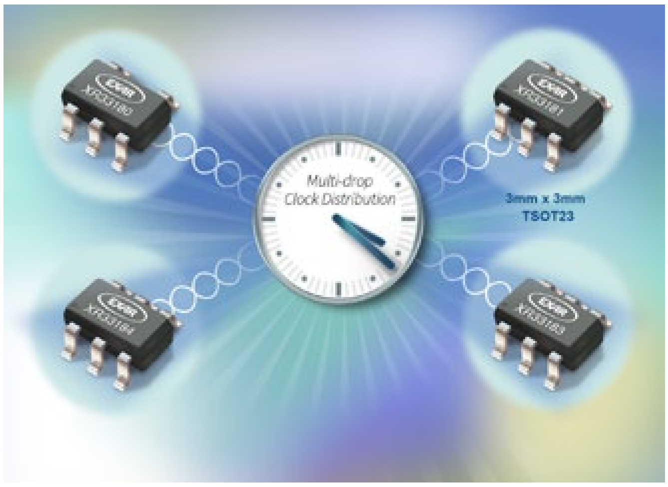

www.exar.com/products/interface/serial-transceivers/rs485-422

Monolithic Power Modules for DC/DC Applications

Mouser Electronics, Inc. is now stocking the Monolithic Power Modules (MPM) from Monolithic Power Systems (MPS). Providing superior performance and inherent reliability by eliminating unnecessary assembly steps and minimizing external components, the MPM family comprises integrated DC/DC solutions that consist of a monolithic regulator, passive components, and a mold compound all in a single chip. Based on MPS' innovative single-step assembly process, these step-down DC/DC converters offer circuit simplicity for ease of design; are highly efficient; yield superior noise, ripple, and transient performance; and are available in a compact module form factor that is up to 50 percent smaller than competing solutions.

The MPS Monolithic Power Modules, available from Mouser Electronics, are high-frequency, synchronous, rectified, step-down, switch-mode converters with built-in power MOSFETs and integrated inductors. Each of the modules can regulate a continuous output current to input voltage with excellent load and line regulation results. The modules operate on a switching frequency of up to 2.4 MHz to achieve a fast load transient response, and feature a wide operating input range of up to 36V. The devices also include a variety of protective features including over-current protection and thermal shut down.

www.mouser.com/new/monolithicpowersystems/mps-mpm-power-modules/

The H-Bridge to up Customers Application's Speed and Efficiency

Vincotech, a supplier of module-based solutions for power electronics announced the launch of a fastPACK 0 HC improving UPS, SMPS, solar and welding applications in speed, efficiency and full-current capability for bidirectional usage. The H-bridge module is available in the low-inductive flow 0 housing.

The fastPACK 0 HC module featuring high frequency 650 V IGBT H5 technology in combination with a fast diode enables outstanding efficiency, reliability and perfectly balances cost and performance. This utmost efficient H-bridge module delivers 30+ kHz fsw and is suitable for soft switching to reduce switching losses.

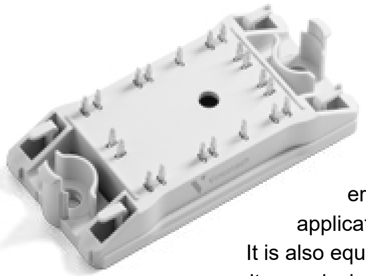

The fastPACK 0 HC enables bidirectional operation for charger and SMPS applications with full current FWD. It is also equipped with integrated capacitors reducing electromagnetic interference. Packaged in the low-inductive flow 0 12 mm housing the module can also be provided with phase-change material on special request.

www.vincotech.com/fastPACK-0-HC

UFHV Series - Fast Axial Lead High Voltage Diodes

Dean Technology, Inc., announced the reintroduction of the UFHV series axial lead high voltage diodes. This series of diodes are available in 2,000, 3,000 and 4,000 volt ratings and all have a 75 nanosecond response time. Recent improvements in manufacturing processes have made this series of diodes a viable offering again. The work we've done to keep the UFHV series cost effective is a perfect example of our commitment. We want to be sure that we offer our customers products that will meet their needs for a very long time." With current ratings ranging from 350 to 550 milliamps, the UFHV series is very flexible and ideal for many uses. These diodes offer exceptional performance for the price, making them a very good value.

Full product details can be found on the Dean Technology website, and the diodes are in stock and immediately available from Dean Technology, or through any approved sales partner or distributor.

www.deantechnology.com

Next-Generation Output Transistor Arrays

Toshiba Electronics Europe has announced a series of next-generation output transistor arrays that feature a DMOS FET type sink output. The TBD62183AFNG and TBD62183AFWG are ideal for level shift applications and for directly controlling photocouplers, LEDs, and relays that require high-voltage input signals.

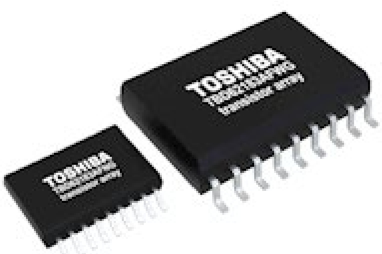

The TBD62183AFNG and TBD62183AFWG deliver high-voltage drive capabilities with an input rating of 30V and output rating of 50V. An 8-channel sink type output is incorporated into the small SMD packages, enabling reduced component count for the control of multiple circuits.

In addition, the TBD62083A-series has an IOUT of 500mA/ch while the TBD2183A-series is designed for low power applications with a maximum IOUT of 50mA/ch.

By adopting a DMOS FET type output, the two new transistor arrays eliminate the need for a base current for the input pin. The devices achieve operation with a low maximum input current of 0.1mA @ VIN=3V, while delivering very low power consumption. They also have output characteristics similar to the Vce (sat) properties of a Darlington Bipolar transistor, making them suitable for replacing in-line bipolar transistors in Toshiba's TD62083A series.

www.toshiba.semicon-storage.com

Advertising Index